SURFACE MODIFICATION OF BIOMATERIALS TO REDUCE POLYETHYLENE WEAR IN METAL-POLYMER CONTACT

TAN MEAN YEE

DEPARTMENT OF MECHANICAL ENGINEERING
FACULTY OF ENGINEERING
UNIVERSITY OF MALAYA
KUALA LUMPUR

2020

Universiti Malaya

SURFACE MODIFICATION OF BIOMATERIALS TO REDUCE POLYETHYLENE WEAR IN METAL-POLYMER CONTACT

TAN MEAN YEE

DISSERATION SUBMITTED IN FULFILMENT OF THE REQUIREMENTS FOR THE DEGREE OF MASTER OF ENGINEERING SCIENCE

DEPARTMENT OF MECHANICAL ENGINEERING
FACULTY OF ENGINEERING
UNIVERSITY OF MALAYA
KUALA LUMPUR

2020

Universiti Malaya

UNIVERSITY OF MALAYA

ORIGINAL LITERARY WORK DECLARATION

Name of Candidate: Tan Mean Yee

(Matric No: KGA 150073

Name of Degree: MASTER OF ENGINEERING SCIENCE

Title of Dissertation: Surface modification of biomaterials to reduce polyethylene wear in metal-polymer contact

Field of Study: Surface modification

I do solemnly and sincerely declare that:

(1) I am the sole author/writer of this Work;
(2) This Work is original;
(3) Any use of any work in which copyright exists was done by way of fair dealing and for permitted purposes and any excerpt or extract from, or reference to or reproduction of any copyright work has been disclosed expressly and sufficiently and the title of the Work and its authorship have been acknowledged in this Work;
(4) I do not have any actual knowledge nor do I ought reasonably to know that the making of this work constitutes an infringement of any copyright work;
(5) I hereby assign all and every rights in the copyright to this Work to the University of Malaya ("UM"), who henceforth shall be owner of the copyright in this Work and that any reproduction or use in any form or by any means whatsoever is prohibited without the written consent of UM having been first had and obtained;
(6) I am fully aware that if in the course of making this Work, I have infringed any copyright whether intentionally or otherwise, I may be subject to legal action or any other action as may be determined by UM.

Candidate's Signature Date:

Subscribed and solemnly declared before,

Witness's Signature Date:

Name:

Designation:

University of Malaya

SURFACE MODIFICATION OF BIOMATERIALS TO REDUCE POLYETHYLENE WEAR IN METAL-POLYMER CONTACT

ABSTRACT

This research focus on studying different surface modification (Texturing and DLC coating) on the metal part of TKR (Total knee replacement) in improving UHMWPE (Ultra-high molecular weight polyethylene) wear. TKR was widely being used to relieve knee pain due to osteoarthritis and further restore knee function of patients. Generally, TKR consists of metal femoral component, metal tibial component, and UHMWPE tibial insert. TKR will fail due to various factors over time, however, this study will be focusing on failure cause by loosening. Loosening failure of TKR was mainly caused by wear debris generated during articulation motion, where UHMWPE wear was one of the main threats toward loosening failure. UHMWPE has many advantages; however, the major drawback of UHMWPE was its hydrophobicity. Protein will more likely being attracted and denatured onto hydrophobic surface and form protein aggregate. The protein aggregates formed on the surface will increase surface roughness and friction which later cause surface wear. However, when two hydrophobic surfaces with protein aggregates interact, protein aggregate from both surfaces will bind together and formed a thin film which protects the surface from wear. Hence, surface modification (Texturing and DLC coating) onto the hydrophilic metal surface will be done in order to alter the surface energy of the metal surface.

Surface texturing using LST method was used to create dimple texture, while surface coating was used to deposit DLC (Diamond-like coating) coating (ta-C, a-C:H) onto the metal surface. Surface characterization (RAMAN, FTIR) was done in order to characterize the surface morphology before wear. Protein absorption and wettability test was done on DLC coating in order to evaluate the relationship between surface energy and protein adsorption towards wear. Wear test was done using reciprocating and pin-on-

Universiti Malaya

disc method under protein (BS, BSA) lubricated condition. Wear surface then was characterized using RAMAN, FTIR, SEM, optical microscope in order to analyze the surface wear mechanism. The results of this research show that UHMWPE wear of tibial insert in TKR will deteriorate over time and was essential to reduce formation of wear in order to improve functionality and performance of TKR. Hence, surface modification was being done. Surface texturing might have the ability to protect its own surface from wear, but it will cause high wear on its counterpart. While DLC coating has the ability to protect its own surface and its counterpart from wear. a-C:H coating can reduce more UHMWPE wear as compared with ta-C coating. The a-C:H coating deposited using different hydrocarbon source will not have much differences in improving UHMWPE wear.

Keywords: Failure analysis; surface modification; surface texturing; diamond-like carbon; protein adsorption.

Universiti Malaya

MODIFIKASI PERMUKAAN BIOMATERIAL UNTUK MENGURANGKAN PENGGUNAAN POLYETHYLENE DALAM HUBUNGAN LOGAM-POLYMER

ABSTRAK

Fokus penyelidik ini ialah mengenai tentang pengubahsuaian permukaan (Penteksturan dan lapisan DLC) pada bahagian logam TKR dalam mengurangkan UHMWPE wear. TKR secara meluas digunakan untuk melegakan sakit lutut akibat osteoarthritis dan memulihkan fungsi lutut pesakit. Secara umumnya, TKR terdiri daripada komponen logam femoral, komponen logam tibial, dan tibial UHMWPE. TKR akan gagal disebabkan oleh pelbagai faktor dari masa ke masa, walau bagaimanapun, kajian ini akan memberi tumpuan kepada kegagalan disebabkan oleh kelonggaran UHMWPE. Kelonggaran TKR terutama disebabkan oleh serpihan yang dihasilkan semasa gerakan artikulasi, di mana serpihan UHMWPE adalah salah satu ancaman utama ke arah kelonggaran UHMWPE. Walaupun UHMWPE mempunyai banyak kelebihan; kelemahan utama UHMWPE adalah hydrophobicity. Protein mudah tetarik dan denatured terhadap permukaan hidrofobik dan bentuk agregat protein. Agregat protein yang terbentuk di permukaan akan meningkatkan kekasaran permukaan dan geseran yang kemudiannya menyebabkan memakai permukaan. Apabila dua permukaan hidrofobik dengan agregat protein berinteraksi, agregat protein dari kedua-dua permukaan akan terikat bersama-sama dan membentuk sebuah filem nipis yang melindungi permukaan daripada haus. Oleh itu, pengubahsuaian permukaan (Penteksturan dan lapisan DLC) ke permukaan logam yang hydrophilic akan dilakukan untuk mengubahsuai tenaga permukaan permukaan logam.

Penteksturan dengan kaedah LST akan digunakan untuk menghasilkan tekstur dimple, manakala lapisan permukaan akan digunakan untuk deposit lapisan DLC (ta-C, aC: H) ke

Universiti Malaya

permukaan logam. Pencirian permukaan (RAMAN, FTIR) akan dilakukan untuk mencirikan morfologi permukaan sebelum memakai. Ujian penyerapan dan kelembapan protein akan dilakukan pada lapisan DLC untuk menilai hubungan antara tenaga permukaan dan penjerapan protein ke arah kehausan permukaan. Ujian kehausan akan dilakukan menggunakan kaedah reciprocating dan pin-on-disk dengan pelincir protein (BS, BSA). Permukaan yang haus akan dicirikan menggunakan RAMAN, FTIR, SEM, optical microscope untuk menganalisis mekanisme haus permukaan. Hasil penyelidikan ini menunjukkan bahawa UHMWPE wear dari tibial UHMWPE di TKR akan merosot dari masa ke masa dan adalah penting untuk mengurangkan pembentukan wear untuk meningkatkan fungsi dan prestasi TKR. Oleh itu, pengubahsuaian permukaan mesti dilakukan. Permukaan tekstur mungkin mempunyai keupayaan untuk melindungi permukaannya sendiri dari wear, tetapi ia akan menyebabkan wear tinggi pada rakan sejawatannya. Lapisan DLC mempunyai keupayaan untuk melindungi permukaannya sendiri dan rakannya daripada memakai. Lapisan a-C:H boleh mengurangkan lebih banyak UHMWPE wear berbanding dengan lapisan ta-C kerana lapisan a-C:H mempunyai tenaga permukaan yang lebih rendah dan penjerapan protein yang lebih tinggi. Lapisan a-C:H yang deposit menggunakan sumber hidrokarbon yang berbeza tiada jauh berbeza dalam peningkatan keupayaan UHMWPE.

Keywords: Analisis kegagalan; pengubahsuaian permukaan; Penteksturan permukaan; diamond-like carbon; penjerapan protein.

Universiti Malaya

ACKNOWLEDGEMENTS

I am indebted to everyone who helped me throughout my research work to make this work successful. Foremost, I sincerely appreciate my supervisor Dr. Shahira Liza for her instruction of the research and support of the personal development. Her advice is not only valuable for my graduate study but also beneficial for my future. Moreover, I express my deepest thanks to my supervisor, Dr. Nurin Wahidah for her consistent trust and support. I am grateful to Dr. Hiroki Akasaka from Tokyo institute of technology for technical support in DLC deposition. I am thankful to Division of Joint Reconstruction, Department of Orthopaedic Surgery, University Malaya Medical Centre for sample contribution and consultation. I am also thankful to Surface lab of Faculty engineering, UM for the equipment. I am also grateful to Triprem Centre, MJIIT, UTM for the equipment used for analyze data. I would like to thank Miss Khadijah for the help in failure analysis study. I am also thankful to Miss Nur Hidayah and Miss Shazwani for the help in experiment procedure and analysis. I also acknowledge the financial support provided by University of Malaya through research grant No. BK070-2015 and Universiti Teknologi Malaysia through Tier2 research grant No. Q.K130000.2643.15J17. Finally, I want to give my special thanks to my family for their unceasing support.

Universiti Malaya

TABLE OF CONTENT

Universiti Malaya

Universiti Malaya

Universiti Malaya

Universiti Malaya

Universiti Malaya

LIST OF FIGURES

University of Malaya

Universiti Malaya

LIST OF TABLES

Universiti Malaya

LIST OF SYMBOLS AND ABBREVIATIONS

a-C	:	Amorphous carbon
a-C:H	:	Hydrogenated amorphous carbon
ATR-FTIR	:	Attenuated total reflection-Fourier transform infra-red
BS	:	Bovine serum
BSA	:	Bovine serum albumin
CVD	:	Chemical vapor deposition
DLC	:	Diamond-like Carbon
DSC	:	Differential scanning calorimeter
FCVA	:	Filtered cathodic vacuum arc
GPC	:	Gel permeation chromatography
LST	:	Laser surface texturing
PJI	:	Periprosthetic joint infection
PVD	:	Physical vapor deposition
SEM	:	Scanning electron microscopy
SS 304	:	Stainless steel 304
ta-C	:	Tetrahedral amorphous carbon
THR	:	Total hip replacement
Ti6Al4V	:	Titanium alloy grade 5
TJR	:	Total joint replacement
TKR	:	Total knee replacement
UHMWPE	:	Ultra-high molecular weight polyethylene

Universiti Malaya

LIST OF APPENDICES

Universiti Malaya

CHAPTER 1: INTRODUCTION

1.1 Overview

In this study, failure analysis of the tibial insert from an early-retrieved TKR implants will first be studied in order to identify the failure mode of the early-retrieved UHMWPE tibial inserts and further revealed the damage mechanism on the UHMWPE tibial insert. Later, different surface modification (surface coating and surface texturing) was done on the metal (Ti6Al4V and SS 304) surface in order to modify the original characteristics of the metal surface and to characterize the effect of different surface modification toward the reduction of UHMWPE wear. The surface modification will be done on the metal part (Ti6Al4V and SS 304) and tribological performance of both metal and UHMWPE part will be evaluated under lubrication condition using bovine serum (BS) and bovine serum albumin (BSA) in order to evaluate the role of synovial fluid toward the modified surface. The study was then continuing by focusing on DLC coating (a-C:H and ta-C) on metal surface (Ti6AL4V). The surface energy, protein adsorption and wear rate of the samples was being done in order to characterize the surface properties and wear behavior a-C:H and ta-C films under protein lubricated conditions. Lastly, hydrogenated DLC coating (a-C:H) deposited using difference hydrocarbon source was being study in order to characterize surface properties of wear and friction behavior of a-C:H films with difference hydrocarbon source.

1.2 Problem Statement

There are many factors to be considered for improving performance of implant due to the severe environment at in-vivo condition. UHMWPE wear and damage are one of the factors that often lead to the failure of implants, in which the surface energy of UHMWPE is believed to have played an important role. Knee implants were commonly manufactured by metal and UHMWPE, where metal was hydrophilic and UHMWPE was

Universiti Malaya

hydrophobic. Surface with low surface energy (hydrophobic) is believed to have high adsorption of protein due to hydrophobic interactions of protein, while hydrophilic surface will less likely to attract protein. When the protein interacts with hydrophobic surface, the protein will unfold and attached on the hydrophobic surface in order to reduce the interaction with the aqueous solution. Later, peptide bond of the protein that attached on the surface will break under several conditions (temperature, ionic strength) and cause protein denaturation. The denatured protein will become gel-like protein aggregate on the hydrophobic surface which increase roughness of the surface and further lead to high wear toward the surface when contact with hydrophilic surface. However, when two hydrophobic surfaces with protein aggregates interact with each other, the protein aggregate on both surfaces will bound with each other to form a thin protein which will protect surfaces from wear.

The role of protein (especially protein albumin) with different surface energy on wear mechanism still remains unclear and not been fully characterized. This study aims to study the tribological properties of metals (Ti6Al4V and stainless steel 304) and UHMWPE with the addition of surface modifications (surface coating and surface texturing) on metal surfaces under protein lubrication (bovine serum, 20mg/ml and bovine serum albumin, 20mg/ml) condition. The metal surface will be modified into the hydrophobic surface to evaluate the tribological behavior between hydrophobic metal surface and hydrophobic UHMWPE surface. The wear mechanism of modified (coating and texturing) metal surface under the influence of protein with effect of surface energy will be evaluated in this study.

Universiti Malaya

1.3 Objectives

The main objective of this study was to modify metal surface into hydrophobic surface in order to improved UHMWPE wear. The sub-objective of this study was;

1. To examine damage mode and wear mechanism of UHMWPE tibial insert of total knee replacement (TKR) in early stage implantation of bilateral total knee arthroplasty.
2. To characterize the surface properties and wear behavior of non-hydrogenated and hydrogenated diamond like carbon (DLC) coatings under protein lubricated condition.
3. To evaluate the surface properties of wear and friction behavior of hydrogenated DLC with different hydrogen source under protein lubricated condition.

1.4 Scopes of Research

The scope of the project is to focus on the study of two type surface modifications (texturing with LST method and DLC coating) to enhance metals which used in manufacture orthopedic implants such as knee replacement. The surface modifications will be focused on improving the wear resistance of the UHMWPE under influence of protein lubricated condition (bovine serum and bovine serum albumin). The scope of this research was as below.

- The early-retrieved TKR implant (less than 1 year) was failed due to infection but wear analysis must be done in order to understand the mechanism that will initiate the formation of wear damage on long term implants, which able to contribute on improving surface properties and longevity of implants in the future.
- The metals used for this study will be titanium grade 5 alloy (Ti6Al4V) and stainless steel 304.

Universiti Malaya

- The polymer counterpart used in this study is ultra-high molecular weight polyethylene (UHMWPE) which was sterilized by exposed directly to nominal doses of gamma radiation at 25 kGy.
- The tribological wear test was tested under slow walking speed of 0.1 ms^{-1}, since the orthopedic patient can only be able to walk under low speed.

Universiti Malaya

CHAPTER 2: LITERATURE REVIEW

This chapter will discuss about all the literature review that related to this study. In this chapter, the latest finding for biomaterials, surface modification, surface texturing, diamond like carbon (DLC) will be discussed.

2.1 Biomaterials for orthopedics application

The first-generation biomaterials used for manufacture orthopedic implants are the common materials for industry (alumina, zirconia, stainless steel, cobalt–chrome-based alloys, titanium alloys, silicone rubber and acrylic resins) used which have the ability to resist corrosion under harsh condition (Navarro, M.et al., 2008). According to Hench, L. L. & Polak, J. M., evolution of biomaterials can be divided into three generations which the first generation is bioinert materials and second generation is bioactive and biodegradable materials (bioactive glass, glass–ceramics, calcium phosphate, polyglycolide and polylactide), while the third generation use materials that are bioactive and bioresorbable that designed for activate genes that stimulate regeneration of living tissue (2002).

2.1.1 Metal

Materials such as titanium alloy (Ti6Al4V), Stainless steel 316, Stainless Steel 304 and cobalt chromium molybdenum alloy (CoCrMo) are some of the commonly used metal in biomedical application (Elahinia, M., et al.,2019; Kovačević, N., 2012). These materials are used for orthopedic implants due to its high corrosion resistance, wear resistance, high hardness (Eliaz, N., 2019). The bearing components of orthopedic implants is as shown in Figure 2.1, while the mechanical properties of metal used for implants is recorded in Table 2.1.

Universiti Malaya

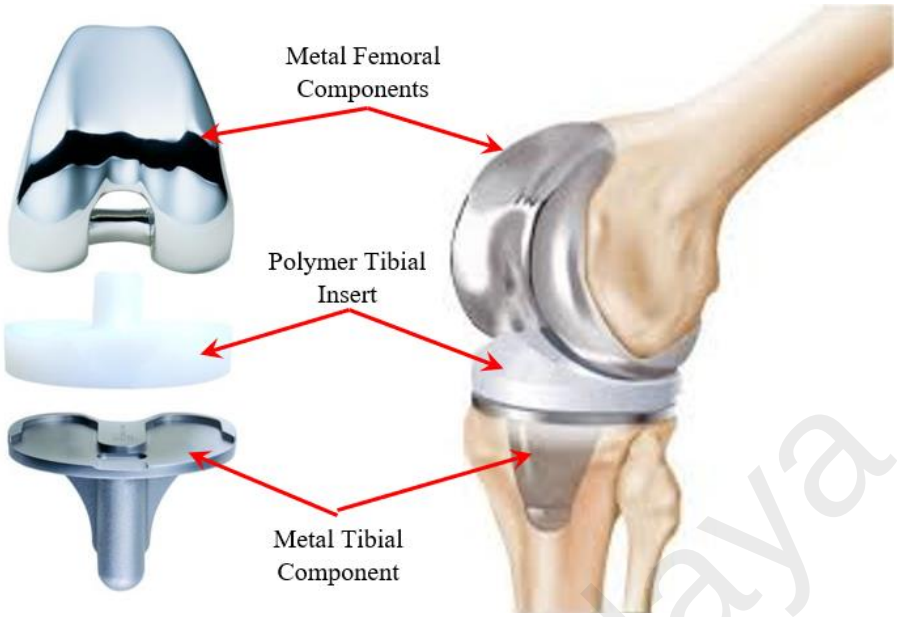

(a)

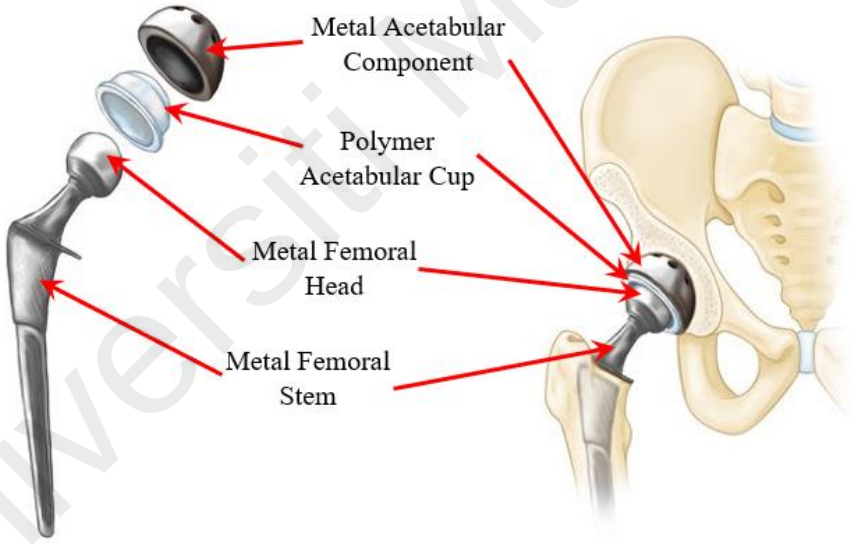

(b)

Figure 2.1 Bearing component of (a) Knee Implant; (b) Hip Implant (May, S., 2014; Sullivan, T., 2010)

Universiti Malaya

Table 2.1 Mechanical Properties of Metal Used for Implants (obtained from: Materials Properties Handbook)

	Density [Mg/m^{3}]	Hardness [MPa]	Tensile Strength [MPa]	Modulus of Elasticity [GPa]	Poisson's Ratio
Ti6Al4V	4.512	3730	1200	119	0.37
SS 316L	8	705	485	193	
CoCrMo	8.4	1190	1280	250	0.29

2.1.1.1 Titanium alloy

The high strength, low weight, excellent corrosion resistance properties has made titanium alloy (Ti6Al4V) have successful application in surgery and medicine which demand high levels of reliable performance (Manmeet, K. & Singh, K., 2019). Corrosion caused by body fluids on the implanted metal will resulted the releasing of ions (Cr, Ni, Co, Al, V and Ti) which will then lead to several diseases (endocrine, hepatocellular necrosis, Parkinson's disease, skin cancer, etc) (Demehri, S. et al., 2014; Sansone, V. et al., 2013). Hence, the corrosion resistance is essential characteristic to be used for implanted metal. Furthermore, titanium alloy also possesses the ability to tightly integrate into the bone, which able to improve the long-term behavior of the implanted devices, and further decrease the risks of loosening and failure (Manmeet, K. & Singh, K., 2019; Nasab, M. B. et. al., 2010). However, the long-term performance of titanium alloy, especially Ti6Al4V, has raised some concerns due to the releasing of aluminum and vanadium, since both Al and V ions are associated with long-term health problems, like Alzheimer disease and neuropathy (Sansone, V. et al., 2013; Yokel R. A., 2000). Moreover, titanium alloy has the high friction coefficient and rather high tendency to seizure, which lead to wear and damage of the alloy have caused its application is limited

Universiti Malaya

to the locations on the implant surface where wear resistance is not of vital importance (Nag, S., et al., 2009; Rack, H.J. & Qazi, J.I., 2006). Hence, several surface treatment methods, such as ion implantation, titanium nitride (TiN) coating, and thermal oxidation, have been proposed to improve the wear resistance by altering the nature of the surface (Budzynski, P. et al., 2006; Shenhar, A., et al., 1999).

2.1.1.2 Cobalt-chromium alloy

Cobalt chromium alloys are generally categorized into two types, which is Co-Cr-Mo alloy (which is usually used to cast a product) and Co-Ni-Cr-Mo alloy (which is usually wrought by hot forging). Co-Cr-Mo alloy has been widely used in dentistry for a long time and have recently used in making artificial joints, while Co-Ni-Cr-Mo alloy is a new material which is used for making the stems of heavily loaded joints such as the knee and hip (Alvarado, J., et al., 2003). Cobalt-chromium alloys have high corrosion resistant even in extreme environment due to the spontaneous formation of passive oxide layer within the human body environment (Navarro, M., et al., 2008; Oztürk, O. et al., 2006; Vidal, C.V. & Muñoz, A.I., 2008). Moreover, cobalt-chromium alloys also have excellent mechanical properties (high fatigue resistance, high crack resistance and excellent wear resistance) and great elongation properties due to high elastic modulus (220–230 GPa) (Alvarado, J., et al., 2003; Ramsden, J.J. et al., 2007). However, element such as Cr and Co that release from the cobalt chromium alloys due to corrosion in the human body is found to be toxic towards the human body. The corrosion products of Co-Cr-Mo are more toxic than those of stainless steel 316L. The thermal treatments used to Co-Cr-Mo alloys modifies the microstructure of the alloy and alters the electrochemical and mechanical properties of the biomaterial (Vidal, C.V. & Muñoz, A.I., 2008).

Universiti Malaya

2.1.1.3 Stainless steel

Stainless steel is the general name for a variety of steels with high Cr contents used due to their high resistance toward corrosion. The Cr elements in stainless steel have a great affinity for oxygen, which allows the formation of chromium oxide film on the surface of steel at a molecular level which is passive, adhesive, tenacious and self-healing (Alvarado, J., et al., 2003; Navarro, M., et al., 2008). In spite, stainless steel implants are often degraded due to pitting, corrosion fatigue, fretting corrosion, stress corrosion cracking, and galvanic corrosion in the body (Singh, R. & Dahotre, N.B., 2007). The wear resistance of austenitic stainless steel is relatively poor; hence, loosening failure is often occurred due to the generate of wear debris. Stainless steel has been used for a wide range of application due to easy availability, lower cost, excellent fabrication properties, accepted biocompatibility and great strength. Stainless steel has various types and the most used stainless steel for manufacturing implants are austenitic stainless steel. Stainless steel 316L is widely used in traumatological temporary devices such as fracture plates, screws and hip nails. Stainless steel 304 was widely used for medical applications due to its high corrosion resistance and low carbon content, which assured stainless steel 304 will not chemically react with body fluids, tissue and sterilize products (Azom, 2012).

2.1.2 Polymer

The first-generation polymers used for implants are mainly polyethylene (PE), polypropylene (PP) and polymethylmethacrylate (PMMA), which later evolve into resorbable biomaterials such as polylactide (PLA), polyglycolide (PGA), polydioxanone (PDS) in second generations (Elahinia, M., et al.,2019).

Universiti Malaya

Figure 2.2 Orthopedics UHMWPE Liner (Ansari, F. et al., 2013)

2.1.2.1 UHMWPE

Ultra-high molecular weight polyethylene (UHMWPE) is commonly used is application of biomedical especially as one of the leading components of orthopedic implant. UHMWPE is widely used is biomedical field due to high wear resistance, self-lubrication ability, and excellent chemical inertness (Elahinia, M., et al.,2019; Suh, N.P., Mosleh M. & Arinez J.,1998). UHMWPE is used as the materials for the bearing part of knee implants (eg.: tibial insert) due to its high wear resistance, self-lubrication ability, and excellent chemical inertness (Jun, F., 2019; Suh, N.P. et al., 1998). However, UHMWPE will undergo oxidation degradation over time due to factors such as gamma sterilization. The energy produced during sterilization process will interrupt C-bonds in the UHMWPE and generates free radicals. The free radicals will then react in three ways (recombination, oxidative Chain Scission and cross-linking) (Musib, M. K. et al., 2011). Chain scission will cause the reduction of molecular weight of UHMWPE, in which caused mechanical degradation (Besong, A.A. et al., 1998; Kurtz S. M. et al., 1999; Kurtz S. M. et al., 2003; McKellop, H, et al., 2000). Mechanical degradation of UHMWPE will cause it more

vulnerable to undergo delamination, molecular weight reduction, fatigue deformation, fracture and abrasive wear (Kurtz S. M. et al., 2000; McKellop, H. A., 2007). Various methods such as cross-linking, vitamin E have been used to prevent the oxidative degradation of UHMWPE (Oral, E. et al., 2007; Oral, E & Muratoglu, O. K., 2011).

2.1.2.2 Cross-linked polymer

The cross-linked polymers are polymer that its molecular chains links one polymer chain to another polymer chain, which cross-linked polymers are polymers that obtained when cross-link bond formed between monomeric units (Zweifel, H. et al., 2009). Cross-linked polymer will form long chains (branched or linear) from the covalent bonds between the polymer molecules, since covalent bonds of the cross-linked polymers are much stronger than the intermolecular forces and resulting a stronger and more stable material. Cross-linked polymer can be manufactured by induced the materials that are normally thermoplastic through exposure to a radiation source, such as electron beam exposure, gamma-radiation, or UV light. Cross-linked polymer has great properties such as stable in mechanical and thermal properties. Cross-linked polymers are thermosetting, which caused it harder to melt or dissolved. However, cross-linked polymer is hard to be manufactured, since, cross-linked polymer is relatively inflexible when it comes to processing properties because cross-linked polymer is insoluble and infusible. The examples of cross-linked polymer are as shown in Figure 2.3.

Universiti Malaya

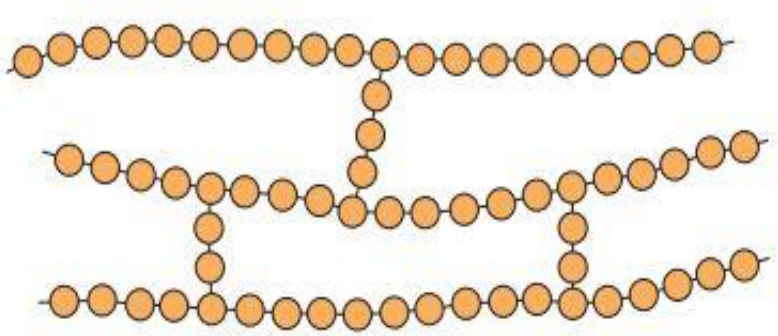

Figure 2.3 Cross-linked polymer

2.1.2.3 Vitamin E blending polymer

Vitamin E (VE) is an effective biological antioxidant, that helps to prevent the oxidative degradation of cell membrane phospholipids. When added to UHMWPE, VE performs a similar role by helping to prevent oxidation of the polyethylene chains (Brigelius-Flohé, R. & Traber, M. G., 1999; Costa, L. et al., 1998; Wang, X. & Quinn, P. J., 2000). VE can be incorporated into the polymer by two methods; blend VE with UHMWPE powder before consolidation (Oral, E. et al., 2005) and diffusion of VE into UHMWPE after radiation cross-linking (Oral, E. et al., 2007).

2.1.3 Failure of implants

Orthopedic surgery or total joint replacement (TJR) can generally be categorized into total knee replacement (TKR) and total hip replacement (THR). TJR has been found to be able to relieve pain due to osteoarthritis and it is effective in improving function and restore the quality of life in patients. In the United States, estimated 4.7 million patients have undergone TKR and 2.5 million have undergone THR. Generally, TKR component consists of three main components: the metal femoral component, metal tibial component, and the joint liner which is made of a polymer (UHMWPE). While THR components consist of four main components: the metal acetabular component, a polymer acetabular cup, metal femoral head and metal femoral stem.

Universiti Malaya

Over time, however, a joint replacement may fail for a variety of reasons and needed a second surgery which called revision TJR. Joints implant can usually last long for 10 - 15 years, depend on the condition of the patients, such as age, weight, gender, activity level (Laska, A. et. al., 2016; Zanasi, S., 2011). UHMWPE damage and wear have is considered a treat to the long-term survival of TKR. Failure occurs most commonly in form of fatigue and adhesive wear that generates submicrometric particulate debris which cause osteolysis around the implant components ultimately leading to loosening and failure of the TJR (Choudhury, D., et al., 2018; Laska, A. et. al., 2016; Lum, Z. C. et al., 2018; Postler, A. et al., 2018; Yan, Y. et al., 2014). In previous failure analysis, the TJR failed within 5 years of the index operation is categorized as an early failure (Fehring, T. K. et al., 2001). Fehring et al. claimed that the reasons for early failure were infection (38%), instability (27%), failure of ingrowth of a porous-coated implant (13%), patellofemoral problems (8%), and wear or osteolysis. (7%) (2001). Infection was found to be the predominant mode of failure to early failure mechanisms of TKR. However, infection can be difficult to diagnose and required multiple approaches to find the cause of failure. Furthermore, bone stiffness another common factors for early failure of knee implants (Dudhniwala, A. G. et al., 2016; Thomas, K. F. et al., 2001). Bone stiffness will influence the implant as the stress distribution will more homogeneous for low-stiffness bone surface (Simon, U. et al., 2003). McTighe, T. stated that early failure due to implant instability are mostly due to misalignment during the surgery (2009).

Although the aseptic loosening, fracture and malalignment is less likely to occur in early failure, but it still has probability to fail due to loosening, fracture and malalignment (Postler, A. et al., 2018). Postler, A. study stated that periprosthetic joint infection (PJI) was the most common reason for early failure factors of TKR, while aseptic loosening and fracture is the least common reason for failure (2018). Infection can occur any time

Universiti Malaya

after surgery with a sign of swelling or redness. Since joint implant is an artificial joint that made by non-organic materials (metal and UHMWPE), therefore, it is harder for body to kill bacteria on them. Thomas, K. F., study stated that third body particle is one of the reasons that caused infection failure in early failure (2001). Third body particle such as foreign metal and UHMWPE debris will causes pit wear damage and scratches on the surface of the implant (Thomas, K. F. et al., 2001).

The UHMWPE tibial component that peel off at the implant-cement interface was the primary factor that caused tibial aseptic loosening, moreover, the un-keeled knee implant has higher chance to undergoes aseptic loosening compare to keeled knee implant (Kutzner, I. et al., 2017). The small UHMWPE debris particles mainly formed due to the formation of scratch, while the large debris particles were produced by fatigue due to the formation of delamination (Hirakawa, K. et al., 1999). During the articulation motion of the implants, the third body particle or UHMWPE debris were being pushed along the surface or being indented into the surface causing wear while forming more debris, which then lead to the occurrence of loosening failure. Arsoy, D. et al. study has found that 25 cases (1.9%) out of 1337 cases of early-retrieved knee implant failure (with a median duration of 39 months) is due to loosening (2012). Furthermore, Lee, B. S. et al. stated that the malalignment of the femoral component is one of the primary factors for the occurrence of aseptic loosening (2018). The factor that causes loosening in early-retrieved failure include frontal misalignment, sagittal overstuffing or mal-positioning, axial malrotation, poor bone fixation, inappropriate constraint or ligamentous balance, and inappropriate level of the joint space (Rousseau, M. A. et al., 2006). Other than that, the human body will attack the UHMWPE debris that formed during the articulation motion, which at the same time attacks the bone cells causing bone loss that induced osteolysis (Abu-Amer, Y. et al., 2007).

Universiti Malaya

2.1.4 Wear of biomaterials

One of the factors that caused implants to fail was due to wear. The wear debris that formed will induce osteolysis which then therefore caused loosening failure. Wear can be affected by many factors such as loading, materials, lubricant and surrounding environment (Shoji, H. et al., 1976). The wear of implant is mainly caused by the friction occurs during the articulation motion of the implant. The friction that occurs during articulation between the parts of the orthopedic implants will caused the temperature to increase in the implants, which the rise in temperature will the affect the wear resistance, fatigue rate and oxidation degradation of the implant and therefore forming the debris (Stanczyk, M. & Telega, J. J., 2002; Liao, Y. S. et al., 2003). The polymer debris that form will then cause the implant to loosen and failed. The formation of polymer debris is said to be mainly related to the mechanical properties of the contacting bodies, counter face roughness, lubricant composition, and loading configuration (Fisher, J. et al.,2009). The polymer particles generated during the articulation are the most common inducer of osteolysis, which will then cause the implant to loosen and eventually against failure of the implant (Ulrich-Vinther, M. et al., 2002). The metal debris and ion from the biomedical tools and implant will cause inflammation to the body tissues (Zhang, T. F. et al., 2015).

According to the previous analysis study, the common wear features to be found on retrieved tibial inserts were pitting, scratching and delamination (Collier, J. P. et al., 1996; Crowninshield R. D., et al., 2008l; Diabb, J. et. al., 2009; Garcia, R. M. et al., 2009; Hood, R. W. et al., 1983; Liza, S., et al., 2011). Hood, R. W. et al. have classified surface damages on the articulating surface of retrieved tibial inserts into seven wear damages modes, which are scratching, burnishing, embedded particulate debris, abrasion, permanent deformation, and surface delamination (1983). While Haman. J. D. et al. indicated that mechanism fatigue was the most common wear mechanism found on

Universiti Malaya

retrieved tibial inserts, in which wear appearance formed due to fatigue were pitting and delamination (2005). Figure 2.4 shows the worn polymer part of orthopedic implants due to mechanical degradation.

Figure 2.4 Worn surface of (a) UHMWPE tibial insert from TKA and (b) UHMWPE acetabular liner from THA (Musib, M. K. et al., 2011; Jonathan Miles FRCS Orth.)

2.1.4.1 Effect of Lubrication on wear

Lubricant is a layer that can be added between two sliding surfaces in order to reduce wear and friction and can form low-shear-strength layer between sliding surfaces. Lubrication regime can be categorized into three conditions as shown in Figure 2.5. Boundary lubrication occurred at high normal load and low speed; the load applied is carried entirely by asperity contact. Mixed lubrication lies somewhere in between boundary lubrication and fluid-film lubrication, the load applied is shared between the asperity contacts and the pressure generated in the fluid-film. Fluid-film

Universiti Malaya

lubrication has no contact between sliding surface and the load applied is entirely supported by the fluid.

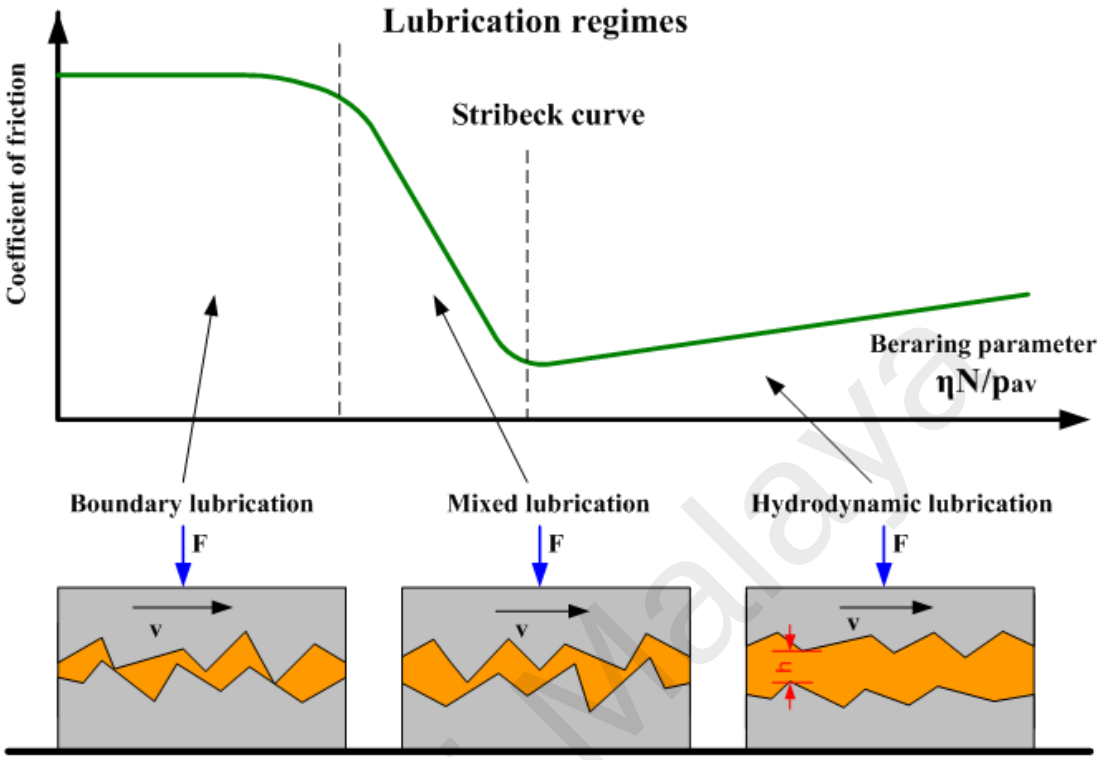

Figure 2.5 Stribeck Curve (Robinson, W. J. et al., 2016)

Boundary lubrication conditions will form a molecular film on the sliding surfaces, by either through absorption process or by the reaction with the contact surface. Generally, the formation of the protective film can be formed under two conditions which is static condition and rolling conditions. During static conditions, the protective film will form through absorption process. While under rolling conditions, protective film will form through protein aggregation under shear and load. Protein aggregation lubrication (PAL) will occur in protein solutions under low speeds, where the increased of protein concentrations occurs in the inlet of the contact surface and the proteins trapped in the inlet will form large aggregates which are attracted into the contact area, which the parting the contact surfaces.

Universiti Malaya

DLC coated artificial knee joint has been done previously and the results were disappointing. The main failure factor is mainly due to aseptic loosening, where the DLC coating delaminated and induced osteolysis (Taeger, G. et al., 2003) Furthermore, the body fluids (such as synovial fluid) able to reach below the coating through the cracks of the surface coating that were formed by several factors such as friction, imperfect coatings, etc (Hauert, R. et al., 2012). Therefore, DLC coated artificial knee joint must also consider the effect of synovial fluids on the behavior of coating. Synovial fluids are the natural lubricant in human body and it contained composition such as albumin protein, globulin protein, hyaluronic acid (HA) and lubricin. Each composition in synovial fluids plays an important role in protecting the knee joints (Ghosh, S. et al., 2014). Synovial fluids are produced by the synovial membrane and cartilage from human joints. After implant surgery, synovial membrane will eventually reform, and later produced a liquid similar to synovial fluid (pseudo synovial fluid) that lubricated the newly implanted device (Roba, M., 2009). The synovial fluid in normal joint will fills the synovial space and provide excellent lubricating properties with the presence of articular cartilage and the lubrication condition are mostly depending on normal load and sliding velocity conditions. While knee implants are mainly lubricated in the boundary and mixed regimes and exhibit much poorer tribological properties (Flannery, M. et al., 2008).

Universiti Malaya

Table 2.2 Biochemical composition of normal synovial fluids and bovine serum (Aurora, A. et al., 2006)

Component	Normal synovial fluid (g/l)	Bovine serum (g/l)	Synovial/serum ratio
Protein (total)	18	70.0	0.26
Albumin	11.3	34.3	0.33
α_1-globulin	1.26	4.2	0.3
α_2-globulin	1.26	8.4	0.15
β-globulin	1.62	11.9	0.14
γ-globulin	3.06	11.2	0.27
Lipid	2.4	7.0	0.34
Phospholipids	0.8	2.0	0.40
Glucose	0.66	0.91	0.73
Hyaluronate (HA)	2–4	4.2×10^{-5}	$\sim 7 \times 10^{4}$

2.1.4.2 Protein

Protein is generally composed by multiple amount of amino acids (a compound made of C, O, N, H) and was linked together by peptide bond. The chemical structure of protein was as shown in Figure 2.6. Protein will naturally fold together in order to perform their biological function by maintaining protein stability and active. Since the physiological environment in the human body are in aqueous state, the non-polar (hydrophobic) side chains of protein will react with each other and caused the protein folding to avoid interaction with the aqueous environment (Pace, C. N. et al., 1996). However, when a protein contacts with hydrophobic surface, protein will tend to attach onto the hydrophobic surface in order to prevent interaction with the aqueous environment. The hydrophobic moieties inside the protein will form weak hydrophobic interactions with hydrophobic which later cause protein denaturation onto the hydrophobic surface (Zhang, C., Fujii, M., 2015; Nygren, H. et al., 1994). Protein denaturation occurs normally due to bonding interactions responsible for the secondary structure (hydrogen bonds to amides) are disrupted (Heni, B., 2019). There are various factors can cause the protein to denature such as increase of temperature, ionic strength, change of pH, etc (Arakawa, T. et al.,

Universiti Malaya

2001; Heni, B., 2019; Hollar, C. M., 1995). The denatured protein attached to hydrophobic surface will accumulate and piled up on the surface, which induced formation of gel-like protein aggregates that might increase surface roughness and friction (Zhang, C., Fujii, M., 2015; Nygren, H. et al., 1994). Unlike hydrophobic surface, protein will less like to attach to the hydrophilic surface to form protein aggregates. Hence, when hydrophobic and hydrophilic surface contact, the protein aggregates on the hydrophobic surface will cause high wear and damage on the surfaces (Heni, B., 2019). However, when two hydrophobic surfaces with protein aggregates interact with each other, the protein aggregate on both surfaces will bound with each other to form a thin protein which will protect surfaces from wear (Escudeiro, A., 2014). The mechanism of protein aggregates on hydrophobic and hydrophilic surface is as shown in Figure 2.7.

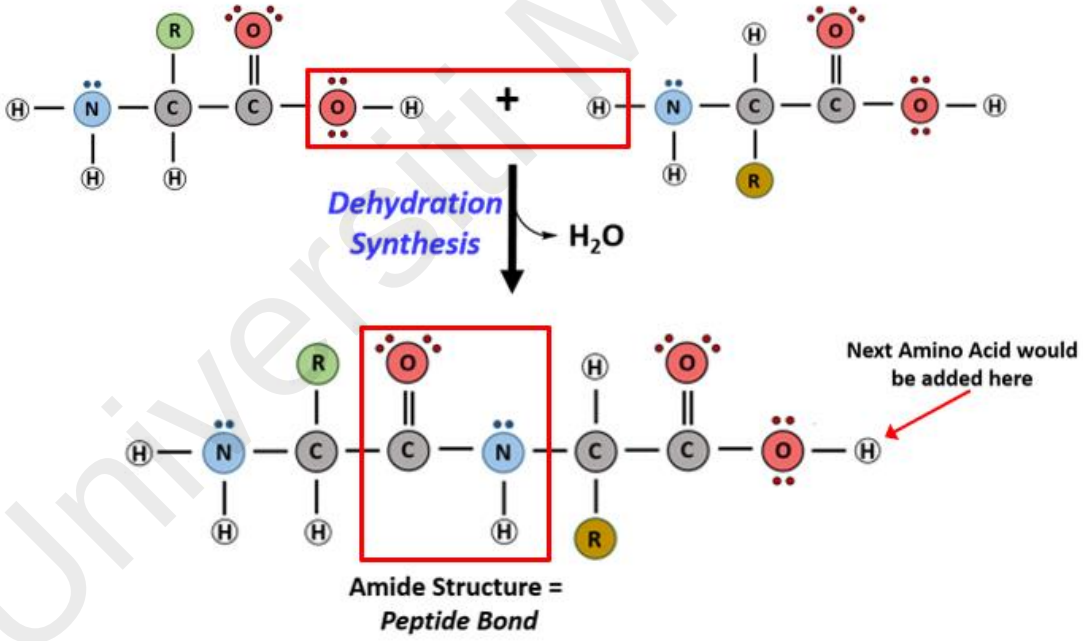

Figure 2.6 Chemical structure of protein

Universiti Malaya

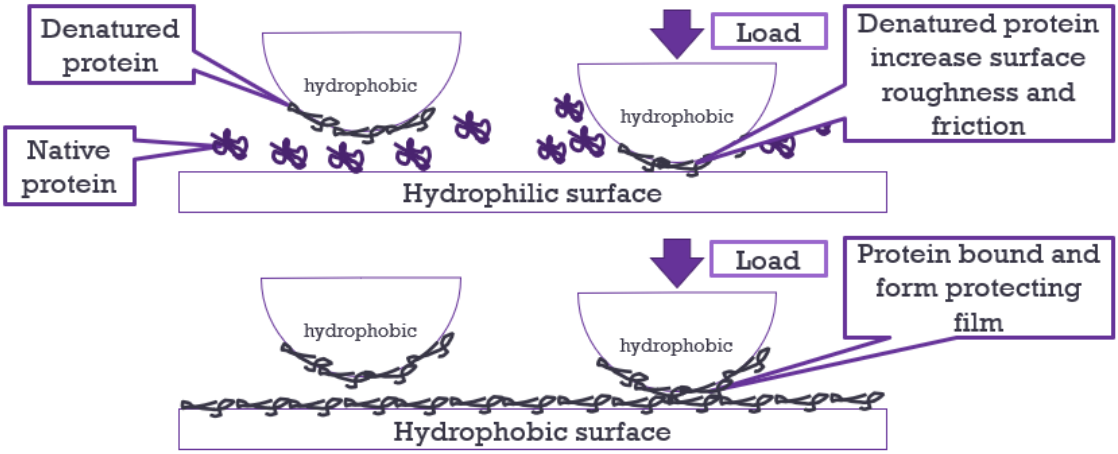

Figure 2.7 Mechanism of protein aggregate on surface (Escudeiro, A., 2014)

2.2 Surface Modification

Surface modification of the material is said to be able to modify the surface of the material in order to improve its tribological performance by not affect the mechanical properties of the materials (Ding, Q. et al., 2010). Material surface can be modified by altering the surface roughness, hydrophilic properties, biocompatibility, etc. Surface modification can be applied in many fields such as electronic, chemical, machine tools, biomedical, etc. Surface modifications have always been used to improve tribological performance of materials by improving wear resistance in many studies (Monsees, T. K. et al., 2017; Capellato, P. et al., 2013; Wang, G. C. et al., 2011). There are many surface modifications techniques that are commonly used to modify the surface of the materials such as ion implantation, coatings and surface texturing (Rautray, T. R. et al., 2009).

2.3 Surface Coatings for Biomaterials

Surface coating is added in order to protect surface of material by increase the performance and lifespan of the biomedical tools. According to Demas N.G. et al. coating of a material can enhance the properties of the material by reducing friction and increase hardness of the material (2016). Surface coating is used to improve the tribological behavior of a material. However, coatings for orthopedics implants must have properties

Universiti Malaya

that will not delaminate in biochemical and biomechanical environments, and furthermore coatings for orthopedics implants must have corrosion resistance against biochemical and biomechanical environments. Surface coatings is done on the metal parts since the UHMWPE part is unable to withstand the high temperature that occurs during the coating deposition process.

Tantalum (Ta), graphite- like carbon (GLC), titanium nitride (TiN) and Diamond- like carbon (DLC) was the common coating used in orthopedic application. Ta was used because it has similar structure as the bone structure and was biocompatible (Balla, V. K. et al., 2010; Zardiackas, L. D. et al., 2001). Ta also have good corrosion resistance and was compatible with all metal materials used for implants. GLC was used due to its high hardness and flexibility (Yang, S. et al., 2000). Furthermore, GLC was hydrogen-free and amorphous coating which was biocompatible. TiN have the ability to increase hardness and reduce metal ion release from the metal (Stone, D. S., 1991). TiN also possess excellent performance in reducing wear against UHMWPE (Ching, H. A. et al., 2014). However, TiN has a drawback in the weak adhesion toward the substrate. DLC was a hard coating form of diamond (sp3) and graphite (sp2) bonds, which give DLC the properties of diamond and graphite. The excellent hardness and toughness of DLC has made DLC being commonly used for biomedical implant applications (Ching, H. A. et al., 2014).

2.3.1 Surface Coating Deposition Method

Coatings have been deposited onto biomaterials in order to improve the mechanical and tribological properties of biomaterials. Coatings such as hydroxyapatite (HAP) coatings, glass–ceramic coatings, SBF coatings and DLC coating are commonly used to coat biomaterials (Monsees, T. K. et al., 2017; Capellato, P. et al., 2013; Wang, G. C. et al., 2011). Coatings on biomaterials can be coated by many methods such as plasma-

Universiti Malaya

spraying, electrophoretic deposition, laser deposition, magnetron sputtering, biomimetic deposition, pulsed laser deposition and micro-arc methods (Monsees, T. K. et al., 2017; Wang, G. C. et al., 2011). DLC are often being deposited by using Polymer Vapor Deposition (PVD) machine (Wiklund & Larsson, 2000) or by Chemical Vapor Deposition (CVD) machine (Gottimukkala, 2005; Grill, 1998). Schematic diagram of CVD machine is as shown in Figure 2.8 and PVD machine is as shown in Figure 2.9.

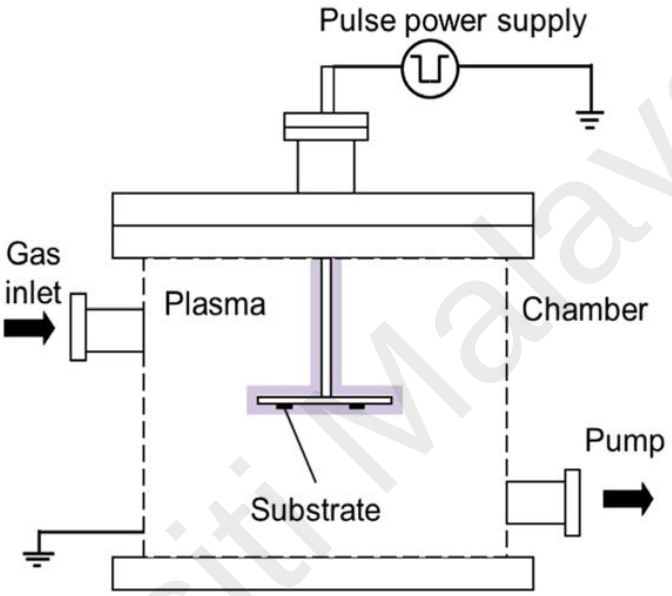

Figure 2.8 Schematic Diagram of Chemical Vapor Deposition machine (Liza et al., 2016)

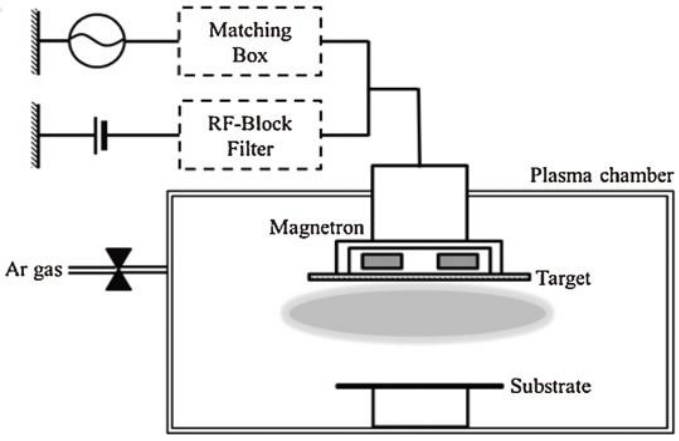

Figure 2.9 Schematic Diagram of both Polymer Vapor Deposition (PVD) machine (Liza et al., 2016)

Universiti Malaya

2.3.1.1 Magnetron Sputtering

Magnetron sputtering method is also known as physical vapor deposition (PVD) method which can be run by PVD machine (Wiklund & Larsson, 2000). Magnetron sputtering method is a type of plasma coating process where an electron is bombarded onto a target in order to sputter the sputtering materials to the specimen to coat a film. Magnetron sputtering method can give excellent layer uniformity and smooth film surface. A carbon target such as graphite will be added in order to deposit DLC on the specimen. Hydrogen free DLC can be deposited by sputtering the carbon target (graphite) in the presence of argon gasses. Discharged will occurs due to the presence of high voltage which will then cause the speed of the electron and the coating process to accelerate. The usage of argon is to help eject the sputtering materials from the carbon target. The schematic diagram of the Magnetron Sputtering process is as shown in Figure 2.10. The parameter that varied during the deposition using magnetron sputtering method mainly are the voltage and the pressure while the other parameter such as time of deposition, flow rate of gas is often being fixed.

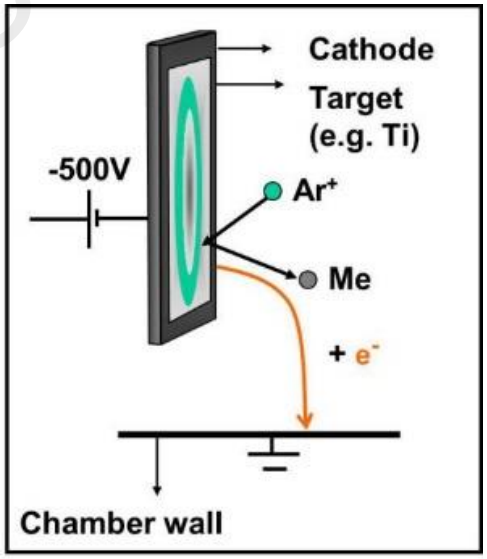

Figure 2.10 Schematic Diagram of Magnetron Sputtering Method (Wiklund & Larsson, 2000)

Universiti Malaya

2.3.1.2 Chemical Vapor Deposition (CVD)

Chemical vapor deposition (CVD) method is a chemical process used for coating process where volatile gas is used to react and form a coating onto the specimen. CVD method is useful in process of atomic layer deposition which allows CVD to produce a thin layer onto specimens. By using methane gas (C_2H_4) as reactive gas, hydrogenated DLC will be able to produce under low pressure condition. Voltage and temperature of the CVD system will increase the speed of the reaction of gas and also enhance the adhesion of the coating towards the specimens. Figure 2.11 shows the schematic diagram of CVD process and Figure 2.12 shows the differences between CVD system and PVD system.

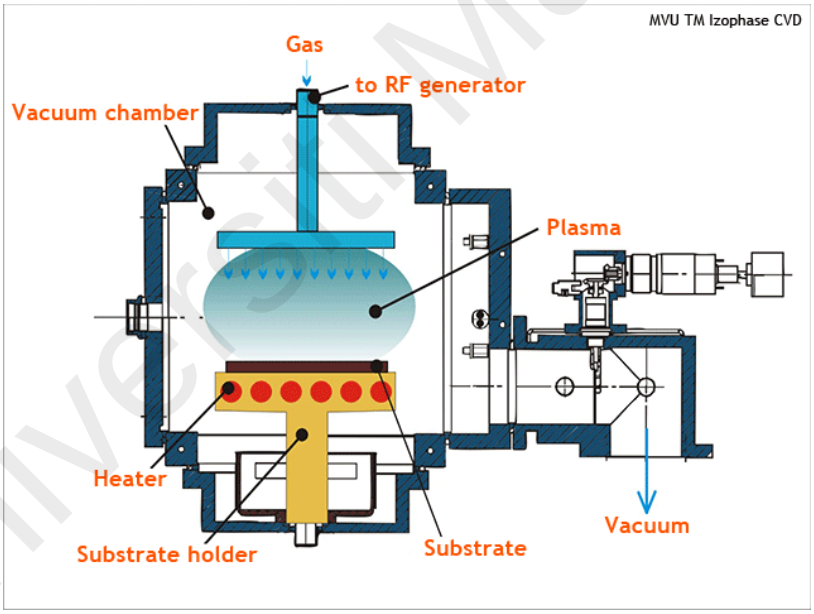

Figure 2.11 Schematic Diagram of CVD Process (obtained from: MVU TM Izophase)

University Malaya

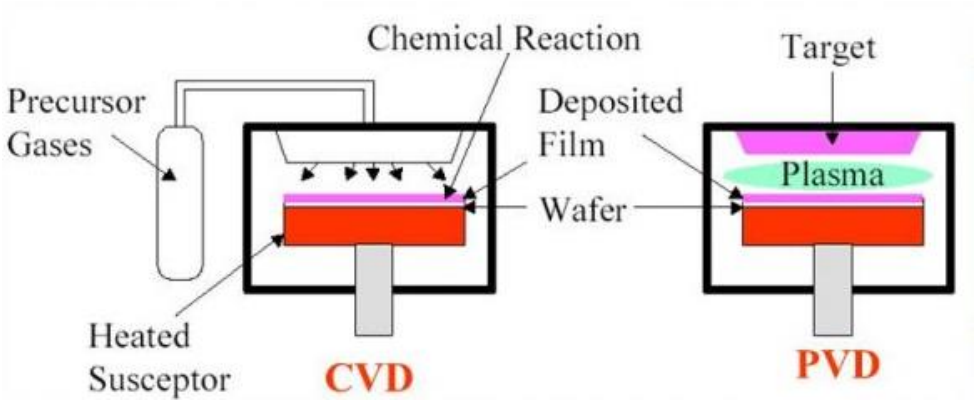

Figure 2.12 Difference Between CVD system and PVD system (The Digital Terror, 2016)

2.3.1.3 Filtered Cathodic Arc Deposition (FCVA)

Filtered Cathodic Arc Deposition (FCVA) are the typical and best technique used to produce hard tetrahedral amorphous carbon (ta-C) thin films. The apparatus is equipped with a magnetic filtering technique that efficiently removes the macro particles and hence improves the smoothness of DLC film even at the room temperature. Graphite is often used as the cathode source and carbon ions are produced in a vacuum, between the graphite cathode and anode. The sp^3 content in films produced by FCVA are normally high and thus the films exhibit high hardness compared to the films deposited by other techniques. The schematic diagram of FCVA system is as shown in Figure 2.13.

Universiti Malaya

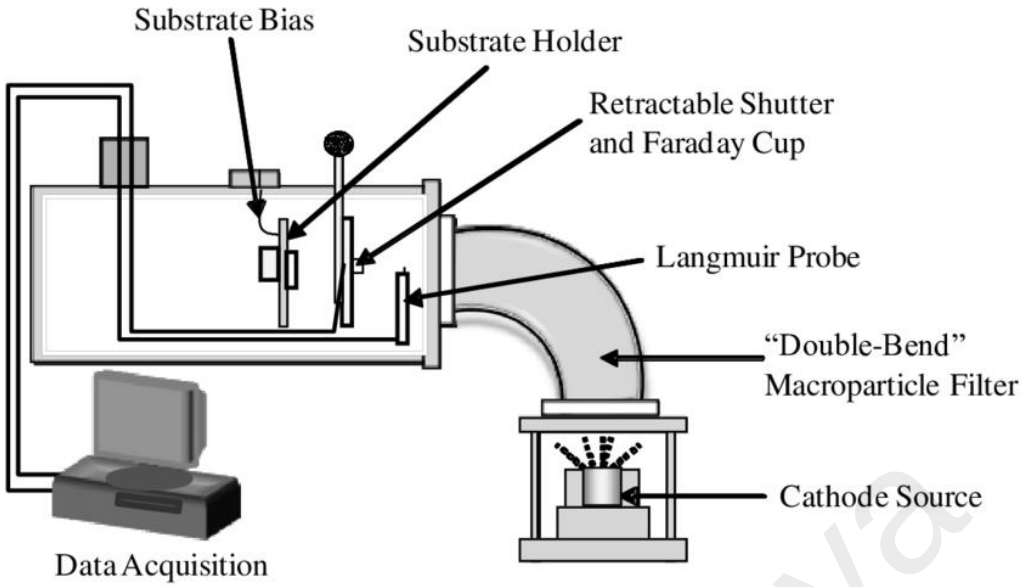

Figure 2.13 Schematic diagram of FCVA system. (Shafiei, M., 2010)

2.3.2 Diamond Like Carbon (DLC)

There are many types of hard coatings have been discovered in order to improve the performance of the tools and equipment (Gupta, 2003; Oohira, 2009). Hard coatings are materials with high hardness in the mechanical and have good tribological properties as defined by Cavaleiro and Hosson (2000). The other types of hard coatings and its properties are as shown in Table 2.3. However, the hard coatings that have been discovered have several limitations which make the application become difficult such as higher deposit temperature, Young Modulus that does not match the substrate and the thermal expansion coefficient that not same with the substrate (Gupta, 2003). Young Modulus that does not match the substrate and the thermal expansion coefficient that not the same with the substrate will cause some internal and thermal stress which will affect the adhesion strength of the coatings towards the substrates. Therefore, DLC is being discovered in order to overcome the limitations that have on other types of hard coatings (Gupta, 2003).

Universiti Malaya

Table 2.3 Properties of Several Hard Coatings (Gupta, 2003)

Coatings	Young's Modulus (GPa)	Poisson's ratio	Thermal Expansion Coefficient	Hardness (kg mm^{-2})	Melting / Decomposition Temperature
TiC	450	0.19	7.4	2900	3067
Cr_3C_2	370	-	10.3	1300	1810
TiN	-	-	9.35	2000	2949
Al_2O_3	400	0.23	9.0	2000	2300
TiB_2	480	-	8.0	3370	2980

DLC is chemical inertness and impermeable to liquids, it can be used as coatings to protect bio-medical tools which will the being used in a human body since DLC is bio-compatible material for orthopedic implants. The bio-medical tools or the metal implant in a human body is necessary to be coated since the wear and corroded implant will generate metal debris and ion which will then cause inflammation to the body tissues (Zhang et al., 2015). Since bio-medical tools will be used inside the human body, bio-compatibility properties are important and lubricated properties is also important in order to reduce the wear rate.

There are many types of DLC coatings due to different methods of deposition, but however Gupta, P. stated that DLC can be classified into 2 groups in general that is DLC which contain carbon only and DLC which contain a mixture of hydrogen and carbon (Gupta, 2003). The DLC which contain carbon only is also named as the amorphous carbon or amorphous diamond while the DLC which contain a mixture of hydrogen and carbon is named as the hydrogenated amorphous carbon. DLC on was first found and being deposited by Aisenberg and Chabot in year 1971, while the hydrogenated DLC coating is found at year 1985 by Kaplan et al. (Grill, 1998). DLC is an amorphous

Universiti Malaya

structure which consists of irregular mixture of sp^2 bonds and sp^3 bonds. The sp^2 bonds is the graphite structure as shown in Figure 2.14(a) while the sp^3 bonds is the diamond structure as shown in Figure 2.14(b) while the structure of DLC is as shown in Figure 2.15 (Oohira, 2009). The composition of DLC which is the ratio of sp^2 bonds to sp^3 bonds in the DLC will affect the coatings and differ the characteristics of the coatings. The composition of the DLC with sp^2, sp^3 and Hydrogen (H) content is shown in Figure 2.16 which adopted from (Robertson, 1993). The differences between hydrogen-free and hydrogenated DLC is recorded in Table 2.4.

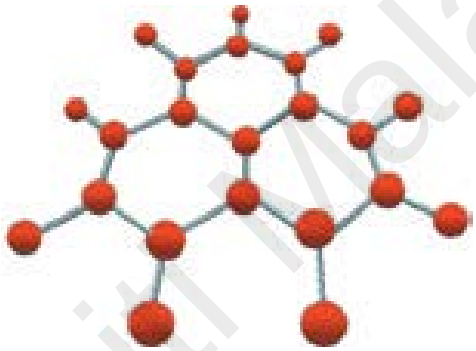

(a)

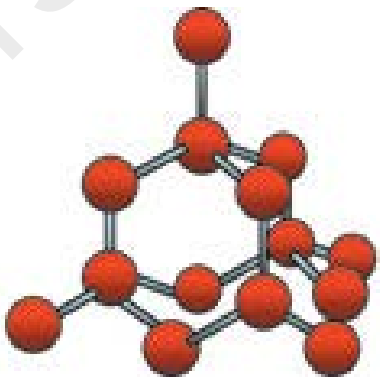

(b)

Figure 2.14 (a) Structure of Graphite (b) Structure of Diamond (Oohira, 2009)

Universiti Malaya

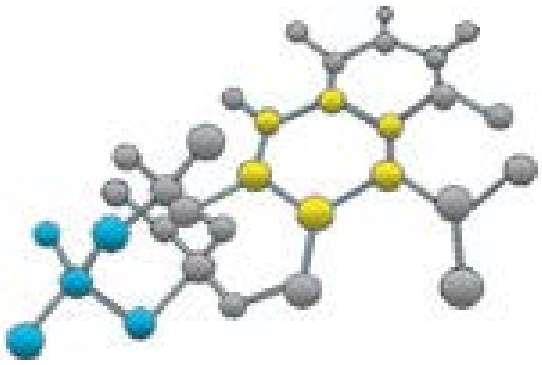

Figure 2.15 Structure of Diamond like Carbon (Oohira, 2009)

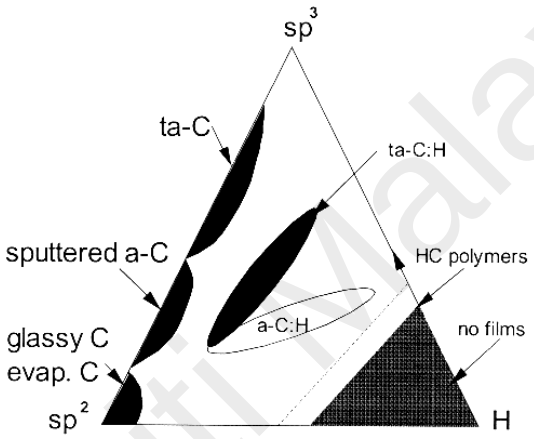

Figure 2.16 Phase diagram showing composition of a-C:H, ta-C and ta-C:H (Robertson, 1993)

Table 2.4 Comparison between hydrogen-free and hydrogenated DLC (Grill, A., 1998)

Hydrogenated DLC (a-C:H)	Hydrogen-free DLC (ta-C)
sp3 fractions smaller than 50%	sp3 fractions more than 85%
softer polymeric network	rigid network
Hardness (10–30 GPa)	Higher hardness (40-80 GPa)
Lower internal stress (0.5–7 GPa)	Internal stress (~13 GPa)

Universiti Malaya

2.3.2.1 Hydrogenated amorphous carbon (a-C:H)

Hydrogenated amorphous carbon (a-C:H) films have varying amounts of sp3, sp2 bonds and hydrogen content, resulting in a wide range of properties of these coatings (Liskiewicz, T. & Al-Borno, A., 2015). The hydrogen in hydrogenated DLC (a-C:H) can help to achieve stability and wide optical band for the hydrogenated DLC. Hydrogenated DLC can improve wear resistance in humid condition according to Park S.J. et al. (2003). The tribological properties of hydrogenated DLC will differ according to different environment and other factors such as load parameters (Ronkainen H., 2001). Hydrogenated DLC is described to be in a structure of 3-dimensional array with six membered rings, which contain 17-61% of hydrogen (Grill, A., 1998).

2.3.2.2 Amorphous carbon (a-C)

Amorphous, non-hydrogenated carbon (a-C) coatings are major dominated by sp^2 bonds and have less than 1% of hydrogen contains (Liskiewicz, T. & Al-Borno, A., 2015). The a-C coatings would have a higher advantage in adsorbing due to the dominant sp^2 bond and lack of hydrogen have given a-C coatings to have free end, and therefore caused a-C coating to have higher surface energy (Mabuchi, Y. et al., 2007).

2.3.2.3 Tetrahedral amorphous carbon (ta-C)

Tetrahedral amorphous carbon (ta-C) coatings have the highest fraction of sp^3 hybridized bonds, which can vary between 50 and 90% depending on the fabrication conditions and ta-C coatings are have the closest properties toward crystalline diamond (Liskiewicz, T. & Al-Borno, A., 2015). Ta-C is relatively more stable and have higher hardness than hydrogenated DLC due to its stability of the tetrahedral C particles structure. Amorphous DLC will have low friction and low wear behavior according to Ronkainen H. & Holmberg K. study (2001).

Universiti Malaya

2.4 Surface Texturing for Biomaterials

Surface texture has always been used to deal with friction, eg. patterns are used to overcome slippery condition at the dynasty of Tong in China (Anno, J. N. et al., 1968). Nowadays, surface texture has been used in many fields in order to deal with various friction condition and to improve tribological performance. Surface texturing has advantages such as the ability to retain fluid, alter hydrodynamic pressure and trap debris (Zhang, B., Huang, W. & Wang, X. L., 2012). Hence, surface texturing has emerged as an essential way to enhance tribological properties started from last decade.

In the last decade, there was a study by Clarke, I. C. stated that the surface of natural joint was not a smooth surface (1971), this finding was then inspired the idea of surface texturing (Zhang, B., Huang, W. & Wang, X. L., 2012). There are many studies have done regarding surface texturing of orthopedic implants (Pou, P. et al., 2017; Ghosh, S., & Abanteriba, S., 2016). According to Zhang, B. et al. study, the optimum friction can be achieved by selecting a suitable dimple texturing parameter. In the case of Zhang, B. et al., dimple textured UHMWPE with a dimple diameter of 50 mm, area density of 22.9% and a dimple depth of 10 mm have the optimum results (2013). Ippolito, C. et al. have studied the optimum procedure and parameter used to create optimum parameters for UHMWPE using hot embossing (2017). From Zhang, Y. L. et al. study, the numerical results have shown that dimple textured surface does influence the load-carrying capacity. Parameters such as dimple diameter and dimple depth are the important parameter that will affect the load-carrying capacity of the dimple texture (2015). Micro-dimpled metal surface was said to be able to improve the UHMWPE wear during a sliding test due to the ability to trap wear particles into the dimples (Sawano, H., Warisawa, S. & Ishihara, S. (2009).

Universiti Malaya

2.4.1 Surface Texturing Method

Various techniques have been used to fabricate surface texture such as reactive ion etching, machining, abrasive jet machining, LIGA, and laser surface texturing (LST) (Zhang, B., Huang, W. & Wang, X. L., 2012). LST method is to create various texture pattern with different geometry using lasering. Surface texturing started to be used to improve tribological performance of implant from last decade by inspired by the study of Clarke, I. C (1971). Lathe CNC machine can also be used for texturing micro size texture by using micro size tools (Groover, M. P. et al.). Nanoimprint lithography (NIL) is commonly used to texture micro and nano-pattern onto polymer and is easy to be operated, low cost and able to produce high resolution pattern (Kustandi, T. S. et al., 2010). Electron beam lithography (EBL) and photolithography both are similar with the only difference is source of the ray. EBL is a method to produce texture pattern by using a beam of electron to texture a surface covered with resist, which is an electron-sensitive film (McCord, M. A. & Rooks, M. J., 2002). On the other hand, photolithography method is a method using light to texture by transferring pattern from a photomask to resist that are light sensitive (Hartley, J. G, 2007).

2.4.2 Parameters of Surface Texture

There many types of surface texture have been fabricated on the substrate and being analyses in previous study, such as nano-wells textured (Al-Azizi & Ala' A., 2014), mesh texture (Shimizu, T., Kakegawa, T. & Yang, M., 2014), micro-groove texture (Aizawa, T. & Fukuda, T. ,2013), micro dimple texture (Arslan, A. et al., 2015), as shown in Figure 2.17, in order to improve the tribological properties of DLC coating. The most common surface texture being used is dimple textured with variable dimple density, depth and diameter.

Universiti Malaya

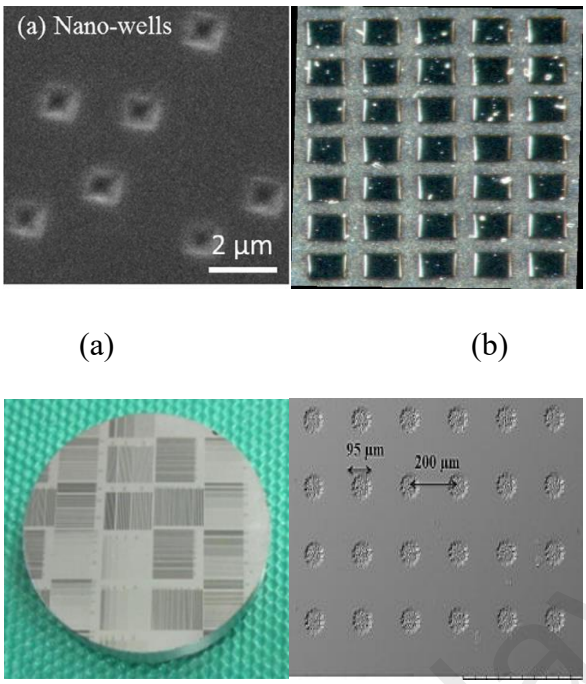

(a) (b)

(c) (d)

Figure 2.17 Types of surface structure, (a) nano-wells texture, (b) mesh texture, (c) micro-groove texture and (d) micro dimple texture

Beside surface structure, the other parameter of texture used on the substrate will affect the tribological performance of the coating as the difference in parameter will vary the pressure distribution towards the coating (Ahmed, A. et al., 2015). As for dimples texture, parameters that can be varied are the dimple density, depth of dimples and diameter of the dimples. However, there are limits to the study about modification of design and parameter of surface texture. Hence, study and analysis about optimum parameter for dimple surface texture will be essential.

2.4.3 DLC combined with surface texturing

There are two types of surface texturing method can be produced with DLC, which are direct and indirect methods. Direct method surface texturing such as by using mesh structure wire (Kondo, S. et al., 2015; Shimizu, T. et. al, 2014) is where a specific texture of the interface layer is placed directly on the substrate, then the interlayer and DLC

Universiti Malaya

coatings are deposited on the textured surface of the substrate. Direct method is easy to perform but the dimensions of the textured depends on the interface layer used while the deposition and cannot be altered easily. Furthermore, direct method is time consuming as time is needed while fabricating the interface layer and.

Indirect method surface texturing is where the deposition of coating is done onto the substrate that have been textured before the deposition process using tools such as laser machine (Arslan, A. et al., 2015). Indirect method has an advantage in fabricating texture with accurate dimension and shape. Moreover, indirect method is not time consuming compared with the direct method as the process is fast and efficient. Indirect method is widely being used for surface texturing with the help of laser machine in fabricating more complex textures in 2-dimensional as well as in 3-dimensional.

2.5 Research gap

Numerous studies have been done in order to improve the performance of orthopedic implants. However, study between the relation of hydrophobic (low surface energy) surface and surface wear behavior was unclear. The present study will focus on the surface modification on the metal part of the implant. The main concern of this study is to study about the effect of surface modifications (mainly focus on modifying surface into hydrophobic surface) toward the tribological behavior of UHMWPE.

Researcher	UHMWPE			Metal		
				Surface coating		
	Cross-linking UHMWPE	Vitamin E blending UHMWPE	Filler reinforce UHMWPE	Increase hardness	Improve coefficient of friction	Increase protein adsorption
Oral, E. et al.		■				
Rachel, L. et al.			■			
Wood, W.J. et al.			■			
Muratoglu, O. K. et al.	■					
Ching, H. A. et al.				■	■	

Universiti Malaya

CHAPTER 3: METHODOLOGY

This chapter will first describe about the sample preparation and the apparatus set-up. The surface texturing method and deposition method will also be discussed in this chapter. Figure 3.1 shown the flow chart of this study in order to achieve the research objectives.

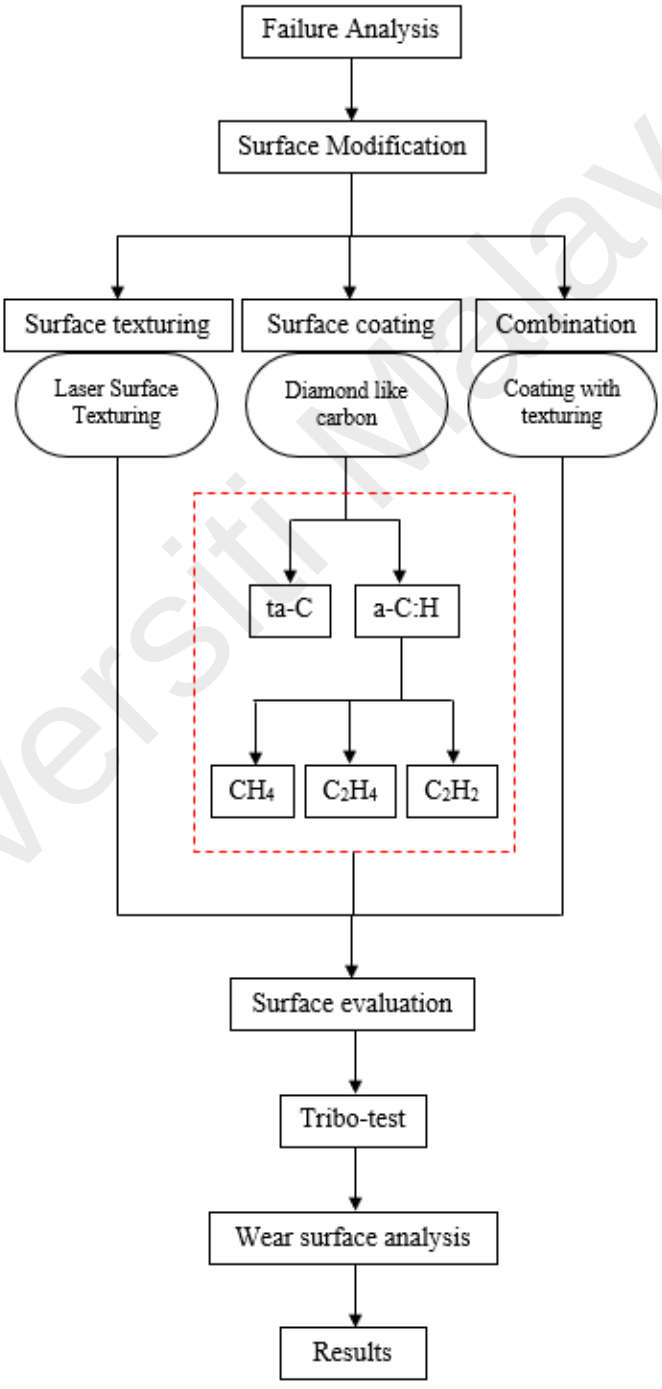

Figure 3.1 Flow chart of methodology

Universiti Malaya

3.1 Failure Analysis

3.1.1 Retrieved sample history

Both the left and right retrieved knees implant was obtained from a 64 years old male patient. The patient had undergone bilateral total knee arthroplasty 6 and 8 months ago for left and right knee respectively.

3.1.1.1 Left knee implant

The left knee implant is from SIGMA® Knee System and was retrieved 6 months after the previous total knee arthroplasty. The femoral component and the tibial tray were made of cobalt-chromium-molybdenum (CoCrMo) alloy, while the tibial insert was made from XLK UHMWPE. The patient underwent revision after his left knee have undergone pain and swelling for 1 month. Upon knee X-rays, his left knee implant is diagnosed to have undergoes loosening failure due to osteolysis posterior of the femoral component and under tibial tray.

3.1.1.2 Right knee implant

Right knee implant is from SIGMA® Knee System and was retrieved 8 months after the previous total knee arthroplasty. The femoral component and the tibial tray were made of cobalt-chromium-molybdenum (CoCrMo), while the tibial insert was made from XLK UHMWPE. Periprosthetic joint infection has been diagnosed after the aspiration diagnosis have been done on the right knee. The x-rays view of the knee is as shown in Figure 3.2.

Universiti Malaya

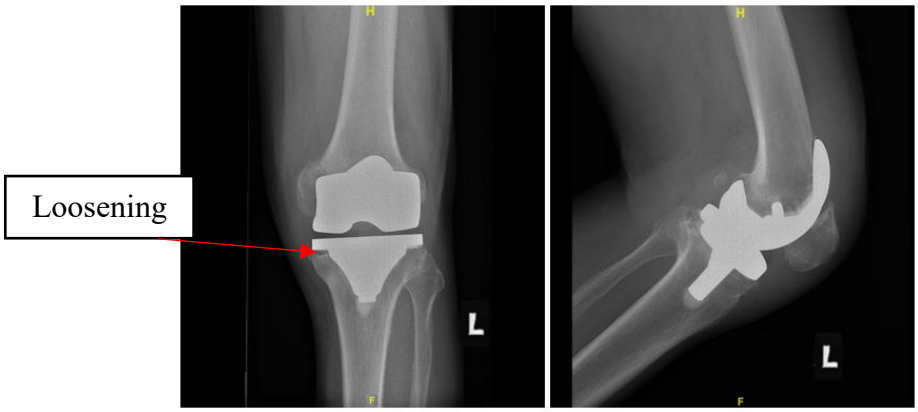

(a)

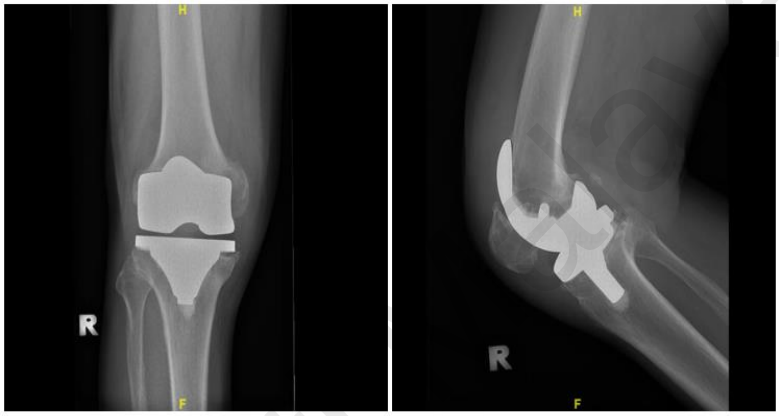

(b)

(c)

Figure 3.2 Radiographs of (a) the left knee of the patient at presentation 6 months after primary total knee replacement (arrow pointing at osteolysis of bone near the implant), (b) the right knee of the patient at presentation 8 months after primary total knee replacement and (c)postoperative view after the left and right knee post revision knee replacement

Universiti Utara

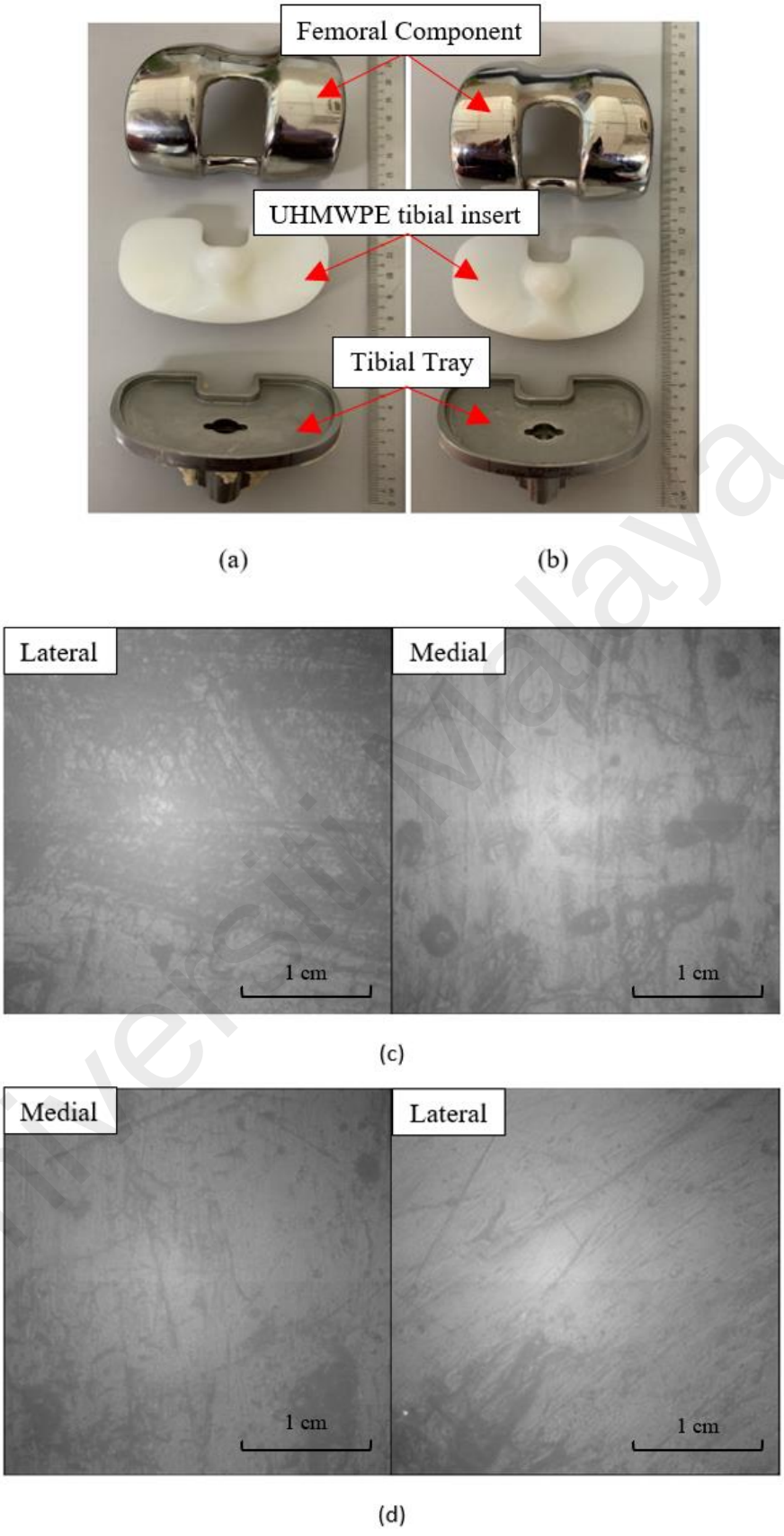

Figure 3.3 Image of (a) Left knee; (b) right knee prosthesis components retrieved; and optical microscope image of (c) left knee tibial insert; (d) right knee tibial insert

Universiti Malaya

3.1.2 Surface evaluation

Surface morphology and surface roughness evaluation is done using optical microscope (KH-8700, HIROX, United States) and 3d imaging microscope (ZeGage, ZYGO, United States) on both sets of samples, right and left knee implant. Microscopic images of tibial insert surfaces were obtained using 3d imaging microscope with 20X magnification, while high resolution topographical and surface roughness were obtained by zygo machine. The hood's grading scale system is used for analyzing the surface roughness and profilometer for both sets of sample, where the tibial insert of the right and left knee were divided into 10 regions (as shown in Figure 3.4) and the sample are categorized into 3 parts, medial (1, 2, 3, 4),lateral (5, 6, 7, 8) and middle (9, 10). The wear damage on the surface was measured based on the extent and severity of seven damage modes (pitting, scratching, burnishing, embedded particulate debris, abrasion, permanent deformation and surface delamination). The analysis of the middle part (9, 10) will not be emphasized in this study due to its complex shape and thus hard to be analyse. The regions with higher surface roughness obtained from profilometer were further analyzed by comparing the features on the sample surface using the electron microscope (JSM-6010PLUS/LV, JEOL, United States).

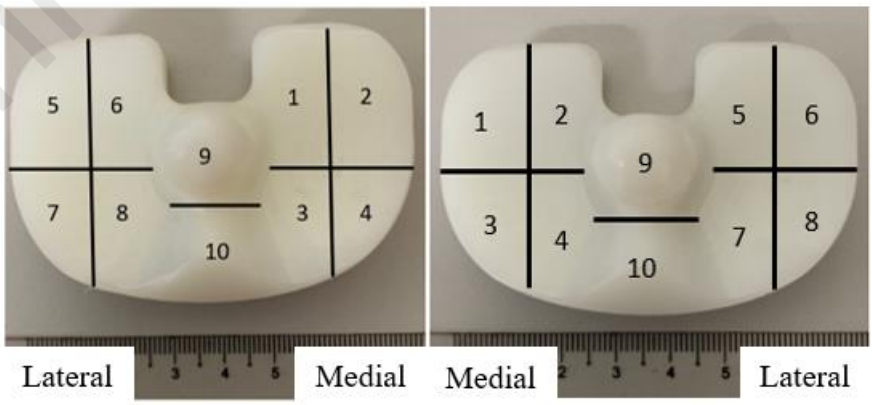

(a) (b)

Figure 3.4 10 region divided on (a) left; (b) right tibial insert

Universiti Malaya

3.1.3 Nano-indentation test

The nano-indentation test was conducted in order to measure the mechanical properties and modulus of elasticity of the UHMWPE tibial insert. The sample was placed on the sample holder of the nano-indenter. Indenter with 0.002 N/s loading rate and the maximum indentation depth of 4 μm is dropped onto the sample. The indenter must be held for 30 s at maximum depth. Average surface hardness was evaluated.

3.1.4 Oxidation characteristics

The oxidation characteristics of the retrieved knee implant samples were analyzed using attenuated total reflection- Fourier transform infra-red (ATR-FTIR) (Spotlight 200i FTIR Microscope System, PerkinElmer, United States) by analyzing the carbon bonding with oxygen molecules. The acquired wavelengths for both bulk and surface area are within intervals of 650 cm^{-1} to 4000 cm^{-1}. The implant samples were put onto the sample holder and the FTIR crystal peak is adjusted to be contacted with the sample in order to obtain precision measurement.

3.1.5 Crystallinity measurements

Crystallinity of UHMWPE were measured using differential scanning calorimeter (DSC) (DSC Q20, TA instrument, New Castle). Sample with weight of < 5 mg were used for the test. The heating was run started from 30°C to 250°C at rate of 10°C/min and the sample was held isothermal at 250°C for 5 min. Later, the sample was cooled until 5° C and the sample was held for another 5 min. Then, the sample was reheated until 250°C in order to obtain the total heat of melting for the sample. The measurement of crystallinity percentage was done by calculating the heat flow from the sample. The measurement of heat flow was recorded during heating and cooling processes of the test. The crystallinity

Universiti Malaya

percentage was evaluated by comparing the total heat of melting ΔH_m to the total heat of fusion where ΔH_f for UHMWPE is 293 J/g (Muratoglu, O. K. et al., 2003).

3.1.6 Molecular weight measurements

The molecular weight of the UHMWPE tibial insert was measured by using gel permeation chromatography (GPC) analysis (Waters 2414 refractive index (RI) detector, Gentech Scientific, New York). The test was conducted on a piece of UHMWPE tibial insert by dissolving the sample in Tetrahydrofuran (THF) at 180 °C.

3.2 Material Selection

Biomaterials of ultra-high molecular weight polyethylene (UHMWPE), titanium (Ti6Al4V) alloy and stainless steel 306 (SS 306) was chosen for this study. There is parameter size of metal substrate, which is square metal substrate and round metal substrate. For square metal substrates (SS 306 and Ti6Al4V) that are all in size of 15mm x 15mm was first being grind using sandpaper from grade 240 to grade 2500 and was mirror-polished using diamond suspension (3μm and 1μm) until the surface was smooth. While round metal substrate was prepared in diameter of 25 mm with 4 mm hole in the middle of the sample [to be placed on sample holder]. The round metal substrate was ground using sandpaper from grade 240 to grade 2500 and was mirror-polished using diamond suspension (3μm and 1μm) until the surface was smooth.

UHMWPE pin in diameter of 6mm was used against square metal substrate with a length of 6 mm and being polished before being used. UHMWPE ball with a diameter of 6 mm was used against a round metal substrate. The UHMWPE pin were exposed directly to nominal doses of gamma radiation at 25 kGy at Radiochemistry and Environment Laboratory (RAS), Malaysian Nuclear Agency. This dose range was suitable for covering the entire range of doses used to sterilize medical devices.

Universiti Malaya

3.3 Surface Texturing

Laser Surface Texturing (LST) Machine were used to introduce the dimple pattern on the metal surface. The plate substrates (15mm x 15mm) have been texturized using laser surface texturing (LST) machine. The choice of circular dimples pattern was used as a geometrical pattern due to easy fabrication and low costs. There are three major parameters involved with surface texturing, such as dimple shape, dimple depth and dimple density. For this study, density of the surface texture used is 10%. The schematic diagram of the texture is as shown in Figure 3.5.

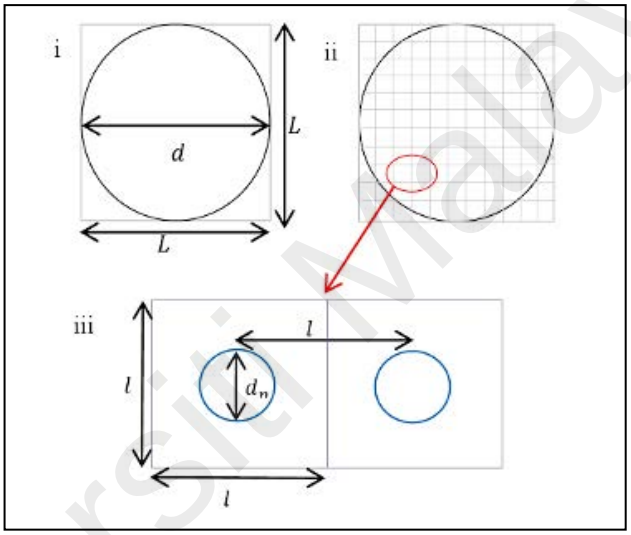

Figure 3.5 Schematic for (i) dimple surface; (ii) imaginary grid and (iii) dimple cell.

Dimple distribution with different dimple density was being calculated using the following calculation. Total surface area of the imaginary square of dimple can be calculated using equation (1). Equation (2) is then used to calculate the area of dimple. The area of dimple density from the total surface area, which also the percentage area was calculated using equation (3) and equation (4) was used to find the grid size on an imaginary square of sample surface. The distance *l* between the micro dimples can be determined by using equation (5). The length of the imaginary square was referred as L and the radius of dimple was referred as r.

Universiti Malaya

$$L \times L = L^2 \quad (1)$$

$$\text{Area of dimple } = \pi r^2 \quad (2)$$

$$\text{Percentage area} = \frac{\text{density}}{100} \times L^2 \quad (3)$$

$$\text{Grid size} = \sqrt{\frac{\text{Percentage area}}{\text{Area of dimple}}} \quad (4)$$

$$l = \frac{L}{Grid} \quad (5)$$

3.3.1 Laser Surface Texturing (LST) Machine

Metal substrates in size of 15mm x 15mm are being texturized using a laser machine (Rofin Starfiber 300 Laser Machine) into dimples with constant diameter (d_n) of 200 µm and the depth of 6 µm. The density of the dimples is 10%. The parameter used for the dimple textured for different density is being calculated and recorded in table 3.1. The dimples were created with constant power of 150 W with speed constant at 200 mm/s using laser machine.

Table 3.1 Parameter of the substrate with different densities for laser machine

Dimple Density (%)	Percentage Area (m^2)	Grid size, $a \times a$	Distance between adjacent dimple, l (m)
10	1×10^{-5}	36×36	2.78×10^{-4}

3.4 Deposition Method

Filtered cathodic vacuum arc (FCVA) system, sputtering system and chemical vapor deposition (CVD) method has been chosen to deposit the DLC film onto the metal substrate. FCVA method was being used to deposit ta-C film, sputtering system was being used to deposit a-C film while CVD method was used to deposit a:C-H film.

Universiti Malaya

3.4.1 Tetrahedral amorphous DLC (ta-C) coating deposition

A FCVA system was used to deposit tetrahedral amorphous carbon (ta-C) film onto Ti6Al4Vsubstrates. The metal substrate was clean using an ultrasonic cleaning machine with ethanol solvent before the deposition. Ti6Al4V substrates were placed on the sample holder and loaded into the deposition chamber. Ar plasma cleaning was applied for 30 min with a flow rate of 200 cm^3/min. For the deposition of ta-C film, bias voltage of -0.4 kV is being applied and the deposition was run for 60 min. The deposition condition of the ta-C film is as shown in Table 3.2.

Table 3.2 Deposition condition of the ta-C film

	Ar plasma cleaning	ta-C film
Flow rate [cm^3/min]	200	-
Duration [min]	30	60
Pressure [Pa]	5	-
Voltage [kV]	0.45	-0.40
Current [A]	0.2	38
Rotational speed [rpm]	-	30

3.4.2 Hydrogenated amorphous DLC (a-C:H) coating deposition

A CVD system was used to deposit a hydrogenated DLC film onto Ti6Al4V substrates. The metal substrates were clean using an ultrasonic cleaning machine with ethanol solvent before placing into the CVD system. Metal substrates were placed on the sample holder and loaded into the deposition chamber. For all a-C:H film with different hydrocarbon source deposition, Ar plasma cleaning was applied for 30 min with a flow rate of 20 cm^3/min. Bilayer of a-SiC:H was being deposited on the substrates by using $C_4H_{12}Si$ with applied voltage of -4.5 kV, flowrate of 15 cm^3/min and deposition duration of 15 min. Later, hydrocarbon source of C_2H_4, C_2H_2 and CH_4 with flowrate of 20 cm^3/min is being introduced into the deposition chamber for the deposition of hydrogenated DLC film. The H/C ratio for C_2H_4, C_2H_2 and CH_4 is 0.24, 0.14 and 0.29 respectively.

Universiti Malaya

Hydrocarbon, a-C:H film was being deposited onto the substrates with an applied voltage of -4.5 kV and deposition duration of 40 min. The pressure was maintained at 3 Pa for the deposition process of Si interlayer and a-C:H film. The deposition condition of the a-C:H film is as shown in Table 3.4.

Table 3.4 Deposition condition of the a-C:H film

Hydrocarbon Source	Parameter	Ar plasma cleaning	a-SiC:H film	a-C:H film
C_2H_4	Flow rate [cm^3/min]	20	15	20
	Duration [min]	30	15	40
	Pressure [Pa]	2	3	3
	Voltage [kV]	-3.5	-4.5	-4.5
C_2H_2	Flow rate [cm^3/min]	20	15	20
	Duration [min]	30	15	40
	Pressure [Pa]	2	3	3
	Voltage [kV]	-3.5	-4.5	-4.5
CH_4	Flow rate [cm^3/min]	20	15	20
	Duration [min]	30	15	40
	Pressure [Pa]	2	3	3
	Voltage [kV]	-3.5	-4.5	-4.5

Figure 3.6 CVD system

Universiti Malaya

3.5 Surface Characterization

The film structure of the DLC film will be characterized by using the RAMAN spectrometer (Raman WorkStation, Kaiser Optical Systems, Michigan, US). The hardness of the film will be by using nano-hardness tester profilometer (Hysitron Ubi 750, USA). The depth of indentation will be 10% of the thickness of the film, load of 1 N and the duration of the indentation was 10 min.

3.6 Surface energy measurement

The contact angle was measured with a droplet angle measuring meter (250-U1, Model 250, Rame Hart Instrument., USA). The droplet angle measuring meter is equipped with an optical subsystem as well as a high-resolution camera to capture the profile of the pure liquid on the solid surface. Droplets (1.0 mL) of distilled water, hexadecane and diiodomethane were dropped onto the metal substrates in order to measure contact angle. For each sample, the measurement was repeated three times in different locations. The contact angle of the droplets is being measured using Laplace-Young method by using $\theta = 2\ arc \tan \frac{2h}{D}$, where h is the height of the droplet and D is the size of the droplet. According to previous studies of Kitazaki and Hata (Hata, T. et al., 1987; Kitazaki, Y. et al.,1972), extended Fowkes theory is being used to calculate the surface energy of the films by using contact angle. The surface energy of a liquid used for the calculation is as shown in Table 3.5.

Table 3.5 Surface energy of the liquids used in calculation (Liza, S. et. al., 2017)

	Liquid Surface energy (mN m–1)			
	Υ_d	Υ_p	Υ_h	Υ_T
Distilled water	29.1	1.3	42.4	72.8
Hexadecane	27.9	0	0	27.9
Diiodomethane	46.8	4.0	0	50.8

Υ_d: dispersion force component, Υ_p: polar force component, Υ_h: hydrogen-bonding force component, Υ_T: total surface energy.

Universiti Malaya

3.7 Protein adsorption

Samples were placed in test tubes filled with diluted bovine serum albumin for incubation before the measurement of protein adsorption film. The samples were placed in an incubator with a constant temperature of 37°C with no rpm for 24 hrs. Later, samples were being cleaned with distilled water and ellipsometer (EC-400, J. A. Woollam Co. Inc., USA) was used for measuring the protein adsorption film thickness.

3.8 Tribological Evaluation

Reciprocating machine (TR 283 Series, DUCOM, Bangalore, India) and pin-on-disc machine was used for the tribological evaluation of this study. The counterpart used for reciprocating machine was UHMWPE pin of 6 mm diameter with 6 mm height and square metal substrate (15 mm x 15 mm) was used. While counterpart used for pin-on-disc machine was UHMWPE ball with 6 mm diameter and round metal substrate with a diameter of 25 mm was used. Tribological evaluation test was done under lubricated condition using bovine serum (BS) and bovine serum albumin (BSA) in order to study the wear mechanisms of film under the existence of BS and BSA. The composition of the lubricant is as shown in Table 3.6.

Table 3.6 Composition of lubricants (Sawae, Y. et al., 1998)

Lubricant	Composition	Protein content
BS	Bovine serum 30 vol.% + distilled water 70 vol.% + sodium azide 0.3 wt.%	10 mg/ml
BSA	Saline + bovine serum albumin 2.0 wt.% + sodium azide 0.3 wt.%	20 mg/ml

Universiti Malaya

3.8.1 Metal Substrate Against UHMWPE Pin

For square metal substrate condition (reciprocating machine), pin used for the test was UHMWPE pin with the size of 6 mm diameter and 6 mm height. UHMWPE pin was used as the counterpart due to UHMWPE was widely used in the making of the implant. The test is run for approximately 40000 cycles with constant frequency of 10 Hz and a constant load of 50 N, which contact pressure was 21.7 MPa. The velocity of the test is 0.1 ms^{-1}, which is same as the mean slow walking speed of OA (Long, L. L., & Srinivasan, M., 2013).

For round metal substrate (pin-on-disc machine), ball with a diameter of 6 mm was used as the counterpart. The test runs for 1500 turns with constant frequency of 20 rpm and constant load of 10 N, which contact pressure was 39.4 MPa. The condition used for all tests was as shown in Table 3.7.

Table 3.7 Tribological Test Condition for Metal Substrate

		Condition
Square metal substrate	Frequency (Hz)	10
	Load (N)	50
	Duration (min)	70
	Cycle	40000
Round metal substrate	Frequency (RPM)	20
	Load (N)	10
	Duration (min)	75
	Cycle	1500

3.9 Worn Surface Characterization

The worn surface film structure of the samples will be characterized by using the RAMAN spectrometer (Raman WorkStation, Kaiser Optical Systems, Michigan, US). The surface structure was then analyzed using attenuated total reflection-Fourier transform infra-red (ATR-FTIR) (Spotlight 200i FTIR Microscope System, PerkinElmer, United States) to analyze the carbon bonding with protein structure after wear test. The acquired wavelengths for both bulk and surface area are within intervals 650 cm^{-1} to 4000

Universiti Malaya

cm^{-1}. The worn surfaces of the deposited films and UHMWPE pins were characterized using scanning electron microscopy (SEM) (JSM-6010PLUS/LV, JEOL, Japan). The chemical composition on the worn surfaces were analyzed via the energy dispersive spectrum (EDS, Oxford Instruments, United Kingdom) attached to the SEM.

3.9.1 Wear Rate Calculation

The wear rate of the substrate and the counterpart was being calculated after the tribological test. Wear rate can be calculated using Equation (6) and the volume loss was being calculated according to the wear track of the substrate or the wear track of the counterpart. Equation (7) and Equation (8) was the used to calculate volume loss of substrate and the volume loss of the counterpart. While Figure 3.7 shows the method in order to calculate the volume loss of the substrate and the volume loss of the counterpart. The worn surfaces of the substrate and the counterpart were characterized using optical microscope.

$$wear\ rate = \frac{volume\ loss}{force \times distance\ slide} \tag{6}$$

$$volume\ loss = depth\ of\ wear\ track \times width\ of\ wear\ track \times pin's\ height \tag{7}$$

$$volume\ loss = Area\ loss \times pin's\ height \tag{8}$$

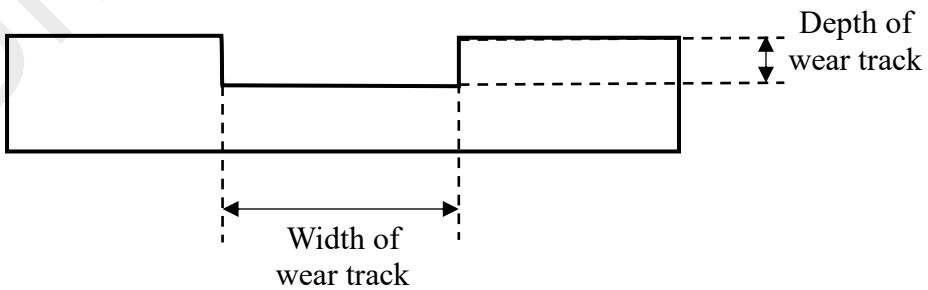

(a)

Universiti Malaya

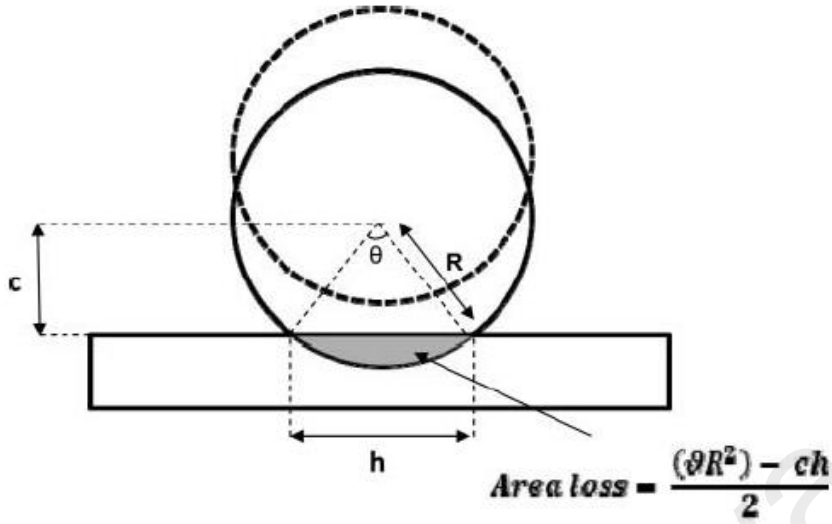

(b)

Figure 3.7 Method to Calculate the (a) Volume Loss of the metal substrate (coated, uncoated) and (b) Volume Loss of the UHMWPE Pin

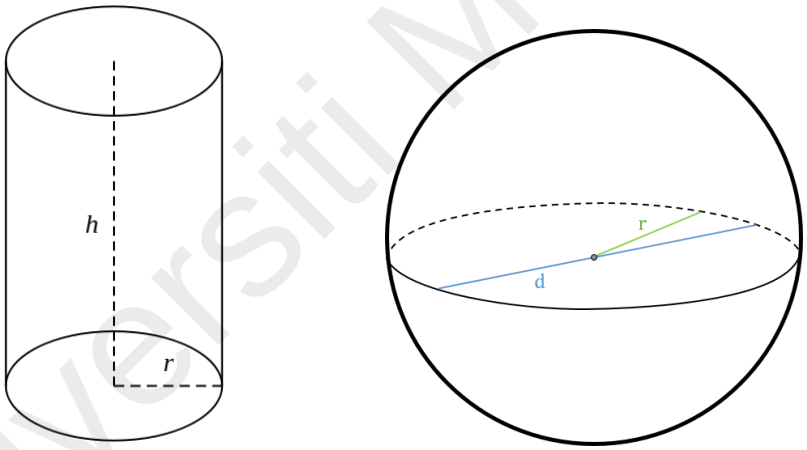

(a) (b)

Figure 3.8 Schematic diagram of (a) pin and (b) ball.

Universiti Malaya

CHAPTER 4: RESULTS AND DISCUSSION

In this study, failure analysis on early retrieved tibial insert was first being studied and noted that improvement need to be done in order to reduce failure risk of implants. Later, surface modification using texturing and coating (ta-C) was studied in order to characterize which surface modifications can improve more on wear resistance. From second stage of study, surface coating was observed to improve on the surface wear resistance, hence, a comparison study between hydrogenated and non-hydrogenated DLC was performed. Since hydrogenated have better ability in improving the surface properties on reducing wear, hydrogenated DLC deposited using different hydrocarbon source was analyzed in order to understand the effect of different hydrocarbon source toward film properties in reducing surface wear. Hence, the study of this thesis will be divided into 4 stages, which is failure analysis, surface modification using texturing and coating, surface coating between hydrogenated and non-hydrogenated DLC, and hydrogenated DLC coated using different hydrocarbon source.

4.1 Failure analysis of early-retrieved left and right knee implants

For the failure analysis of the implants, we have acknowledged several limitations to this current study. First, there is inadequate information on the patient's medical history. Second, information on implant prior the replacement surgery such as original dimensions and treatment were unavailable. Despite these limitations, this study helps to define damage mechanisms on the surface of revision insert in less than 1 year of implantation. The predominant reason for revision in both UHMWPE inserts is infection and the knee implant failures are not caused by UHMWPE wear. Although the cause of the failure was not related to wear, surface analysis was performed to obtain information on surface damage mode for early implanted insert in order to evaluate the early effects of in vivo

Universiti Malaya

and provide information to understand the evolution of surface feature with longer term in vivo durations for further future investigation.

Early retrieved tibial inserts are tibial inserts that retrieved within 5 years after implantation (Fehring, T. K. et al., 2001). The tibial inserts sample for this study were retrieved at 6 and 8 months after the implantation. Early retrieved tibial insert was studied in order to characterize the wear damage on the surface of tibial insert, and hence, able to understand the formation of wear damage on the long-term tibial insert. By understanding the formation of wear damage, the risk of failure for tibial insert will be reduce and the usage life of the tibial insert will be improved, which reduce the revision rate for implants. There are many studies in describing the retrieval analysis of UHMWPE tibial inserts (Bahçe, E. & Emir, E., 2019; Brandt, J. M. et al., 2011; Crowninshield, R. D., et al., 2008; Diabb, J. et. al., 2009; Garcia, R. M. et al., 2009; Hirakawa, K. et al., 1999; Haman. J. D. et al., 2005; Hood, R. W. et al., 1983), and this study will focus on early retrieved study for UHMWPE tibial inserts. The main focus of this study is to describe the severity and location of damage qualitatively which can discuss the damage mechanism on the early-retrieved implants. In order to examine the severity, graded distinctive surface damage is visualized. After that, it is correlated with mode of damage.

4.1.1 Surface characterization of the early-retrieved implants

The surface characterization of both the early-retrieved implants was done using optical microscope and 3d imaging microscope. Figure 4.1 revealed that both inserts (6 and 8 months) posseses numerous scratch marks oriented in various directions and pits. In this study, most scratching and pitting features present on UHMWPE surfaces can be classified as a wear damage. Early surface analysis indicates that the 6 months old insert had predominantly more wear damage compared to the 8 months old insert.

Universiti Malaya

According to the previous analysis study, the common wear features to be found on retrieved tibial inserts were pitting, scratching and delamination (Bahçe, E. & Emir, E., 2019; Brandt, J. M. et al., 2011; Crowninshield, R. D., et al., 2008; Diabb, J. et. al., 2009; Garcia, R. M. et al., 2009; Hirakawa, K. et al., 1999). Hood, R. W. et al. have classified surface damages of articulating surface of retrieved UHMWPE tibial inserts into seven wear damage modes, which are scratching, burnishing, embedded particulate debris, abrasion, permanent deformation, and surface delamination (1983). While Haman. J. D. et al. indicated that fatigue mechanism was the most common wear mechanism found on retrieved tibial inserts, in which wear appearance formed due to fatigue were pitting and delamination (2005). Visually; pitting and scratching appears more prevalent on both 6- and 8-month inserts. It was also interesting to observe surface delamination for 6-month insert.

The condition of these surfaces were further analyzed by the SEM for better visualization of wear damage. For SEM observation, it is confirmed that the most common wear damage feature on the articulating surface of both retrieved UHWPE tibial insert was pitting. It is followed by scratches, delamination, ripples (as shown in Figure 4.2). Pitting of the surface of the 6-months old insert was observed most, followed by scratches and delamination. The surface of 8-months old insert also was dominated by pits, followed by scratches and ripple marks were the least.

In order to confirm the 6 months insert surface incidence of high-grade wear, the condition of the surface was further analyzed by comparing surface roughness using 3D microscope. The dimensional surface profile of UHMWPE tibial inserts (Figure 4.3 and Figure 4.4) taken from 3D microscope image has revealed that the wear features in a more specific way. Moreover, surface roughness of the inserts that obtained from the 3D microscope have been recorded in Table 4.1. From Figure 4.3 and 4.4, the pit depth of the 6-months insert is observed more deeper (approximately 27.5 μm) than 8-months

Universiti Malaya

insert (approximately 18 μm) and Table 4.1 results have also shown that the average surface roughness of 6-months insert is higher than 8-months insert. The average roughness of lateral part (2.096 μm) is higher than medial part (1.264 μm) for 6 months insert and the average roughness of lateral part (1.331 μm) is higher than medial part (1.145 μm) for 8 months insert. Rough surface on 6 months insert indicates surface might undergo more wear than 8 months insert (smoother surfaces). The rough surface (4.207 μm) of region 4 at the lateral compartment proves that the 6 months insert suffered from high damage. The higher surface roughness and deeper pit depth of 6 months implants may be the reason where the loosening of left knee implants is detected to be more severe than right knee. Patient seem to be putting more load on the lateral side of 6 months implant while standing and walking due to loosening factor (Mohd, J. et al., 2014), since the increase in applied load usually results in detrimental behaviour in surface and wear properties (Han, J. et al., 2008; Windarta, M. & Khairul, F., 2011).

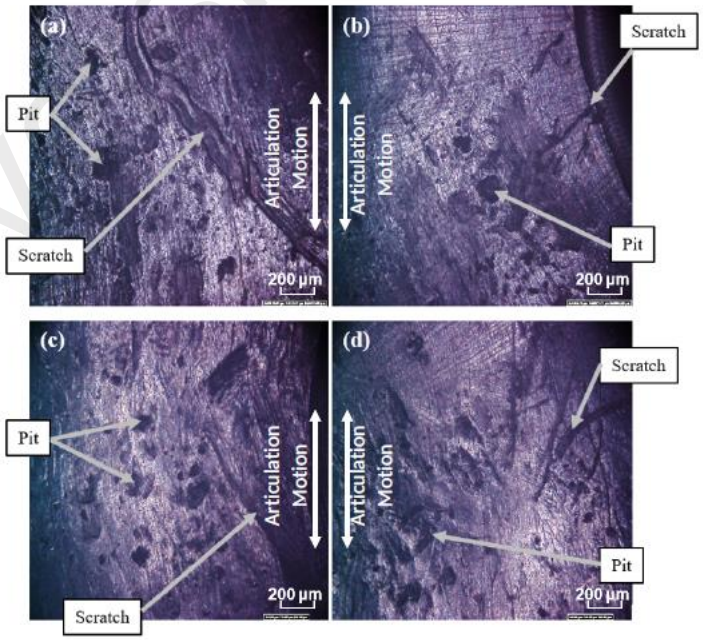

Figure 4.1 Optical microscopic image of the surface of 6-month tibial insert (a) lateral; (b) medial compartment; and 8-month tibial insert (c) lateral; (d) medial compartment.

Universiti Malaya

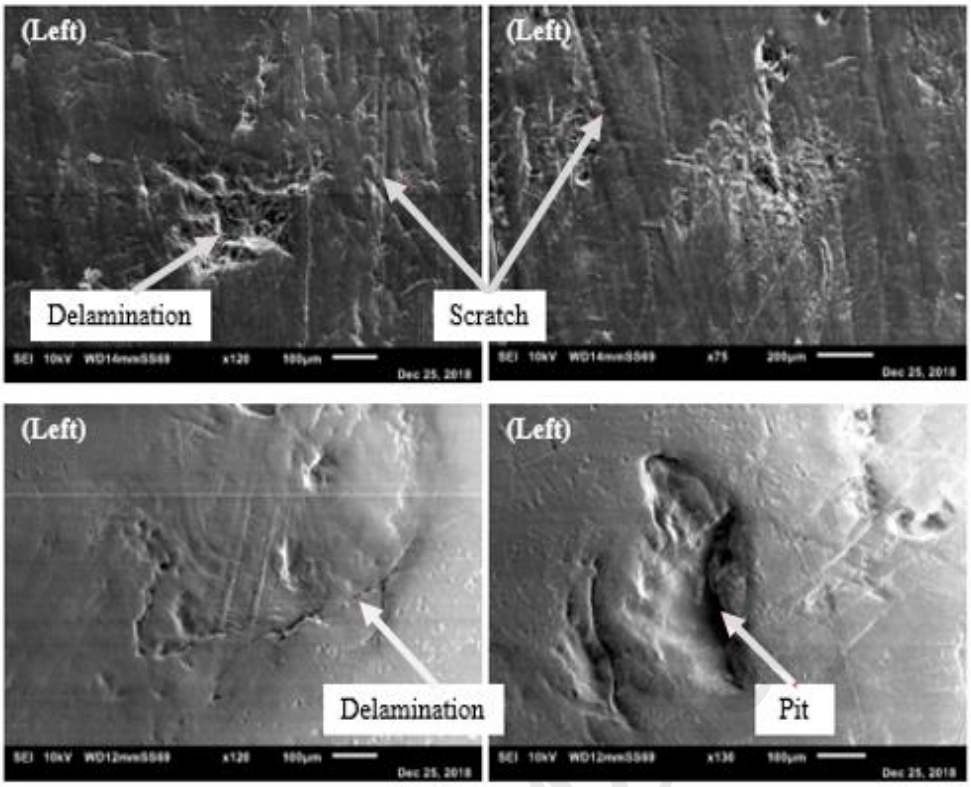

(a)

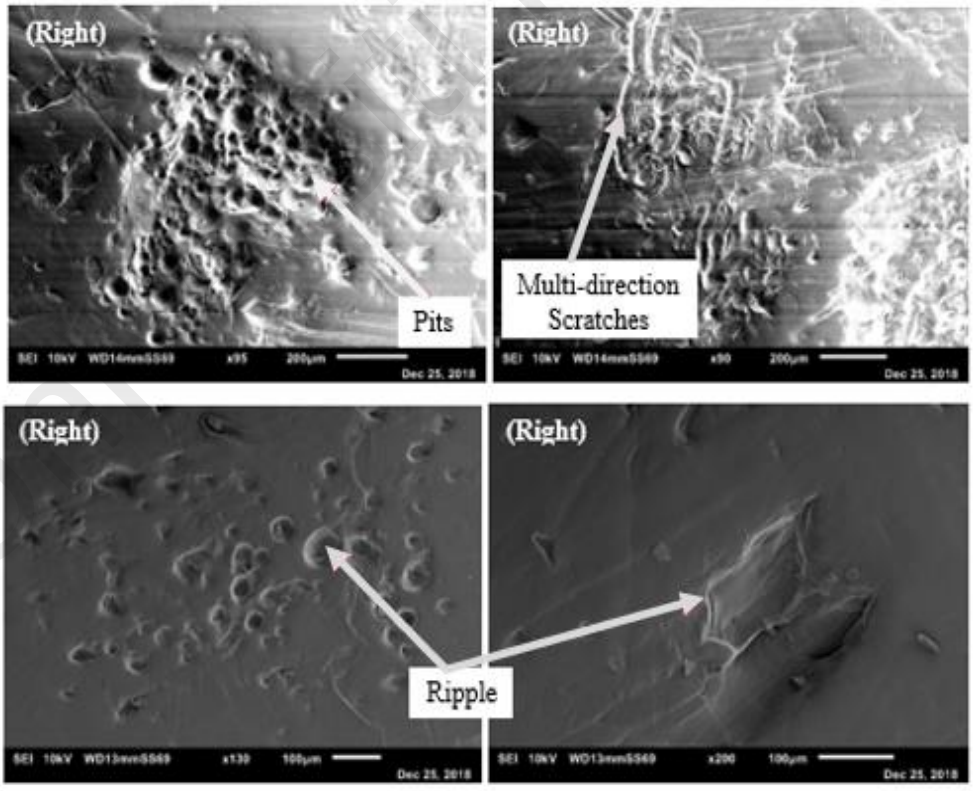

(b)

Figure 4.2 SEM wear characteristics micrographs on (a) 6 month; and (b) 8 months UHMWPE tibial insert.

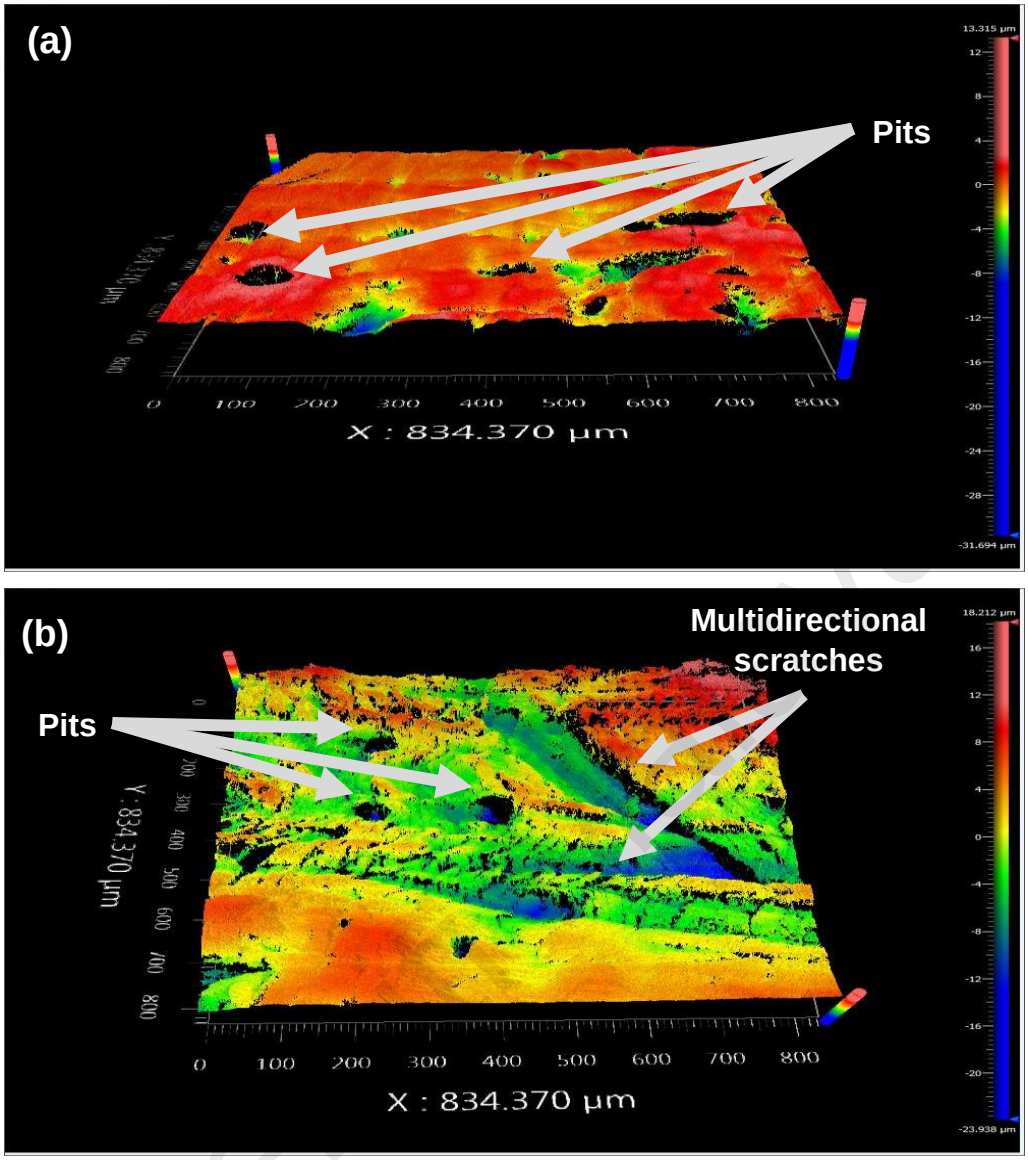

Figure 4.3 3D laser images taken for surface roughness measurement of 6 months UHMWPE tibial insert; (a) medial and (b) lateral compartment

.

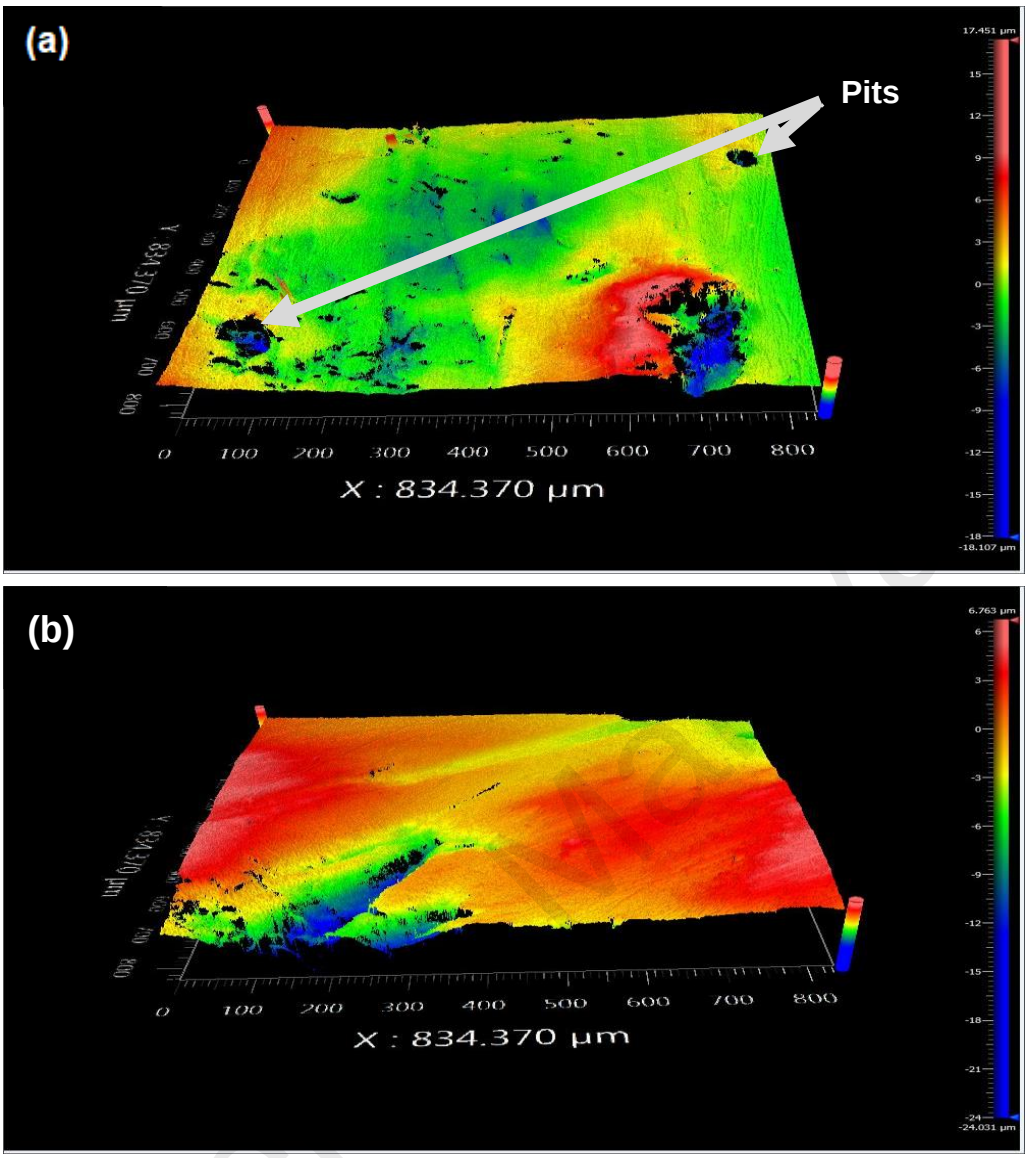

Figure 4.4 3D laser images taken for surface roughness measurement of 8 months UHMWPE tibial insert; (a) medial and (b) lateral compartment

Table 4.1 Surface roughness categorized by compartment of 6- and 8-months UHMWPE tibial inserts.

UHMWPE	Lateral				Medial				Average
tibial insert	1	2	3	4	5	6	7	8	[µm]
6 months	1.186	2.120	0.870	4.207	1.254	1.253	1.568	0.980	1.6798
8 months	0.992	1.467	1.498	1.366	1.763	1.243	1.021	0.551	1.2376

A correlation between implantation time and surface damage score was found by Garcia, R. M. et al. (2009). Greater levels of damage were present with longer in vivo implantation time (from 0.3 to 191.3 months). However, while we anticipated less wear damage from short implantation time (less than 8 months), the current study revealed that three from seven main common surface wear damage modes were present on the inserts. The development of pitting, scratching, and surface delamination at this relatively short implantation time may imply that higher prevalence of wear was found. Although the implantation period is very short but based on the identified damage modes, even inserts with short periods of implantation had severe damage and wear. More precisely, according to Ho, F.Y.et al., the retrieved sample more likely to achieve the failure state is categorized as high-grade wear which consists at least three modes of surface damage namely pitting, scratching, and delamination (2005). Hence, in the present study, retrieved UHMWPE inserts with short implantation duration was considered to have high-grade wear modes. While the wear damage on the 8 months old insert exhibits incidence of low-grade wear since there was no delamination wear observed on the articulating surfaces (Ho, F.Y., 2007).

In this study, the form of pitting on the surface appeared to be indentations can also suggest that there are significant material loss during the articulation motion of the implant (Muratoglu, O. K. et al., 2003). The loss of material in particulate form is known as third body particles or wear debris, where small debris particles mainly formed due to the formation of scratch, and large debris particles were produced due to the formation of delamination (Hirakawa, K. et al., 1999). Previous study suggested that pitting and scratching on the articulating surface are initiated by the hard wear debris which entering the articulation and locally deforming the soft UHMWPE surface (Muratoglu, O. K. et al., 2003; Crowninshield R. D., et al., 2008). In addition, wear scratches caused by wear debris where it embeds into the softer surface or rolls or tumbles through the contact, a

Universiti Malaya

series of indentations is found which further causes groove formation. Based on this observation, it can be suggested that the wear features of 6 months old insert indicates that the wear mechanism of this case can be characterized as a abrasive wear. However, this study is limited by assumptions like the absence of third body wear in order to prove the cause of third bodies for pitting and scratching formation. Scratches found on the surface of insert was not originated from surgical retrieval process. The surgeons was confirmed that the surgeons followed the standard operating procedures (SOPs) for the implant retrieval process including; using an instrument designed for removal of the UHMWPE insert from the tibial tray by disengaging the locking mechanism from the UHMWPE tibial tray interface which is located away from the articulating surface (the underside of the UHMWPE inserts). The femoral component was loosened from the implant-bone cement interface and this was also not involving the articulating surface of the femoral component.

Many retrieval studies reported surface damage features such as pitting and delamination are often observed in retrieved UHMWPE inserts due to fatigue wear (Crowninshield, R. D., et al., 2008; Diabb, J. et. al., 2009; Garcia, R. M. et al., 2009; Hood, R. W. et al., 1983; Liza, S., et al., 2011). In TKR, fatigue phenomenon usually associated with cyclic stress on the contact area between the insert and femoral component. Because of this, at first, we assume an increasing number of cycles will increase in the incidence of pitting and delamination, due to repetitive forces on different axes. For example, Muratoglu, O.K., et al. reported that during 5 million cycles of simulated normal gait, the conventional UHMWPE insert showed large areas of delamination (2004). In contrast to previous study, Flannery, M. et al. reported the fatigue related wear characteristics such as delamination and pitting was not detected on the surface of UHMWPE after short simulator wear test (2008). In their study, wear knee simulator tests were carried out under 2200 N for two million of cycles which considered

Universiti Malaya

representative of 2 years' service of the TKR joint. On the other hand, fatigue tests were performed by Villa, T. et al. using different load, 500, 2000 and 4000 N (2004). As expected, fatigue tests on the prostheses at 500 and 2000 N reached five million cycles each without any sign of failure. However, the fatigue test failed at 4000 N after 1.7×10^5 and 3.8×10^5 cycles, respectively. The findings from above studies, explains millions of cycles might be required to cause fatigue wear. In addition, by considering the gait cycle, delamination should not appear on the insert at least within 5 years of implantation. Study by Zahiri, C. A. et al. reported that the average walking activity of the men with a total joint prosthesis were about 1.07 million cycles per year (1997). Hence less gait cycle indicates there is no effect of fatigue cycle on the formation of delamination in current study.

In the meantime, the early sign of surface damage such as pitting and scratching can lead to severe surface damage. Normally the pit growth rate increases as a function of time. For example, in this study the average size of pit for 6 and 8 months was 27.5 μm and 18 μm, respectively. Pit depth as large as 60 μm was measured on the 10 years implanted UHMWPE insert surface (Crowninshield R. D., et al., 2008). Overtime, the formation of surface damage modes was related to each other, there is possibility that the pit becomes larger and may contribute to development of delamination under the repetitive load cycle. Scratching also could have high potential in producing debris where the wear debris agglomerate aggressively on the surface during sliding can lead to severe surface damage. According to previous study, wear features such as delamination and pitting were found on 6.3 years and 14.2 years retrieved tibial inserts, where 14.2 years retrieved tibial insert was observed to have more severe wear damages (Brandt, J. M. et al., 2011). The 14.2 years retrieved tibial insert was observed to have more delamination features, while 6.3 years retrieved tibial insert was observed to have more pitting features (Brandt, J. M. et al., 2011). The occurrence of this phenomenon was due to pitting features

Universiti Malaya

that have growth severe with time which later induced the formation of delamination features (Bahçe, E. & Emir, E., 2019). These studies show that tibial insert will degrade and deteriorate over time under in-vivo condition, in which, wear damage features occur on late retrieved tibial insert were most likely to be initiated at the early stage of the implantation, and gradually degrade over time. If early stage damage of tibial insert continues to degrade and deteriorate, it will cause the implants to have a high risk of undergoes failure. Hence, understanding wear damage features that occur on tibial insert at an early stage, will help in the contribution of reducing the risk of failure for long term implants.

4.1.2 Mechanical properties of early-retrieved implants

Hardness test was conducted using nano-indentation test in order to measure the mechanical properties and modulus of elasticity of the UHMWPE tibial insert. The hardness and modulus of elasticity of the tibial inserts are recorded in Table 4.2. The hardness and modulus of elasticity of the retrieved tibial inserts were slightly lower compared to the hardness and modulus of elasticity of a new tibial insert; where hardness of new tibial insert is approximately 30 MPa and modulus of elasticity of a new tibial insert is approximately 1.8 GPa (Zanasi, S., 2011; Kang, X. et al., 2014). Although both of the samples just been employed in patient's body for a short implantation time (6 and 8 months). The hardness to modulus of elasticity ratio (H/E) of 6- and 8-months inserts were 20.07×10^{-3} and 20.0×10^{-3}, respectively.

Result indicates that there is a degradation in mechanical properties of the inserts (Zanasi, S., 2011; Kang, X. et al., 2014). Furthermore, the 6 months insert has lower hardness compare to 8 months insert even though it only employs to the patient's body for 6 months. The previous result of surface roughness (Table 4.1) and the formation of wear (Figure 4.1 and 4.2) is believed to be high due to the degradation of the hardness of

Universiti Malaya

insert where it is easier to wear and form wear debris. This phenomenon may partly explain the reason of the insert's wear.

Table 4.2 Hardness and modulus of elasticity of retrieved UHMWPE tibial inserts

UHMWPE tibial insert	Hardness [MPa]	Modulus of elasticity [GPa]
6 months	28.7	1.43
8 months	29.2	1.46

4.1.3 Oxidation characterization of the early-retrieved implants

The oxidation characteristics of the retrieved knee implant samples were analyzed using attenuated total reflection- Fourier transform infra-red (ATR-FTIR). The mechanical degradation of retrieved insert was possibly induced by oxidation. Further analysis on oxidative degradation intervention on retrieved inserts by FTIR was done in order to confirm the possibility occurrence of oxidation. The ATR-FTIR spectra recorded for both 6 and 8 months inserts on surface and bulk region is as shown in Figure 4.5. There are several evident peaks recorded at 2918 and 2916 cm^{-1} (C-H stretching), 1460 and 1464 cm^{-1} (C-H bending alkane), 726 and 714 cm^{-1} (C-H bending monosubstituted) due to absorption. Additionally, there are a number of small absorption peaks at surface and bulk regions which can be assigned to oxidation products. These are acids in the range of 1239 to 1264 cm-1 and carbonyl group in the range of 1712 to 1729 cm-1 (Medel, J. et al., 2009). Absorption peaks that indicate the occurrence of oxidation was detected on both surface and bulk region for both inserts, which shows that the inserts have undergone oxidative degradation. Even though the inserts have only implanted in-vivo condition for a short period of time, it still will undergo oxidation degradation (Hall, R. M. et al., 2001).

Oxidised insert is necessary to be avoid since it has limited success in dynamic applications, due to the delamination tendencies. The oxidative degradation in early stage

Universiti Malaya

of implantation could lead to future fatigue where UHMWPE may lose mechanical properties and have the compromised ability to withstand mechanical loading under the repetitive cycles.

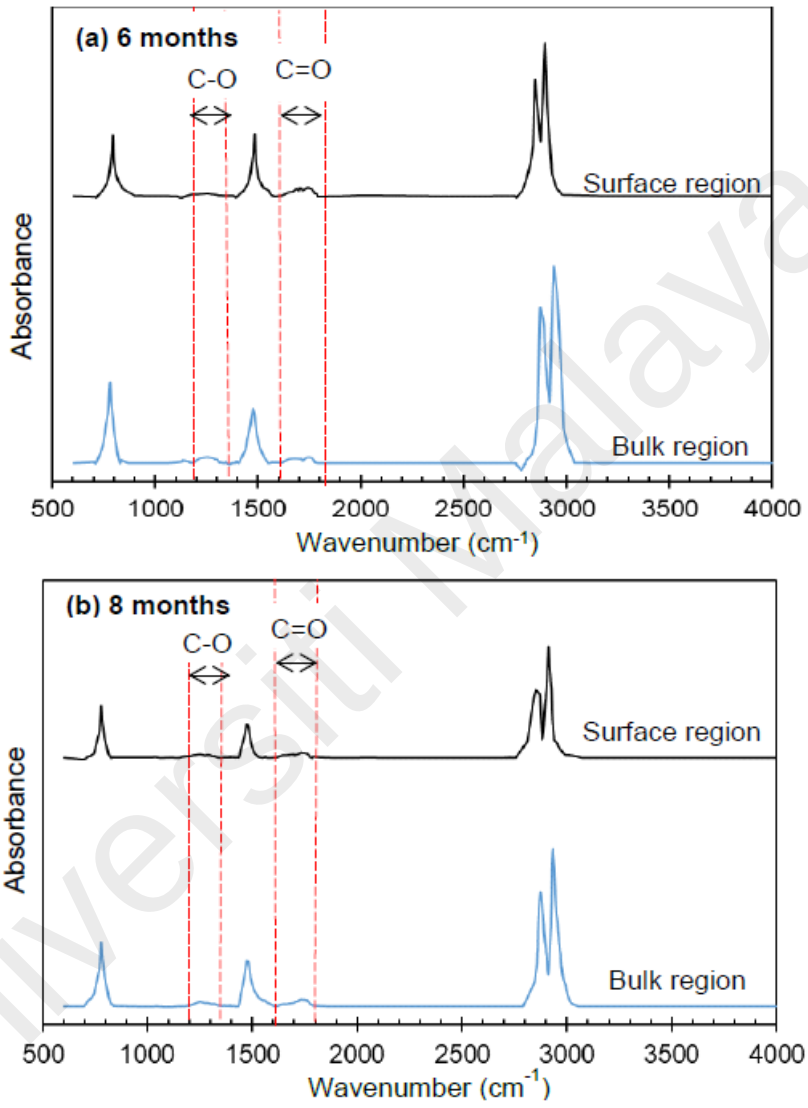

Figure 4.5 ATR-FTIR spectra for (a) 6 months; and (b) 8 months retrieved UHMWPE tibial inserts.

Universiti Malaya

4.1.4 Crystallinity measurement of the early-retrieved implants

The degree of crystallinity of the early retrieved UHMWPE tibial inserts was evaluated by using DSC to determine its crystallinity percentage. The crystallinity difference of the inserts was unable to be characterize due to lack of initial crystallinity percentage record of prior to implantation. The degree of crystallinity of the inserts is shown in Table 4.3, where the crystallinity was 53.79% and 53% for 6-month and 8-month tibial insert respectively. There is not much different on crystallinity of the both inserts, since the obtaining crystallinity was both approximately 53%. Some limitations have been noted about crystallinity assessments because both inserts fall between the acceptable medical range, 39% to 75% and there was lack of initial crystallinity percentage recorded of prior to implantation (Kurtz, S., 2004). Hence, the degree of crystallization of both inserts fall between acceptable medical range.

Table 4.3 Degree of crystallization of retrieved UHMWPE tibial inserts

Sample	Melt Onset Temperature [°C]	Melt peak Temperature [°C]	Enthalpy [J/g]	Crystallinity [%]
6 months	123.0	136.9	157.6	53.79
8 months	120.1	134.0	155.3	53.0

4.1.5 Molecular weight measurement of the early-retrieved implants

The molecular weight of the UHMWPE tibial insert was measured by using gel permeation chromatography (GPC) analysis and the results was recorded in Table 4.4. Molecular weight has a strong influence on the properties of polymer since its rigidity is primarily due to immobilization and entanglement of the chains (Wong, J. Y. & Bronzino, J. D., 2007). It indicates the elasticity, impact resistance, chemical resistance and viscosity of the polymer. Degradation of molecular weight of polymer will cause the polymer

Universiti Malaya

chains to be shorter, where the polymer will have more end groups. The increment of end group in polymer will increase the molecular mobility which causes the polymer chains to become easier to respond to stress (Wong, J. Y. & Bronzino, J. D., 2007). Hence, it reduced the strength and modulus of polymer.

In this study, both 6- and 8-months inserts have undergone approximately 86.4% and 83.1% of weight reduction respectively from the standard medical grade which should be 1.5×106 g/mol (Kurtz, S., 2004). There are similar findings from a study by Diabb, J. et. al. has reported that there is a molecular weight reduction of approximately 88.7% for an insert that retrieved after 7 months of TKR which lead severe wear (2009). The common factors for degradation of molecular weight in early-retrieved implant are most likely due to the sterilization process that conduct on the implant. The irradiation that the implants undergoes will cause surface oxidation which then leads to reduction of molecular weight of the inserts (Diabb, J. et. al., 2009). The reduction of molecular weight of retrieved both inserts has suggested that UHMWPE properties have changed, and the changes are believed to have contributed to the mechanical degradation (low hardness to modulus of elasticity ratio) and ultimately led occurrence of the wear damage.

Table 4.4 Molecular weight of retrieved UHMWPE tibial inserts from GPC analysis

UHMWPE tibial insert	Elution Volume [ml]	Retenti-on time [min]	Adjust-ed RT [min]	Mn	Mw [g/mol]	MP	Mz	Mz+1	Mz/ Mw
6-month	19.775	19.775	19.775	158570	204050	459100	258090	306380	1.2647
8-month	19.727	19.727	19.727	198410	254010	479280	317647	420642	1.2505

Universiti Malaya

The wear features of both tibial inserts were observed to exhibit similar properties [pitting, scratches, and delamination] compare with other long-term retrieval tibial inserts from the previous study (Brandt, J. M. et al., 2011; Collier, J. P. et al., 1996; Crowninshield, R. D., et al., 2008; Diabb, J. et. al., 2009; Garcia, R. M. et al., 2009; Haman. J. D. et al., 2005), but at the initial state of wear damages that will gradually growth severe over time.

The wear of the 6 months old insert is associated with fatigue wear caused by oxidation due to the presence of delamination features on the articulating surface. The wear damages (pits and scratches) caused by wear debris where it embeds into the softer surface or rolls or tumbles through the contact, will then further degrade and caused severe wear such as delamination (Bahçe, E. & Emir, E., 2019). Numerous studies reported the cause of delamination including the degradation of mechanical properties such as reduction of tensile strength and poor elongation will lead to the formation of delamination and cracking (Collier, J. P. et al., 1996; Burnett, R. S. J. et al., 2007). Other than that, it is also believed that the fatigue wear (delamination) can be a result of repetitive cyclic loading during daily activities, since formation of large wear debris (known as delamination) was started by wear from the cyclic stress at the contact surface of inserts (Blunn, G. W. et al., 1992).

The wear damage on the 8 months old insert exhibits incidence of low-grade wear since there was no delamination wear observed on the articulating surfaces. The ripple occurred due to the wear debris produced during the articulating motion have accumulated and piled up on the edge of motion surface. The accumulated wear debris is being pushed along the surface and after sufficient resistance is offered, the ripple is then formed (Yan, Y. et al. (2014); Sinha, S. K., 2006). The damage of 8 months insert is associated to abrasive wear caused by formation of wear debris as material loss during the articulating motion.

Universiti Malaya

Although many studies have reported on in vivo degradation of UHMWPE insert related to fatigue wear, in vivo oxidation was also ultimately recognized as probably the most important contributor to delamination. In this study, from FTIR analysis confirms that oxidation degradation had occurred in the both UHMWPE inserts. It has long been known that oxidation severely degrades the mechanical properties such as loss of toughness can also lead to a decrement in wear resistance (Kurtz, S., 2004; Wannomae, K. K. et al., 2006).

Overall, 6-month tibial insert (left) have observed to undergo high grade wear, while 8-month tibial insert (right) have observed to undergo low grade wear. Surface of both tibial inserts was dominated by pits and scratch, and delamination wear feature was seen to start deformed on the surface of 6-month tibial insert. Both inserts have noted to undergo oxidation and mechanical degradation even though with only short implantation time. Fatigue and applied load were believed to have contributed to the wear formation and degradation of both tibial inserts. Hence, modification needed to be done on the implant to improve performance of implants.

Universiti Malaya

4.2 Effect of laser surface texturing (LST) combined with non-hydrogenated tetrahedral amorphous DLC coatings on tribological behavior of UHMWPE.

Wear on the tibial insert will continuously growth severe over time, which caused implant to have higher risk to undergo failure. Hence, improvement needed to be done on the implant material in order to improve the functionality and longevity of the implants. In this study, surface modification will be used to improve performance of implants. There are many surface modification techniques, but surface texturing and surface coating will be used to evaluate which modification techniques will more suitable to improve performance of implants.

Tetrahedral amorphous carbon (ta-C) film was coated onto textured and untextured metal substrates (SS 304 and Ti6Al4V) by using FCVA system. Texture with dimple density of 10% was being applied onto the metal substrate prior to the deposition. This study was conducted in order to understand the effect of textured surface with combination of DLC film toward the UHMWPE wear, while neat and bare textured metal will be used for reference. Surface texture has been used in many fields in order to deal with various friction condition and to improve tribological performance. There are many methods used for surface texturing such as indentation, laser surface texturing (LST), reactive ion etching, machining and abrasive jet machining (Zhang, B., Huang, W. & Wang, X. L., 2012). In this study, LST method will be used for texturing the samples. LST method was chosen due to its ability to create various texture pattern with different geometry using lasering and also was easy to fabricate. Surface texturing has the ability to improve performance of a system by generating additional hydrodynamic pressure, act as lubricant reservoirs, capture wear debris to avoid third body abrasion (Zhang, B., Huang, W. & Wang, X. L., 2012). On the other hand, surface coating has been widely used to protect material surfaces and also improve surface tribological properties (Demas

Universiti Malaya

N.G. et al, 2016). However, the characteristics for surface texture combine with surface coatings was unclear. Hence, ta-C DLC film and surface texture of 10% dimple density was used in this study to evaluate the role of surface coating, surface texturing and surface coating combine with surface texturing toward UHMWPE wear. ta-C DLC film was chosen because ta-C DLC was easy to be deposited using sputtering method, while 10% dimple density was chosen because it was the commonly used parameter for surface texturing (Zhang, B., Huang, W. & Wang, X. L., 2012). DLC film on metal substrates is first being characterize using RAMAN spectrometer before the tribological test. The coating hardness were being characterize using nano-indentation test before the tribological test. After the tribological test, the substrates wear rate is being calculated and analyze.

4.2.1 Surface structure Characterization before wear test

Dimple texture on both SS 304 and Ti6Al4V was observed using optical microscope and as shown in Figure 4.6. According to the measurement obtained, the dimple textured on both substrates using same parameter by LST have almost same dimple diameter. However, the dimple diameter on Ti6Al4V was slightly smaller (approximately 2%) than dimple on SS 304. Since, Ti6Al4V was a harder material than SS 304, hence, is understandable that dimple diameter on Ti6Al4V will slightly smaller than the dimple diameter on SS 304.

Universiti Malaya

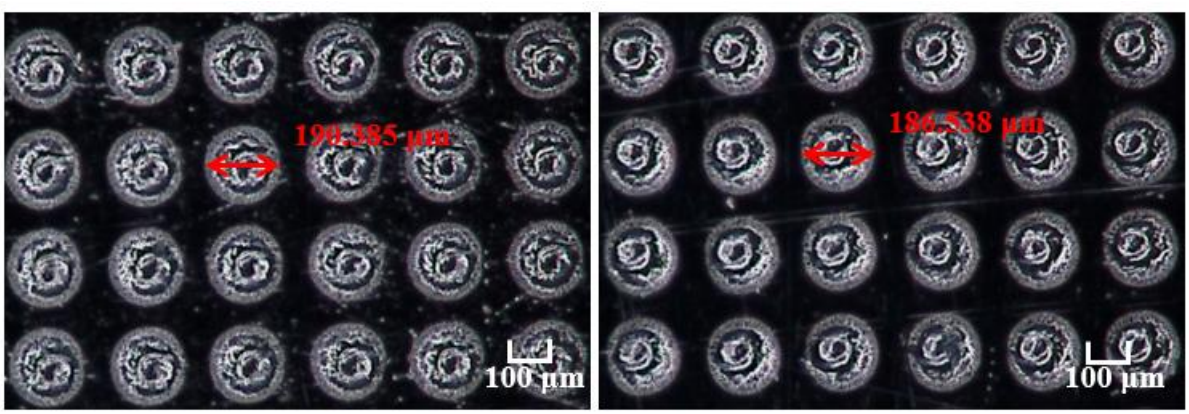

(a) (b)

Figure 4.6 Dimple textured on (a) SS 304; (b) Ti6Al4V.

The thickness of ta-C film deposited on both SS 304 and Ti6Al4V substrate was measured using profilometer. The thickness of the film was as shown in Table 4.5. The thickness of ta-C film on both metal substrates was almost similar since the deposition condition for the film are the same. Hence, the metal substrates use for the deposition of film does not have a large effect towards the deposition rate of the film.

Table 4.5 Thickness of film.

	taC/SS 304	taC/Ti6Al4V
1	313.5	310.2
2	321.7	325.7
3	318.9	321.9
Average [nm]	**318.0**	**319.3**
Deposition rate [nm/s]	**0.088**	**0.089**

Structure characterization of the DLC coating was done using RAMAN spectrometer. The RAMAN spectrometer graph and RAMAN data are as shown is Figure 4.7 and Table 4.6 respectively. By comparing with a previous study, RAMAN spectrum for DLC film involves two broad peaks should be around 1200 - 1450cm^{-1} for the D band and 1500 - 1700cm^{-1} for the G band (Pang, H. et al., 2010). For Figure 4.7, D band of the RAMAN graph is about 1422 cm^{-1} and G band of the RAMAN graph is about 1530 cm^{-1}. The results indicate that ta-C film does successfully being deposited onto both SS 304 and

Universiti Malaya

Ti6Al4V substrate. The relative ratio of the D peak and G peak (I_D/I_G) is proportional to the ratio of sp^2 /sp^3 (Al Mahmud et al.,2014). The I_D/I_G ratio plays an important role in analyzing the RAMAN. The I_D/I_G ratio of all film have similar value, which indicate that all film has similar cluster size.

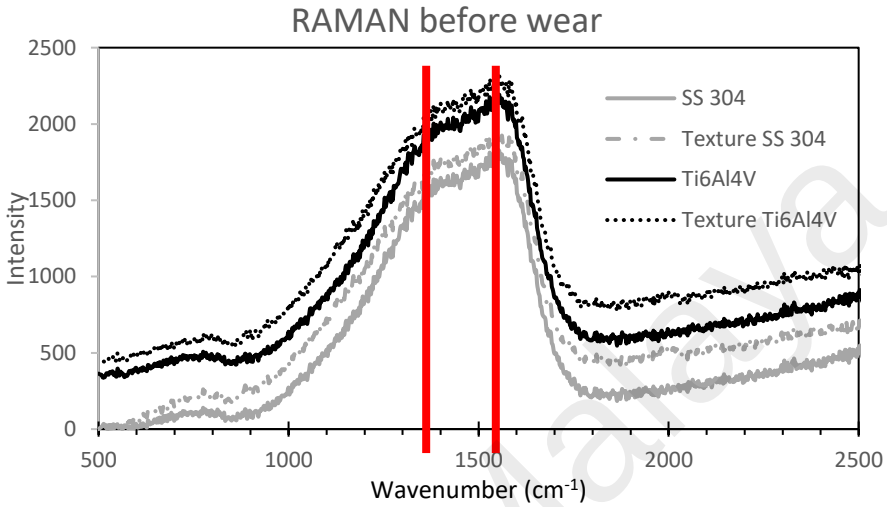

Figure 4.7 RAMAN spectra of textured DLC coatings before wear test.

Table 4.6 Variation of position and I_D/I_G of Raman D and G peak before wear test

Substrate	D peak [cm^{-1}]	G peak [cm^{-1}]	I_D/I_G
SS 304	1388.47622	1572.08974	1.7575
Ti6Al4V	1442.79312	1539.79929	1.5685
Textured SS 304	1386.57685	1563.84017	1.7307
Textured Ti6Al4V	1420.64197	1547.17549	1.7169

4.2.2 Wear Test

Tribological test was done using reciprocating machine with the Pin-On-Disc method under bovine serum lubricated condition. The counterpart pin used for the test is Ultra-high-molecular-weight polyethylene (UHMWPE) pin with the diameter of 6 mm and the height of 6 mm. The wear rate of the UHMWPE pin counterpart is as shown in Figure 4.8. Since the wear rate of DLC film was unable to observed visible scratch, the results of their counterpart were being measured to be analyzed.

The wear of UHMWPE counterpart between all samples were calculated and

Universiti Malaya

compared (Figure 4.8). The UHMWPE counterpart for untextured ta-C film has lower wear rate, followed by textured ta-C, uncoated texture and bare sample. This phenomenon was due to the coating have the ability to protect the surface and reduce the wear of UHMWPE counterpart (Grill, A., 1998). However, surface texturing may have the ability to protect its own textured surface but will increase wear towards their counterpart (Zhang, B. et al., 2013). Since the textured surface will have dimples textured which will increase the surface roughness of the surface, it will also increase wear towards its counterpart (Zhang, B., Huang, W. & Wang, X. L., 2012). On the other hand, the wear rate of UHMWPE counterpart against both DLC coated SS 304 and Ti6Al4V are almost similar with the counterpart for DLC coated Ti6Al4V have a slightly lower wear rate. Since the deposition condition the film on both metal substrates are the same, hence, it was understandable to not have much difference on the wear rate.

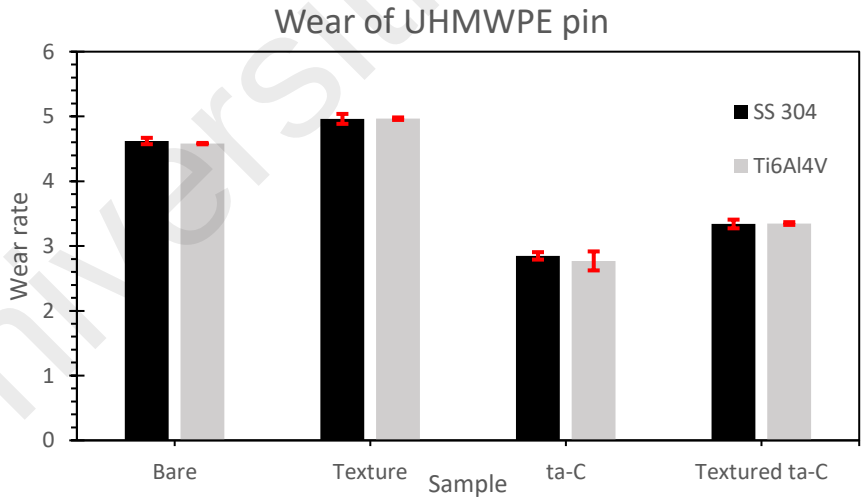

Figure 4.8 Wear rate of UHMWPE counterpart under different DLC film.

Universiti Malaya

4.2.3 Structure Characterization after wear test

RAMAN characterization was conducted on the sample after wear test in order to characterize structural change of the film after the wear test. From the results, it was observed that the intensity peak for all film have reduced and graphitization was observed to occur less likely on all films. Since ta-C film has a strong sp3 bond that prevents graphitization. Furthermore, the intensity of RAMAN spectra after wear test (Figure 4.9) for all film have reduced compared to the intensity of RAMAN spectra before wear test (Figure 4.7). The differences of the peak indicated that there are film residues left on the surface. Furthermore, by comparing the data from Table 4.6 and 4.7, the I_D/I_G value of textured sample have reduce more as compared with untextured sample. The reduction of I_D/I_G value shows that graphitization has occurs more on textured sample, which explained the higher wear rate of textured ta-C sample as compared with untextured ta-C sample.

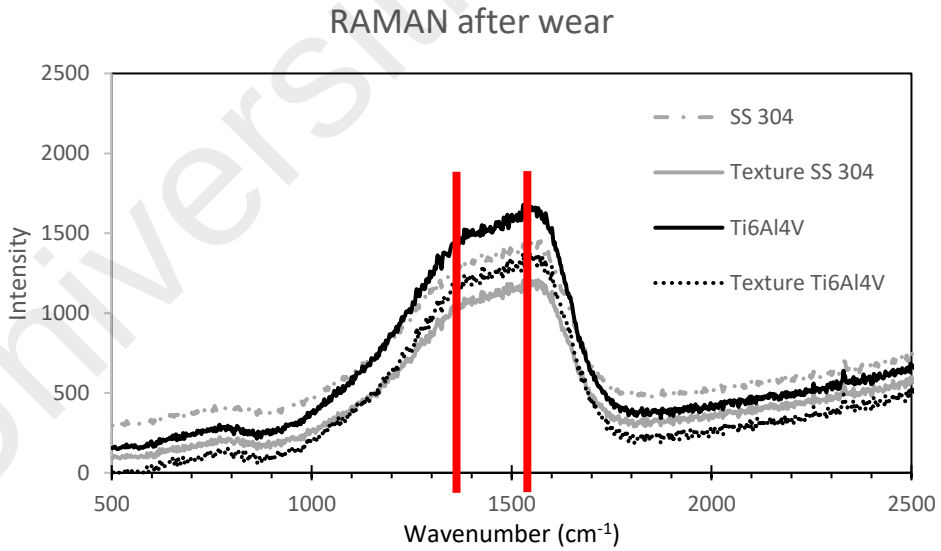

Figure 4.9 RAMAN spectra of textured DLC coatings after wear test.

Universiti Malaya

Table 4.7 Variation of position and I_D/I_G of Raman D and G peak with different type of DLC films after wear test

Film	D peak [cm^{-1}]	G peak [cm^{-1}]	I_D/I_G
SS 304	1374.89742	1557.51472	1.2279
Ti6Al4V	1394.98753	1574.51078	1.2978
Textured SS 304	1359.85844	1574.98705	1.1323
Textured Ti6Al4V	1380.15443	1554.12991	1.1618

Overall, all UHMWPE counterpart on both metal substrate has similar wear trends for the same films, where counterpart for textured surface has high wear. Although surface coating on textured surface able to reduce wear on the UHMWPE counterpart, surface coating on untextured surface still has the better ability in protecting the UHMWPE counterpart.

Universiti Malaya

4.3 Effect of hydrogenated and tetrahedral amorphous DLC coatings on tribological behavior of titanium (Ti6Al4V) alloy and UHMWPE under protein lubricated condition.

Although dimple texture has the ability to protect its own surface from wear, however, the textured surface will cause wear on its counterpart. While DLC coating has the ability to protect both contacting surfaces from wear, hence, more evaluation of DLC coating on the tribological behavior of Ti6Al4V and UHMWPE will be studied in this objective. Tetrahedral amorphous carbon (ta-C) and hydrogenated amorphous carbon (a-C:H) DLC coatings was coated onto Ti6Al4V alloy by using FCVA system and CVD system respectively. From the previous section (4.2), DLC deposited sample on both SS 304 and Ti6Al4V does not have much difference on the wear resistance properties. Hence, this part of the study will focus on Ti6Al4V as the metal substrate used for deposition. This study was conducted in order to evaluate the effect of different type of DLC film toward the UHMWPE wear under protein lubricated condition. Ti6Al4V alloy and UHMWPE were used for the test because these materials were common materials used for manufactured bio-implants. Different types of DLC film on metal substrates of Ti6Al4V is first characterized using RAMAN spectrometer before the tribological test. The coating hardness were characterized using nano-indentation test before the tribological test. After the tribological test, the substrates wear rate is calculated and analyzed.

4.3.1 Surface characterization before wear test

Hardness test is being done using nano-indentation machine. The results from the nano-indentation test is as shown in Figure 4.10. The hardness of ta-C film is higher since the film has strong sp^3 bond compared to a-C:H film which have sp^2 bond. The sp^3 bond in ta-C film strongly attach to each other which cause the bond is hard to be break (Oohira, K., 2009).

Universiti Malaya

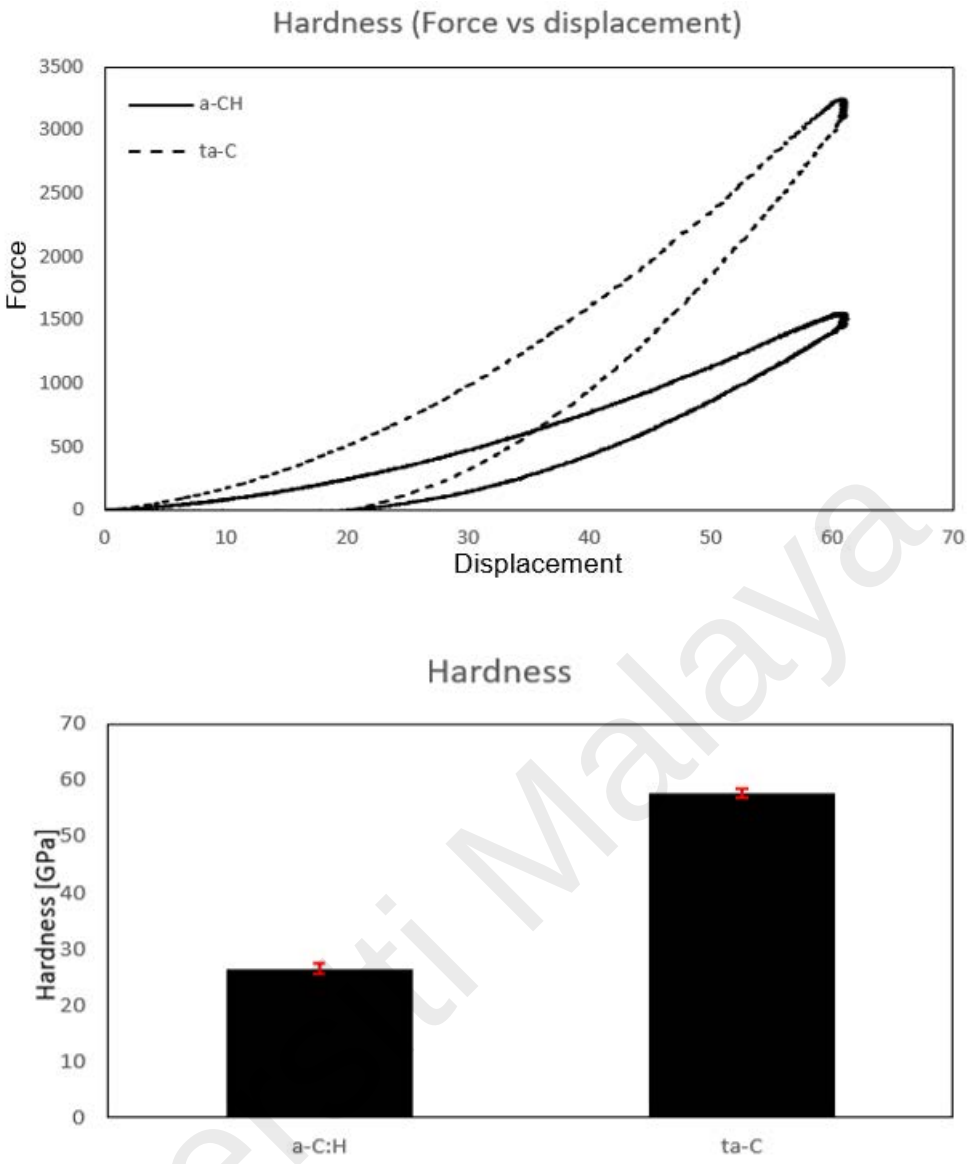

Figure 4.10 Variation of indentation hardness for different DLC films

The FTIR spectrum of the films was as shown in Figure 4.11. All DLC films (a-C:H and ta-C) shows the same trend with difference in absorbance intensity. Strong =C-H bending vibration (675-1000 cm^{-1}), C=C stretching (1500-1680 cm^{-1}), C≡C stretching (2100-2260 cm^{-1}) and C-H stretching (2850-3000 cm^{-1}) was present for both a-C:H and ta-C films. The peaks show that DLC films have successfully deposited on the metal substrate.

Universiti Malaya

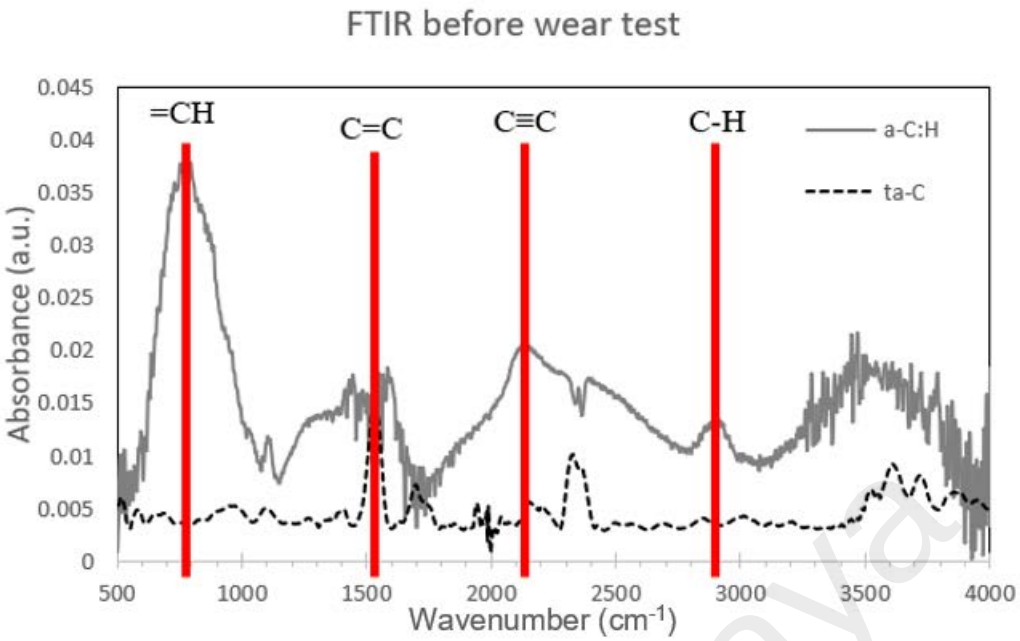

Figure 4.11 FTIR spectrum of the films

4.3.2 Surface energy and wettability of different type DLC films

Wetting is the contact and spreading of a liquid on the surface of a solid object and plays an important role in biomedical applications. From the tribological prospective, wettability plays an important role for improving lubrication properties of the tribo-pairs. Wettability behavior depends on two factors: the first factor is the level of surface free energy and the roughness and topography of the surface. Surface wettability can be estimated by measuring a contact angle (θ). A surface is defined as a wet-able or hydrophilic surface if θ less than 90º, while others are non-wet-able or hydrophobic surface (θ>90º). Contact angle of distilled water, hexadecane and diiodomethane on the ta-C film and a-C:H film is later used to calculate surface energy using extended Fowkes theory. The surface energy of the liquids shows in Table 3.5 is used to calculate the surface energy of the film. The surface energy of the film is shown in Figure 4.12. The total surface energy (Υ_T) of the ta-C film and a-C:H film is the sum of the dispersion component (Υ_d), the polar component (Υ_p), and the hydrogen bonding component (Υ_h).

Universiti Malaya

In this study, higher surface energy was observed on ta-C film, followed by a-C:H. The increasing surface energy was due to the increase in the polar and hydrogen-bonding components due to strong dipole-dipole and hydrogen-bonding interaction at the surfaces. In this study, the best hydrophobic surface occurred at the a-C:H film with lowest surface energy approximately at 47.2346 $mN.m^{-1}$. The film which is more hydrophobic will have lower surface energy. According to Figure 4.12, Υ_p and Υ_h is the dominant factor that contributes to the low surface energy of a-C:H film. The C-H bonding in a-C:H film have contribution in the low surface energy of the film. C-H bond has relatively low polarity than C-C bond, which caused the Υ_p of a-C:H films to be lower. Other than that, hydrogen bonding of the hydrogen of a-C:H films with the hydrogen bond donor (N, O) of protein structure have resulted in the high Υ_h of a-C:H film. Furthermore, protein will fold to become hydrophobic to repel polar solution in order to maintain protein stability and active. When protein interacts with hydrophobic surface, protein will attach on the hydrophobic surface to reduce the interaction with the polar solution, which later denatured onto the hydrophobic surface due to various factors (temperature, ionic strength) (Zhang, C., Fujii, M., 2015; Nygren, H. et al., 1994). The C-H bonding of a-C:H films will interact with the C-H components in the protein to form a hydrophobic interaction in order to repel polar solution.

Further measurements of the contact angle for diluted BS was done in order to see if the DLC films surface change its wettability when in contact with protein solution. The results show that the contact angle consistent with surface energy of the film, which means that the DLC surface does not lose its hydrophobicity/hydrophilicity. Whereas, protein solution does not modify the chemical structure of DLC films.

Universiti Malaya

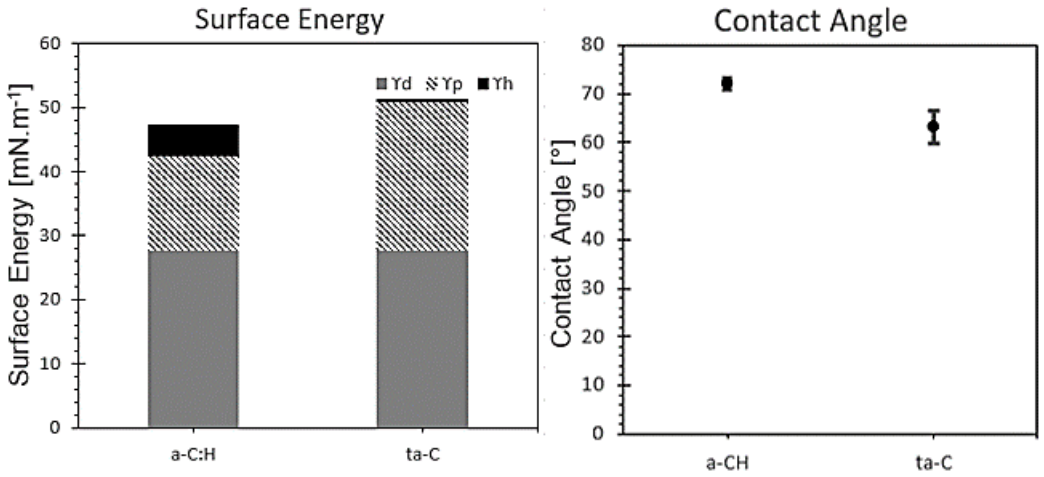

Figure 4.12 (a) Surface energy; and (b) contact angle of different DLC films

4.3.3 Protein absorption

According to Table 4.8, a-C:H film has a thicker adsorption film thickness (313.85 ± 6.347 nm) as compared with ta-C film (93.66 ± 0.533 nm). This result shows that a-C:H film has better protein adsorption ability as compared with ta-C film. The hydrophobicity of a-C:H films (Figure 4.12) was one of the factors that resulting the high protein adsorption of a-C:H films. Wettability has been characterized as the dominant factor for the protein adsorption process, and it is generally stated that hydrophobic surfaces adsorb more proteins than hydrophilic surfaces (Wang, K. et al., 2012). According to Nygren, H. et. al, hydrophobic surface will have high adsorption for protein due to the hydrophobic interaction of proteins (1994). Protein structure will cause the hydrophobic moieties inside the protein to form weak hydrophobic interactions with hydrophobic surface in order to compensate the dehydration of hydrophobic surface.

Furthermore, the low polarity of a-C:H films (Figure 4.12) also have effect on the protein adsorption of the film. Hydrophobic moieties inside the protein will more likely to interact with low polar surface in order to prevent interaction with polar solution, which able to keep the activeness of protein (Nygren, H. et. al, 1994). Hence, increase the protein adsorption toward the surface.

Universiti Malaya

Other than that, protein adsorption is also affected by the chemical composition of the film, where hydrogen bonding of the film will induce the protein adsorption (Verzola, B. et. al., 2000; Wang, K. et al., 2012). The hydrogen in the films will reacts and attract the hydrogen donor particles (N, O) from the protein, which then increase the protein adsorption rate.

Table 4.8 Protein adsorption film thickness measured using ellipsometer

	Solution	Film thickness [nm]
ta-C	BSA	93.66 ± 0.533
a-C:H	BSA	313.85 ± 6.347

4.3.4 Wear test

In order to evaluate the wear performance of different type of DLC films wear tests were carried out. Figure 4.13 shows the wear rate of DLC films and UHMWPE as a counterpart in ambient air under bovine serum and bovine serum albumin lubricated condition. Both ta-C and a-C:H films show relatively low wear rates indicate films had demonstrated similar wear resistance. The wear rate difference of ta-C and a-C:H films was not significant under same lubricant. However, wear rate difference has significant different when compared between difference lubricant used. Nevertheless, the wear of the UHMWPE as counterpart was slightly reduced when testing against a-C:H film, although the difference was not significant when compared with counterpart of ta-C film. This result might be related to the structural differences within the films and the hydrophobic character in a-C:H film under protein lubrication condition (Zhang, C., Fujii, M., 2015). Hydrophobic film surface tends to bind more protein through hydrophobic interactions in which a protein aggregates will form between two hydrophobic surfaces which will then protect both surface (Zhang, C., Fujii, M., 2015; Nygren, H. et al., 1994). Hence, the

Universiti Malaya

UHMWPE counterpart of hydrophobic a-C:H film has slightly lower wear rate than the ta-C film. Further analysis will be done on the worn surfaces to characterize the structural changes and wear mechanism of DLC films under protein lubrication condition.

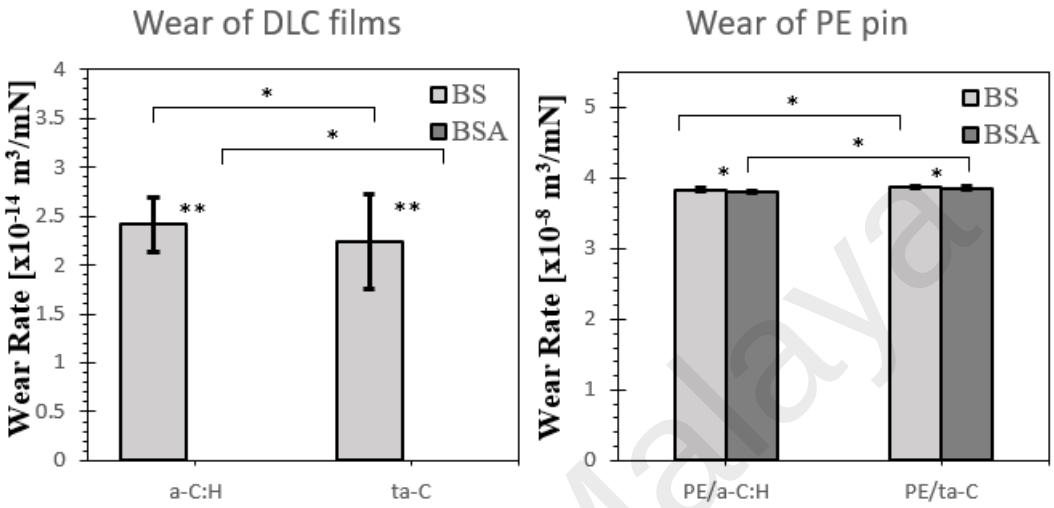

Figure 4.13 Wear rate of DLC films and UHMWPE (counterpart); where, ** P < 0.05 = significant, * P > 0.05 = not significant

4.3.5 Surface characterization

RAMAN spectrometer was done in order to characterize the structural change of the film before and after wear test. RAMAN spectrometer of all film under both proteins was as shown in Figure 4.14, where RAMAN peaks was compared between before and after wear test. All peak before wear test have peak at D peak (~1350) and G peak (~1530), indicate that DLC films was successfully deposited onto the metal substrate. Peak intensity for all films has reduced after wear test. Moreover, amide I (~1665) and amide III (~1242) was observed on the worn side. This shows that protein adsorption might have happened on the film during the wear test, hence, FTIR was done in order to confirm the existence of protein adsorption of the film.

Universiti Malaya

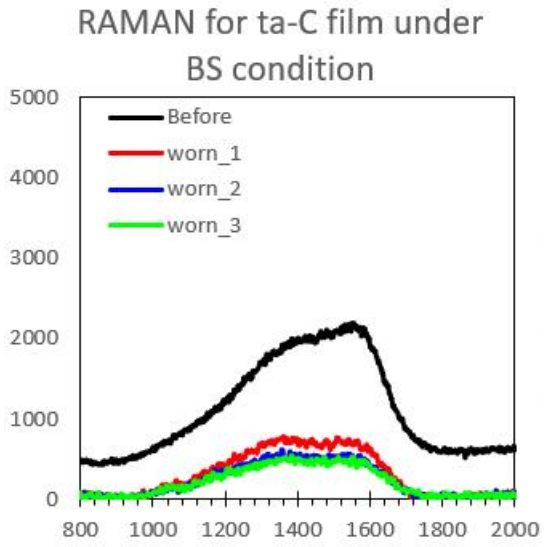

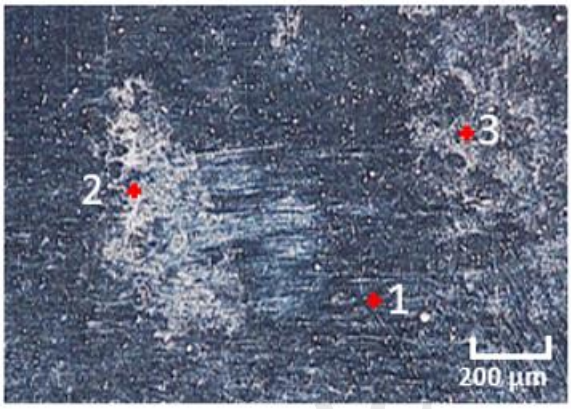

(a)

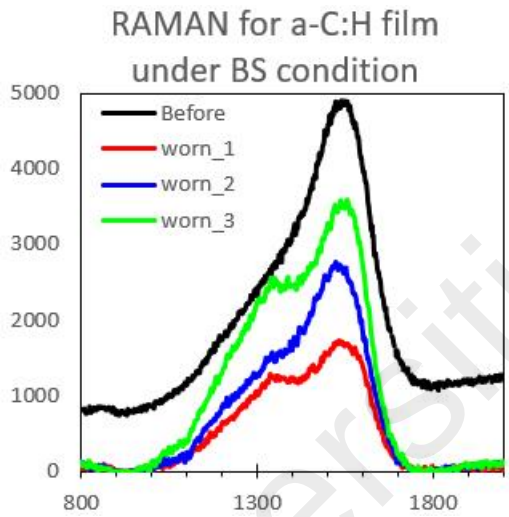

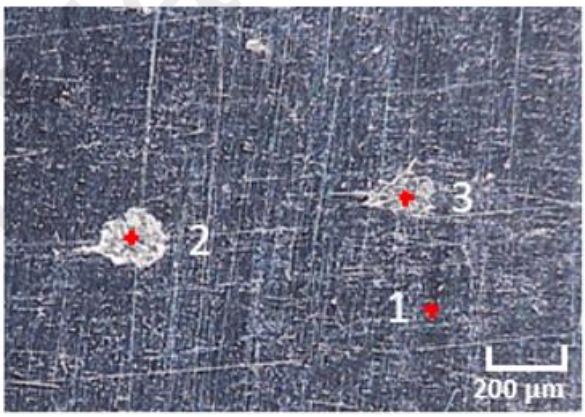

(b)

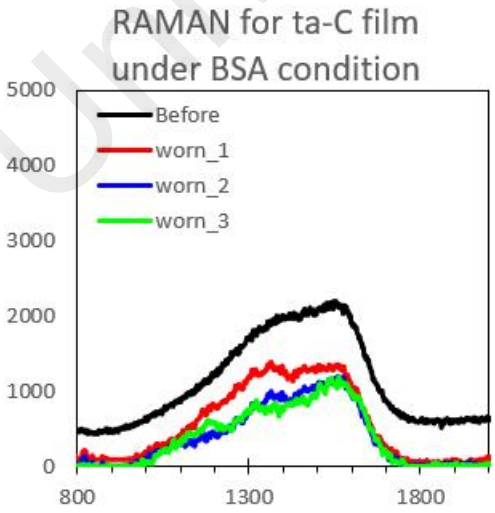

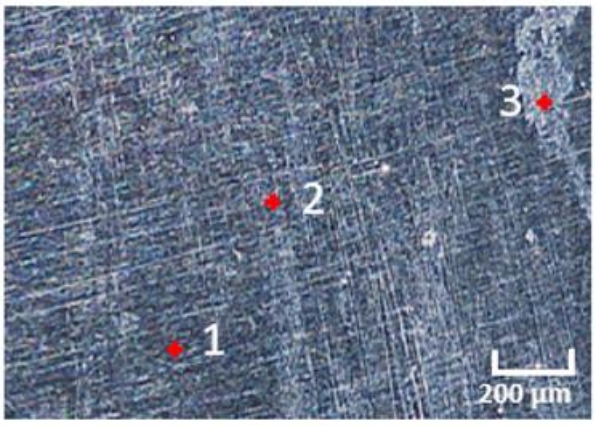

(c)

Universiti Malaya

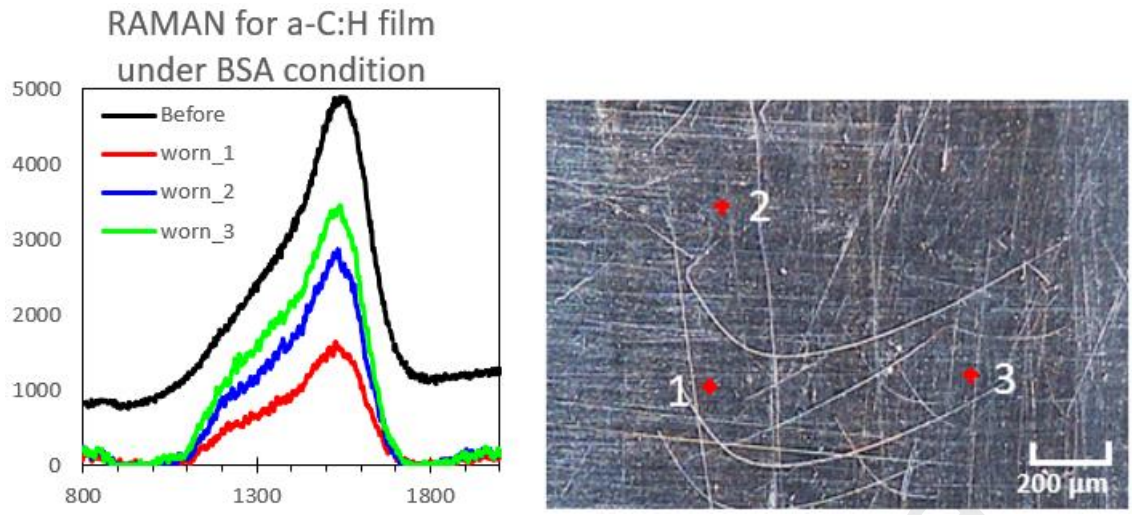

(d)

Figure 4.14 RAMAN spectrometer of (a) ta-C and (b) a-C:H film under BS condition; (c) ta-C and (d) a-C:H film under BSA condition.

FTIR spectrometer was done in order to confirm the existence of amide on the film surface. The FTIR spectrum was as shown in Figure 4.15. Amide I (1610-1700 cm^{-1}) and amide II (1500-1590 cm^{-1}) was observed in both films, although the peak intensity was low. The amide I indicate C=O bond and amide II indicate N-H bond, in which also recognized as a secondary protein structure. Protein is known to formed by peptide and amino acids. When protein denaturation occurs, the peptide chain breaks, and the protein attracts and bind towards the hydrophobic surface due to hydrophobic interactions. Protein denatured often occurs on secondary protein due to secondary protein has a weak N-H bond that easily breaks, which then caused protein denatured. The high amide I peaks intensity for the absorption spectrum indicate the non-denatured protein detected on the surface, where the lower peak shows more protein has denatured on the surface. Hence, the low and saturated peak intensity of all films as shown in Figure 4.15 indicate that the protein has been absorbed and denatured on the surface. Hydrophobic surface will have high adsorption for protein due to the hydrophobic interaction of proteins (Nygren, H. et al., 1994). Other than that, protein adsorption is also affected by the chemical composition

Universiti Malaya

of the film, where hydrogen bonding of the film will induce the protein adsorption. a-C:H film have the higher hydrogen content compared to ta-C film, and the hydrogen interaction from surface energy (Figure 4.12) also shows that a-C:H film has more hydrogen interaction. Hence, the lower and saturated intensity peak (more denatured protein) of a-C:H film than ta-C film is highly caused by the hydrophobicity of the film and the high content of hydrogen of the film. Furthermore, the saturated peak also indicates that there are only amide residues on the surface (no peptide detected).

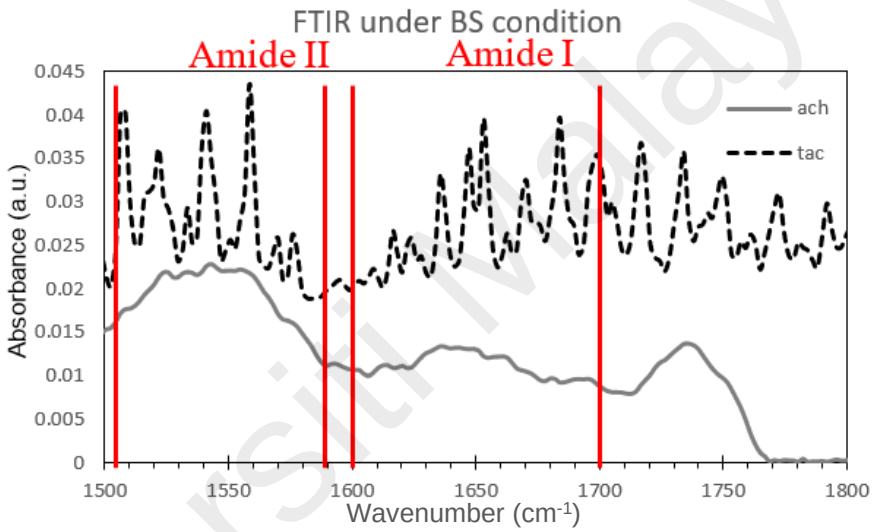

(a)

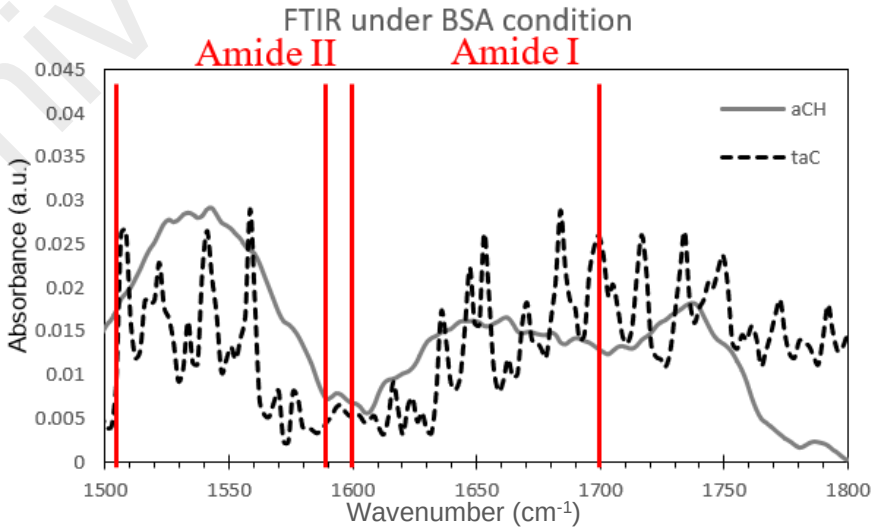

(b)

Figure 4.15 FTIR spectrometer after wear test under (a) BS; (b) BSA conditions.

Universiti Malaya

SEM images of wear traces (Figure 4.16 and 4.17) were obtained for different type of DLC films after wear test. The EDS detection of the white particles on all film surfaces denotes that it contains distinguished elements from DLC film which is N, Cl, Ca and Na elements. These elements were precipitated from diluted BS and BSA solution. In this case, we are able to reveal the adsorption of protein occurs onto those surfaces, which confirm the result from Figure 4.14 and 4.15. There is element of nitrogen (N) which attributed to the amino acid residue or peptide bond in the protein are observed to confirm the occurrence of protein adsorption (Ishihara and Choi, 2010). Figure 4.16(b) and 4.17(b) shows clearly that the adsorbed protein was dominant on a-C:H film surface. The adsorption of protein has a significant effect on the wear behavior. As the mechanism, it was a possibility that there are protective layers through protein adsorption between the contact surfaces. As a result, less wear was observed on worn surfaces of UHMWPE which slides against a-C:H film (Figure 4.13).

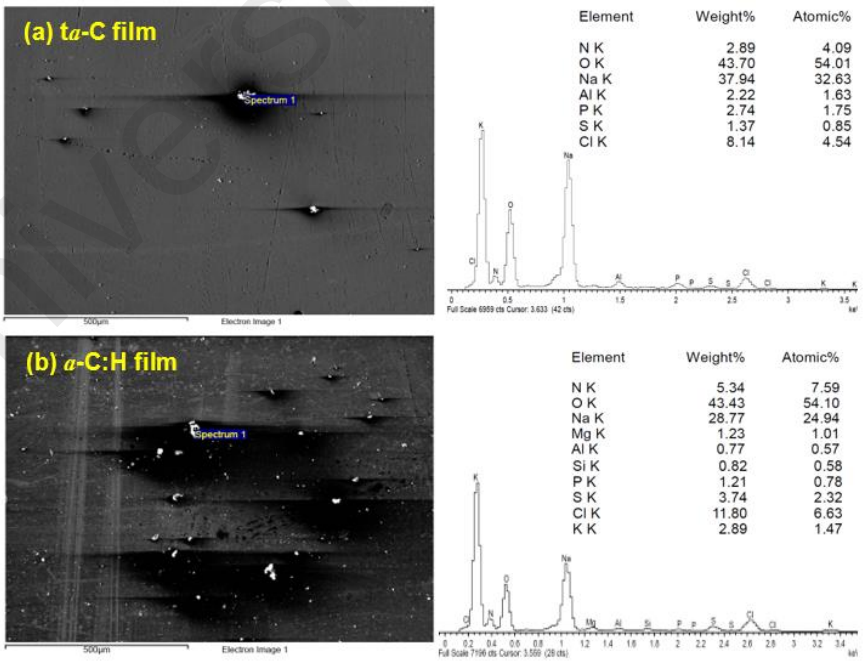

Figure 4.16 SEM-EDS of all films after wear test under BS condition

Universiti Malaya

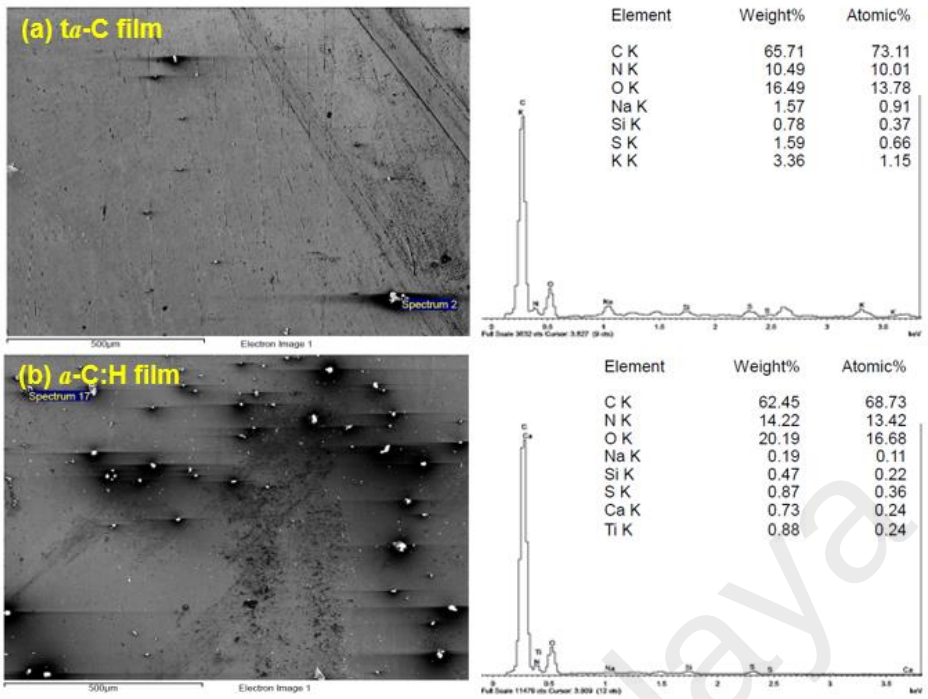

Figure 4.17 SEM-EDS of all films after wear test under BSA condition

Researchers have identified a correlation between surface wettability and wear rate (Zhang et al.,2015), and in this study, it has been found that the surface of a hydrophobic a-C:H film tends to bind more protein from diluted BS and BSA solution through "hydrophobic interactions" and decrease the wear of UHMWPE by protecting the surface from damage. a-C:H film is effective for protein absorption and the driving force of this phenomena is mainly due to the polarity and hydrogen bonding between the protein and the film (Pace et al., 2014). In addition, the hydrogen component of the total surface energy for a-C:H film was significantly larger than those of ta-C film. Thus, the presence of hydrogen in film may allow control of protein adsorption to the surface.

Universiti Malaya

4.4 Effect of hydrogenated amorphous DLC coatings with different hydrocarbon source on tribological behavior of titanium (Ti6Al4V) alloy and UHMWPE under protein lubricated condition.

Hydrogenated amorphous carbon (a-C:H) DLC coatings was observed to obtain better ability in protecting the surface from wear. However, a hydrocarbon source with difference chemical structural may have vary effect on tribological behavior of deposited a-C:H films. Hence, effect of a-C:H films deposited using different hydrocarbon source will further being study in this section. Hydrogenated amorphous carbon (a-C:H) DLC coatings was coated onto Ti6Al4V alloy by using CVD system with different type of hydrocarbon source (C_2H_4, C_2H_2 and CH_4). From previous test (4.3), hydrogenated DLC (a-C:H) have better wear resistance as compared with tetrahedral amorphous DLC (ta-C). However, a-C:H film deposited using difference type of hydrocarbon may have difference properties in mechanical and tribological behavior. Hence, this part of study will focus on studying the effect of a-C:H film deposited using different hydrocarbon source on the tribological behavior of the films and UHMWPE counterparts under protein lubricated condition. Ti6Al4V alloy and UHMWPE was used for the test because these materials were common materials used for manufactured bio-implants. a-C:H deposited using different hydrocarbon source on metal substrates of Ti6Al4V is first being characterize using RAMAN spectrometer and FTIR before the tribological test. The coating hardness were being characterize using nano-indentation test before the tribological test. After the tribological test, the substrates wear rate is being calculated and analyze. The worn surface was then being characterized using RAMAN spectrometer, FTIR and SEM-EDX.

Universiti Malaya

4.4.1 Structure characterization before wear test

Hardness test is being done using nano-indentation machine. The results from the nano-indentation test is as shown in Figure 4.18. Although all samples contain sp bond, sp^2 bond, sp^3 bond and hydrogen, however, films deposited using difference hydrocarbon source will have difference properties due to difference in chemical structure (Oohira, K., 2009). However, a-C:H film deposited using C_2H_2 was observed to obtained higher hardness, followed by a-C:H film deposited using C_2H_4 and CH_4. This was due to the sp bond of C_2H_2 film (triple bond), which have low bond length and high bond energy that make the film to be harder (Oohira, K., 2009).

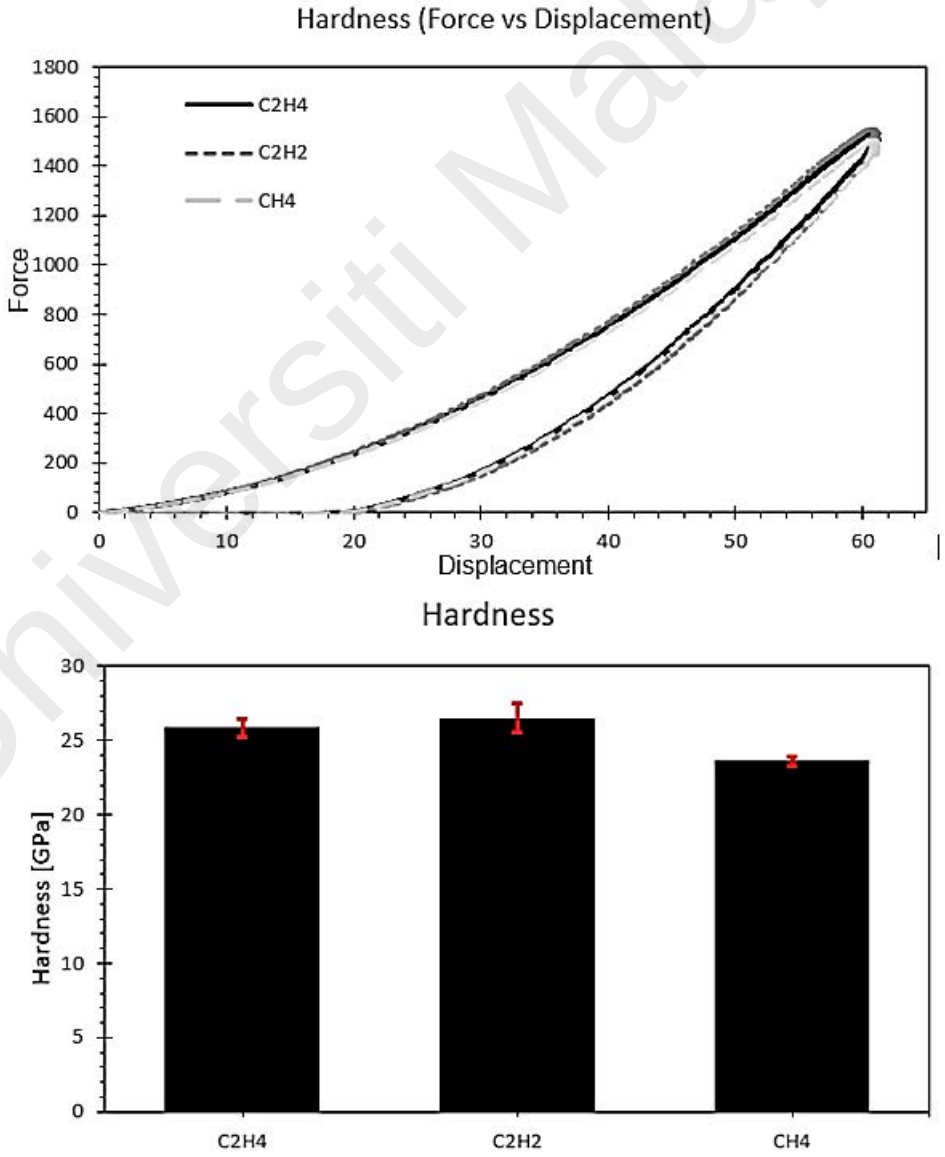

Figure 4.18 Variation of indentation hardness for different DLC films

Universiti Malaya

The FTIR spectrum of the films was as shown in Figure 4.19. All a-C:H films deposited by difference hydrocarbon source (C_2H_4, C_2H_2 and CH_4) shows the same trend with difference in absorbance intensity. Strong =C-H bending vibration (675-1000 cm^{-1}), C-O bending (1032-1085 cm^{-1}), C=C stretching (1500-1680 cm^{-1}), C≡C stretching (2100-2260 cm^{-1}) and C-H stretching (2850-3000 cm^{-1}) was present for all samples (C_2H_4, C_2H_2 and CH_4). The peaks show that DLC films have successfully deposited on the metal substrate.

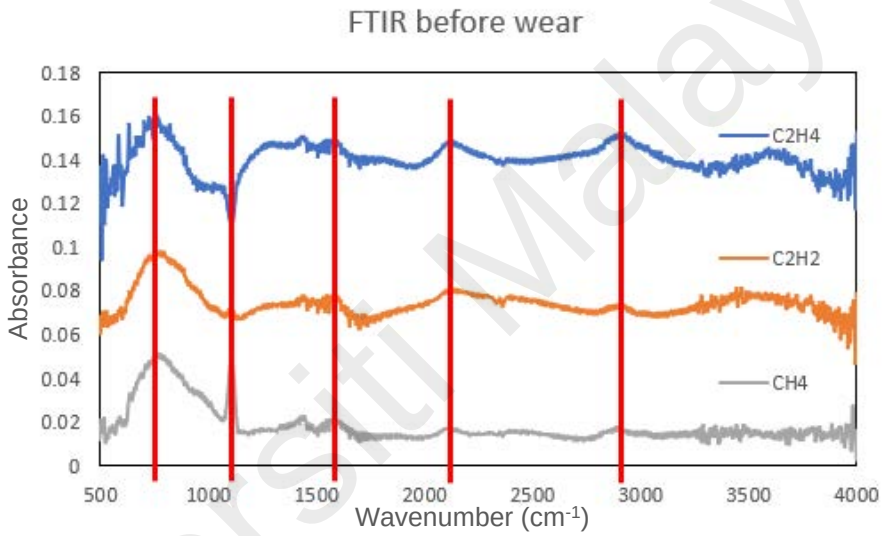

Figure 4.19 FTIR spectrum before wear test

4.4.2 Surface energy and wettability of a-C:H film deposited by different hydrocarbon source

Wetting is the contact and spreading of a liquid on the surface of a solid object and plays an important role in biomedical applications. From the tribological prospective, wettability plays an important role for improving lubrication properties of the tribo-pairs. Contact angle of distilled water, hexadecane and diiodomethane on films deposited using C_2H_4, C_2H_2 and CH_4 is later used to calculate surface energy using extended Fowkes theory. The surface energy of the liquids shows in Table 3.5 is used to calculate the surface energy of the film. The surface energy of the film is shown in Figure 4.20. The

Universiti Malaya

total surface energy (Υ_T) of the films deposited using C_2H_4, C_2H_2 and CH_4 is the sum of the dispersion component (Υ_d), the polar component (Υ_p), and the hydrogen bonding component (Υ_h).

In this study, higher surface energy was observed on CH_4 sample, followed by C_2H_2 sample and C_2H_4 sample. The film which is more hydrophobic will have lower surface energy. The different of surface energy was due to differences in polar and hydrogen-bonding components due to strong dipole-dipole and hydrogen-bonding interaction at the surfaces. In this study, C_2H_2 sample and C_2H_4 sample have similar wettability with surface energy approximately at 56.1033 $mN.m^{-1}$ and 55.1021 $mN.m^{-1}$. According to Figure 4.20, Υ_p and Υ_h is the dominant factor that contribute toward the difference of surface energy.

Although C_2H_2 sample and C_2H_4 sample have similar wettability, C_2H_2 sample was observed to have higher Υ_p and lower Υ_h, while C_2H_4 sample was observed to have lower Υ_p and higher Υ_h. The polar component of the film has the higher tendency to attract the polar liquids and was depend the electronegativity of sample, hence, C_2H_2 was observed to be more polar compare to C_2H_4. The difference in the electronegativity of C_2H_2 sample and C_2H_4 sample has contributed in the difference of Υ_p. C_2H_2 sample have high electronegativity, high polarity and was highly reactive as compare with C_2H_4 sample. Moreover, the existence of H-bond in the film also have contribution in the differences in surface energy of the film. The H-bond in the film are easily attached to the molecule of the liquid, such as the oxygen particle and nitrogen particle in proteins, thus cause the film to have higher Υ_h. Further measurements of the contact angle for diluted BS was done in order to see if the DLC films surface change its wettability when in contact with protein solution. The results show that the contact angle consistent with surface energy of film, which means that the DLC surface does not loses its

Universiti Malaya

hydrophobicity/hydrophilicity. Whereas, protein solution does not modify the chemical structure of DLC films.

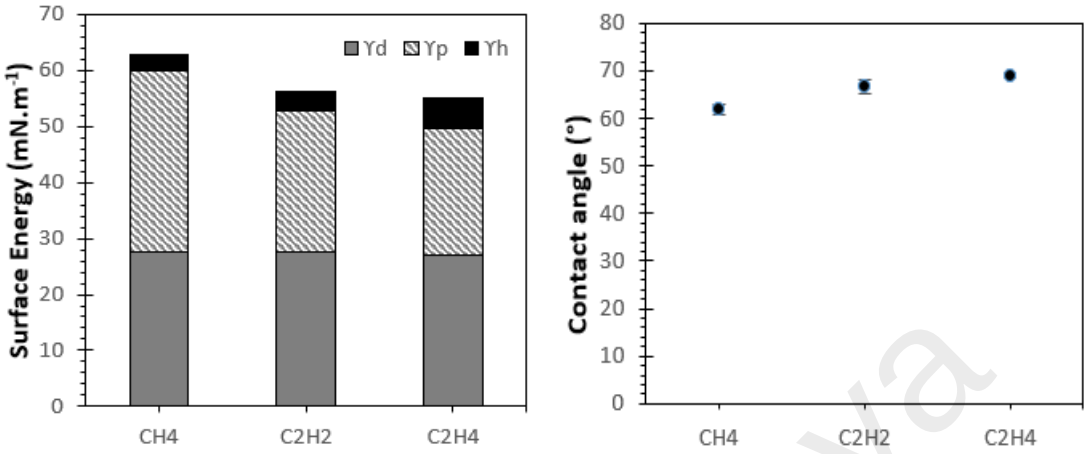

(a) (b)

Figure 4.20 (a) Surface energy; and (b) contact angle of different DLC films

4.4.3 Protein absorption

C_2H_2 sample have the thicker adsorption film thickness (313.85 ± 6.347 nm), followed with CH_4 (280.72 ± 2.265 nm) and C_2H_4 (277.09 ± 4.513 nm) as recorded in Table 4.9. The surface energy and chemical structure will play role in the protein adsorption ability of film. Wettability of surface has been characterized as the dominant factor for the protein adsorption process, and hydrophobic surfaces will have better ability in adsorbing proteins than hydrophilic surfaces (Wang, K. et al., 2012). Hydrophobic surface has high protein adsorption ability due to the hydrophobic interaction of proteins (Nygren, H. et. Al, 1994). When proteins were exposed towards hydrophobic surface, it will tend to being adsorbed strongly towards the hydrophobic surface (Hlady, V. et al.,1999). Thus, increase the proteins adsorption toward the surface. The high polarity resulting in high electronegativity and reactivity of C_2H_2 sample (Figure 4.20) have cause nitrogen and oxygen particles in protein solution can easily attract toward C-H bonding of C_2H_2 sample due to the differences in electronegativity (Hlady, V. et al.,1999). Electronegativity is the measurement of how strongly an atom can attract bonding electrons toward themselves.

Universiti Malaya

Nitrogen and oxygen were more electronegativity than hydrogen, hence, will attract electrons from hydrogen and form a polar bond with hydrogen (Allred, A. L. & Hensley, A. L., 1961).

Table 4.9 Protein adsorption film thickness measured using ellipsometer

a-C:H source	Solution	Film thickness [nm]
C_2H_4	BSA	277.09 ± 4.513
C_2H_2	BSA	313.85 ± 6.347
CH_4	BSA	280.72 ± 2.265

4.4.4 Wear test

In order to evaluate the wear performance of a-C:H films deposited using difference hydrocarbon source wear tests were carried out. Figure 4.21 shows the wear of UHMWPE ball in ambient air under bovine serum and bovine serum albumin lubricated condition. UHMWPE counterpart of C_2H_4 sample was observed to obtained lowest wear under both protein lubricated condition, followed by UHMWPE counterpart of CH_4 and C_2H_2 sample. Since the hardness of film was almost similar, the wear behaviors were mostly due to the surface energy of the films, since film with lower surface energy (more hydrophobic) will have better ability to attract protein due to protein interaction. When two hydrophobic surface contact under protein lubricated condition, protein will form aggregates between both surface which then combine to form a thin protein film that will protect the surface and hence reduce surface wear (Zhang, C., Fujii, M., 2015; Nygren, H. et al., 1994). However, C_2H_2 sample have high wear even though it has similar wettability as C_2H_4. According to Figure 4.20, C_2H_2 and C_2H_4 sample have similar wettability and surface energy with the difference in Υ_p and Υ_h, in which cause the difference of wear for C_2H_2 and C_2H_4 sample.

Universiti Malaya

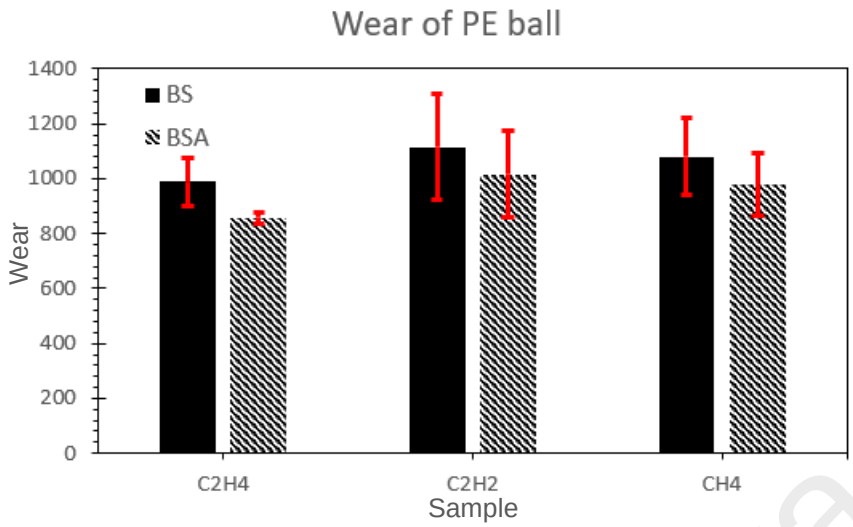

Figure 4.21 Wear rate of UHMWPE (counterpart)

The friction graph obtained from during the wear test was as shown in Figure 4.22. All sample have similar trend, and similar COF before the lubricant dry out. The BS lubricant of all samples was dry out at approximate 1000 cycles, while BSA lubricant of all sample dry out at approximate 1300 cycles. Since the test was run under boundary condition, hence, it was normal for the lubricant to dry out after some turns. After the lubricant dry out, COF for all sample under both protein lubricant condition was seen to rise drastically. This phenomenon was because of the dried-out surface will increase the friction between contact surface, hence, increase COF. C_2H_4 sample was observed to have slightly better ability in sustaining protein on the surface, in which explain the low wear of UHMWPE counterpart for C_2H_4 sample. The protein on C_2H_4 sample under both protein condition has dry out the slowest compared to other samples. This phenomenon was also due to the effect from the surface energy of the C_2H_4 sample (Figure 4.20). The chemical bonding of the films caused by the difference of Υ_h was suspect to have contribute toward the wear behavior and friction behavior of the films. Hence, further analysis will be done on the worn surfaces to characterize the structural changes and wear mechanism of DLC films under protein lubrication condition.

Universiti Malaya

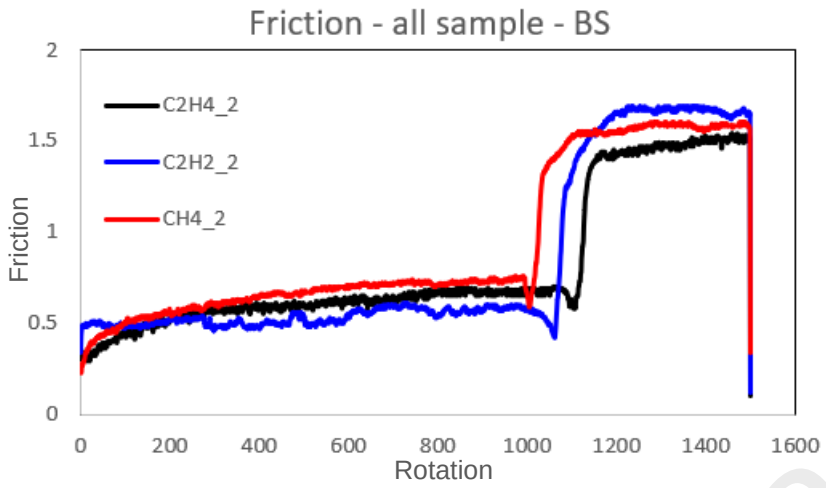

(a)

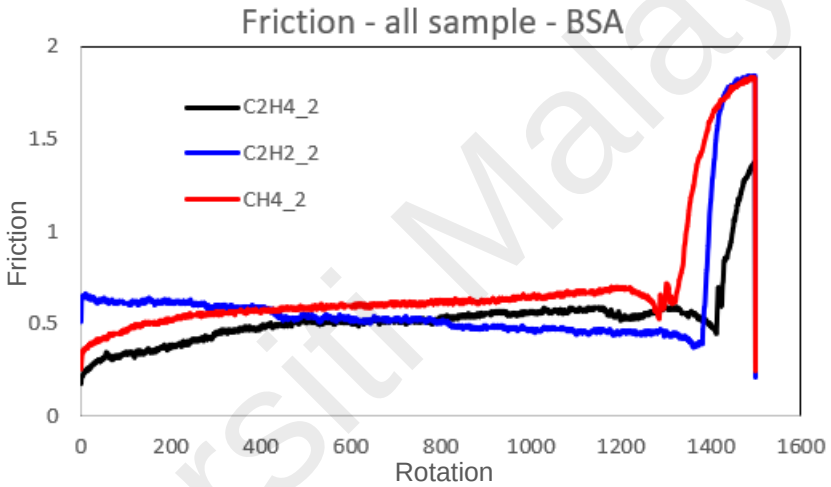

(b)

Figure 4.22 Friction of samples under (a) BS and (b) BSA condition.

4.4.5 Surface characterization

RAMAN spectrometer was used to characterize the structural changes of the film before and after wear test. The RAMAN spectrum of all film under both protein lubrication condition was as shown in Figure 4.23, where RAMAN peaks was compared between before and after wear test. All peak before wear test have peaked at D peak (~1350) and G peak (~1530), indicate that DLC films was successfully deposited onto the metal substrate. Peak intensity for all films has reduced after wear test. Moreover, amide I (~1665) and amide III (~1242) was observed on the worn side.

Universiti Malaya

The I_D/I_G ratio of all films was as recorded in Table 4.10 and 4.11, where I_D/I_G ratio for all film have reduced after wear test. The relative ratio of the D peak and G peak (I_D/I_G) is proportional to the ratio of sp^2 /sp^3 (Al Mahmud, K. et al., 2014). C_2H_4 sample shows lower I_D/I_G ratio than C_2H_2 and CH_4 samples. This finding has revealed that the smaller sp^2 cluster size in C_2H_4 sample the other samples. Reduction of I_D/I_G ratio indicates there was graphitization occurs during the wear test.

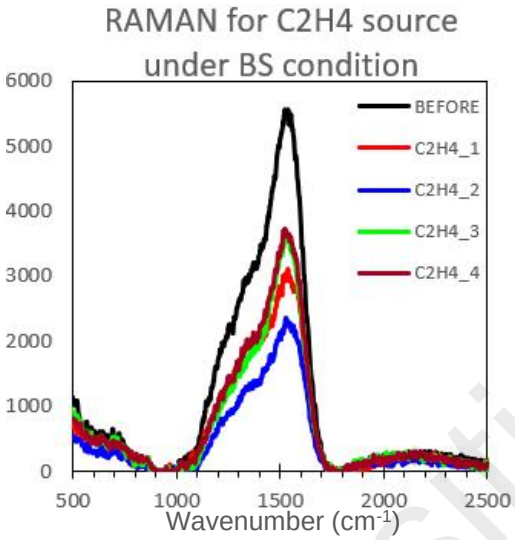

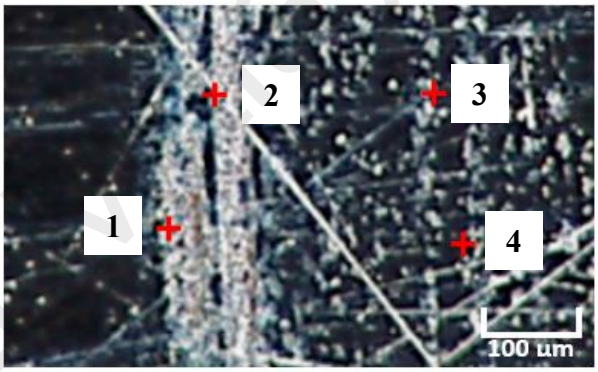

(a)

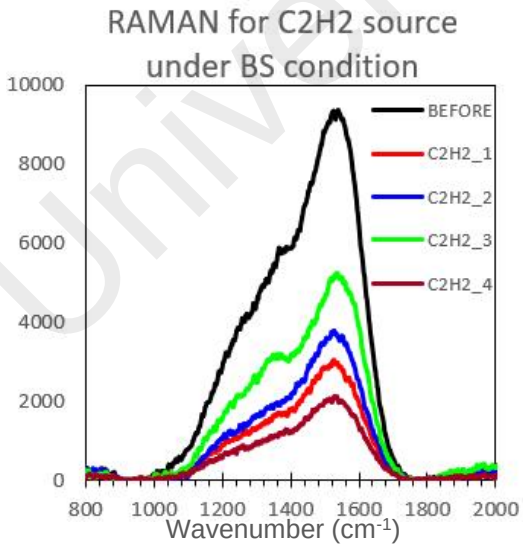

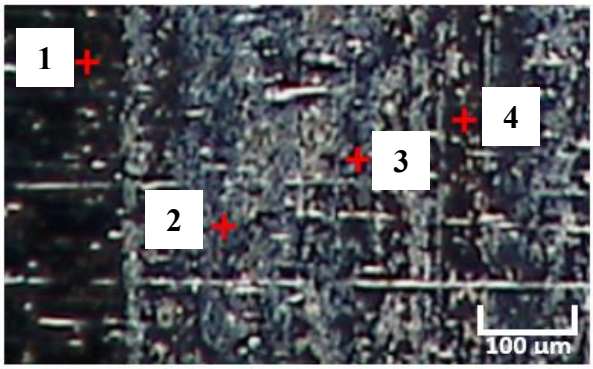

(b)

Universiti Malaya

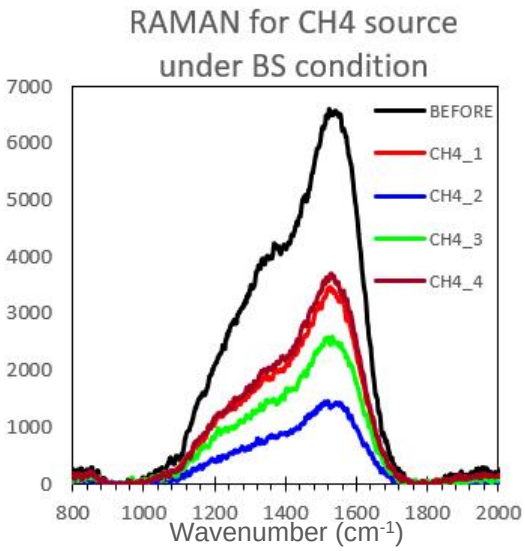

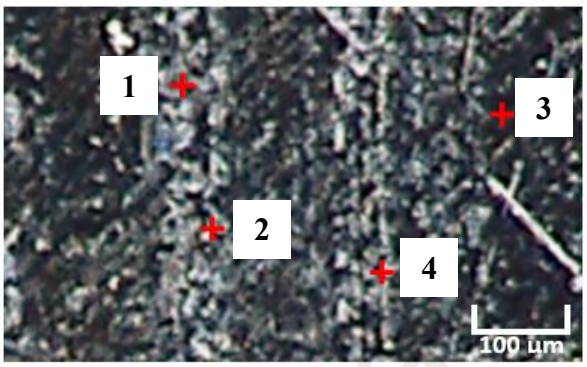

(c)

Figure 4.23 RAMAN spectrometer of (a) C_2H_4; (b) C_2H_2 and (c) CH_4 samples under BS condition.

Table 4.10 Variation of position and I_D/I_G of Raman D and G peak with different type of DLC films

Sample	C_2H_4			C_2H_2			CH_4		
	D peak [cm^{-1}]	G peak [cm^{-1}]	I_D/I_G	D peak [cm^{-1}]	G peak [cm^{-1}]	I_D/I_G	D peak [cm^{-1}]	G peak [cm^{-1}]	I_D/I_G
Before	1361	1544	1.67	1366	1545	1.67	1364	1549	1.49
1	1374	1556	1.39	1344	1537	1.10	1350	1542	1.30
2	1369	1552	1.33	1320	1537	0.72	1371	1546	1.43
3	1323	1542	0.72	1354	1551	1.39	1347	1542	1.06
4	1357	1545	1.25	1352	1540	1.20	1358	1544	1.35

Universiti Malaya

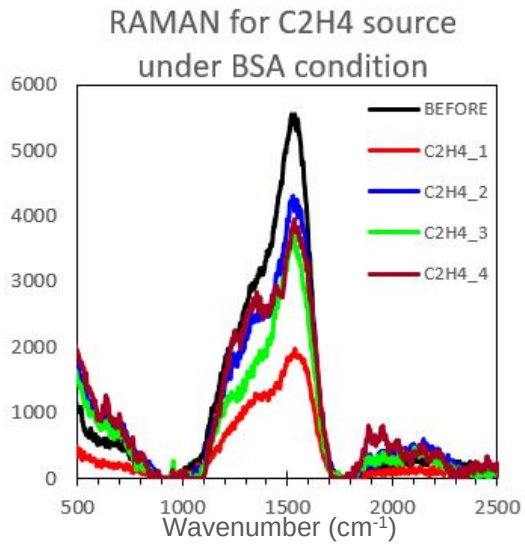

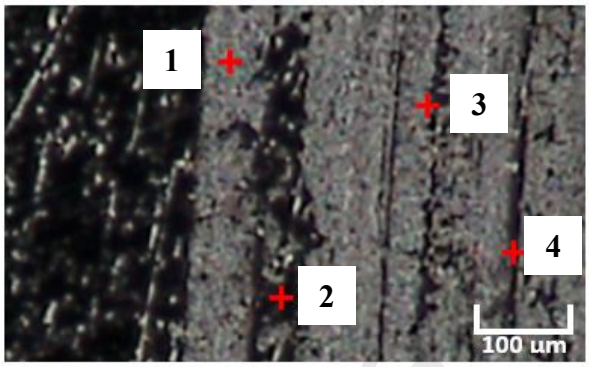

(a)

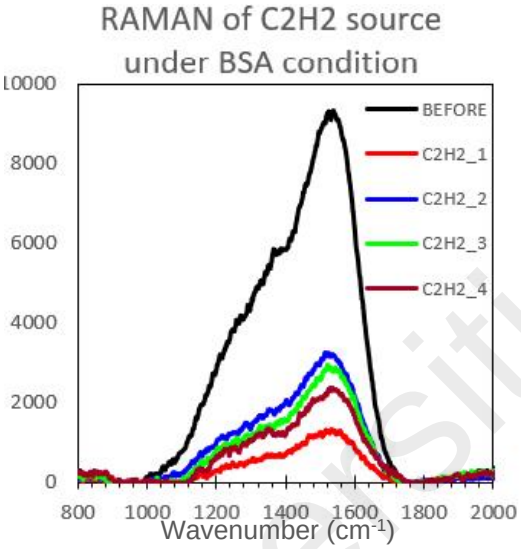

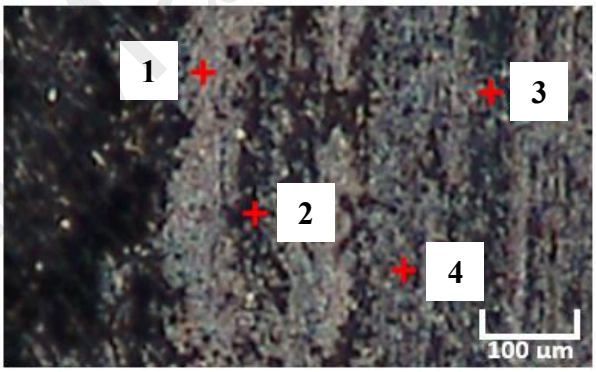

(b)

Universiti Malaya

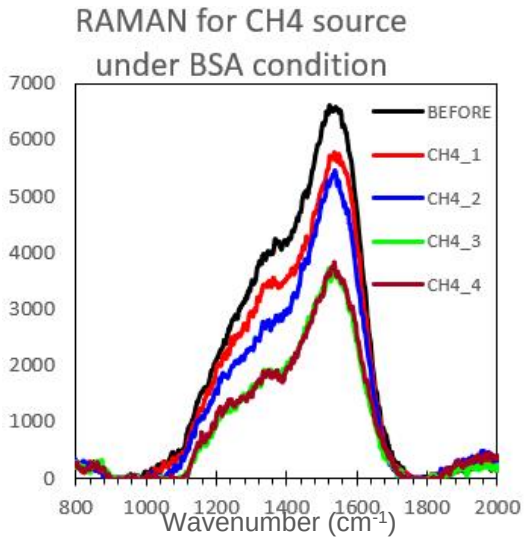

(c)

Figure 4.24 RAMAN spectrometer of (a) C_2H_4; (b) C_2H_2 and (c) CH_4 samples under BSA condition.

Table 4.11 Variation of position and I_D/I_G of Raman D and G peak with different type of DLC films

	C_2H_4			C_2H_2			CH_4		
Sample	D peak [cm^{-1}]	G peak [cm^{-1}]	I_D/I_G	D peak [cm^{-1}]	G peak [cm^{-1}]	I_D/I_G	D peak [cm^{-1}]	G peak [cm^{-1}]	I_D/I_G
Before	1361	1544	1.67	1366	1545	1.67	1364	1549	1.49
1	1371	1556	1.04	1345	1538	0.80	1356	1553	1.32
2	1350	1552	1.25	1349	1540	1.23	1352	1546	1.18
3	1334	1541	0.88	1339	1541	0.83	1331	1540	0.76
4	1339	1558	1.33	1324	1538	0.66	1331	1544	0.82

FTIR spectrometer was done in order to confirm the existence of amide on the film surface. The FTIR spectrum was as shown in Figure 4.25. FTIR peak after wear test of 800 turns and 1500 turns under BSA condition was being measured. Since the protein have already dried out on 1500 turns (Figure 4.22), hence, FTIR measurement on 800 turns was characterized. Films after 1500 turns have lower peaks compared with films after 800 turns, which was probably due to the protein was totally dried out and damage on the film surfaces.

Universiti Malaya

From Figure 4.25 (a), the amide peak was observed to be saturated and low indicate there are denatured protein detected on the film surfaces. All films show similar peak intensity trends after the wear test. Although peak intensity was low, amide I (1610-1700 cm^{-1}) and amide II (1500-1590 cm^{-1}) were able to observe in all films. The amide I indicate C=O bond and amide II indicate N-H bond, in which also recognized as a secondary protein structure (Banker J., 1992). High amide peak intensity indicates the non-denatured protein detected on the surface whereas the lower peak shows more protein has denatured on the surface (Schestkowa, H. et al., 2020). Hence, the low and saturated peak intensity of all films as shown in Figure 4.25 indicate that the protein has been absorbed and denatured on the surface. Furthermore, the saturated peak also indicates that there are only amide residues on the surface (no peptide detected).

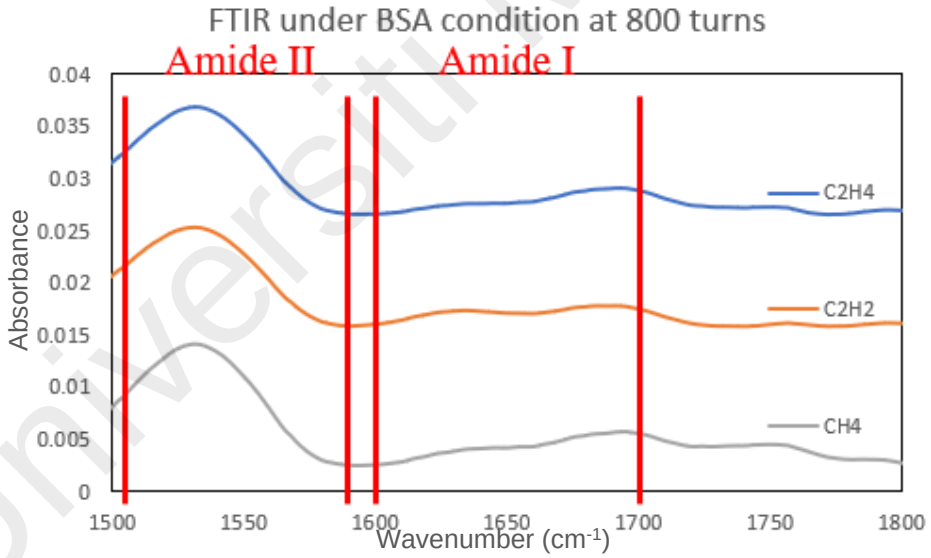

(a)

Universiti Malaya

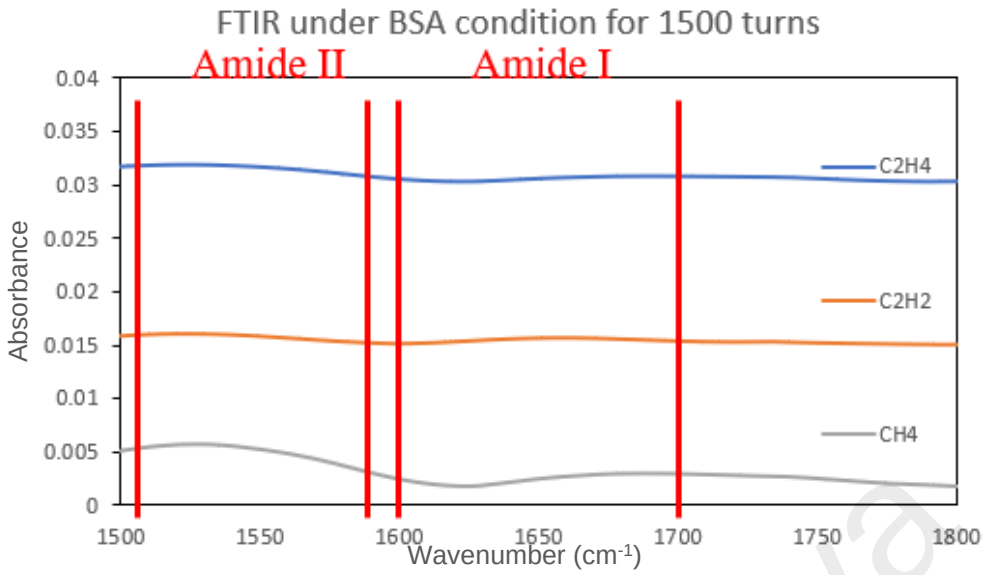

(b)

Figure 4.25 FTIR spectrometer after wear test under BSA condition for (a) 800 turns; (b) 1500 turns.

SEM images of wear traces (Figure 4.26 and 4.27) were obtained for a-C:H deposited using different type of hydrocarbon (C_2H_4, C_2H_2 and CH_4) after wear test. Figure 4.26(b) and 4.27(b) shows clearly that the adsorbed protein was dominant on C2H2 sample surface under both BS and BSA conditions. The EDS detection of the white particles on all film surfaces denote that it contains distinguished elements from DLC film which is N, Cl, Ca and Na elements. These elements were precipitated from diluted BS and BSA solution. In this case, we are able to reveal the adsorption of protein occurs onto those surfaces, which confirm the result from protein adsorption (Table 4.9), where C_2H_2 sample have better protein adsorb ability. There is element of nitrogen (N) which attributed to the amino acid residue or peptide bond in the protein are observed to confirm the occurrence of protein adsorption (Ishihara and Choi, 2010).

Universiti Malaya

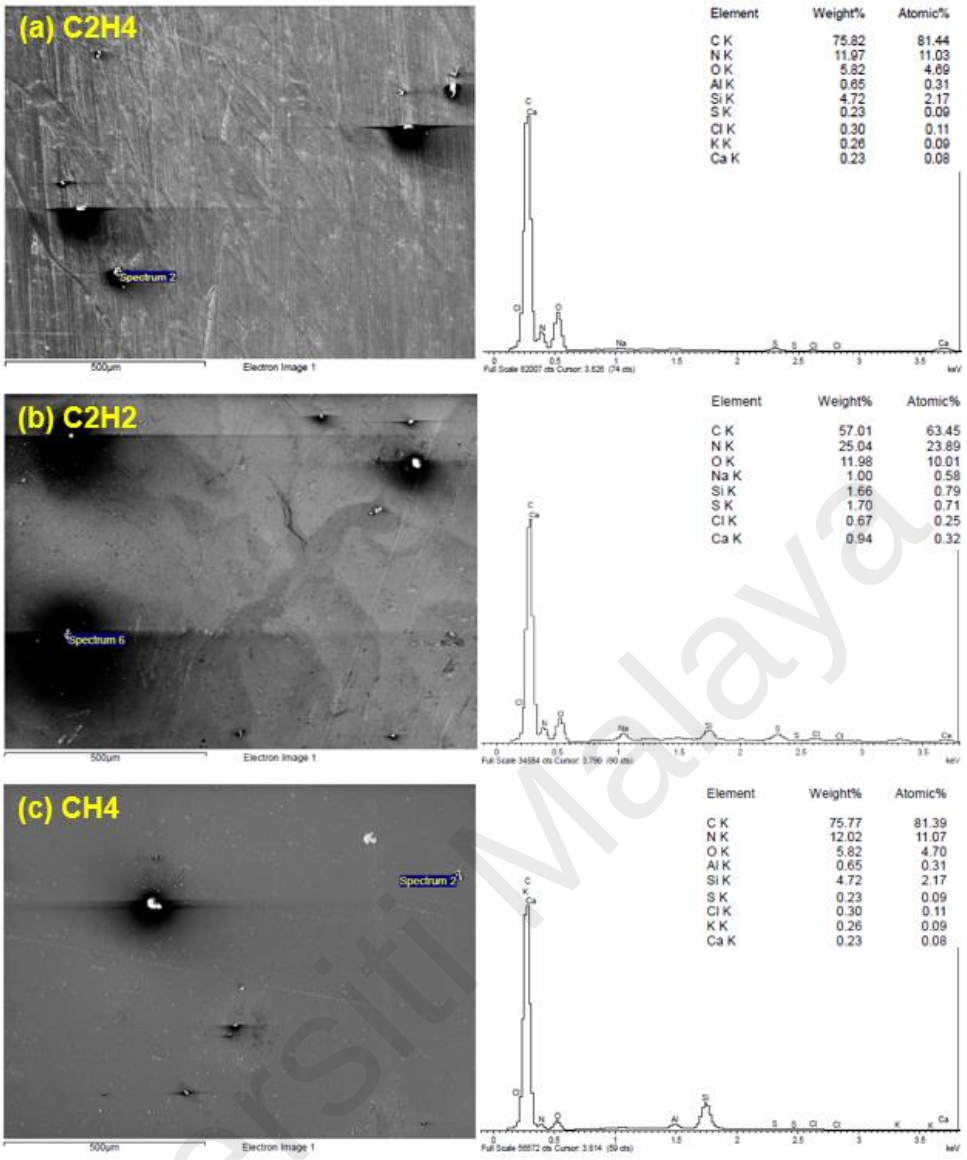

Figure 4.26 SEM-EDS of all films after wear test under BS condition.

Universiti Malaya

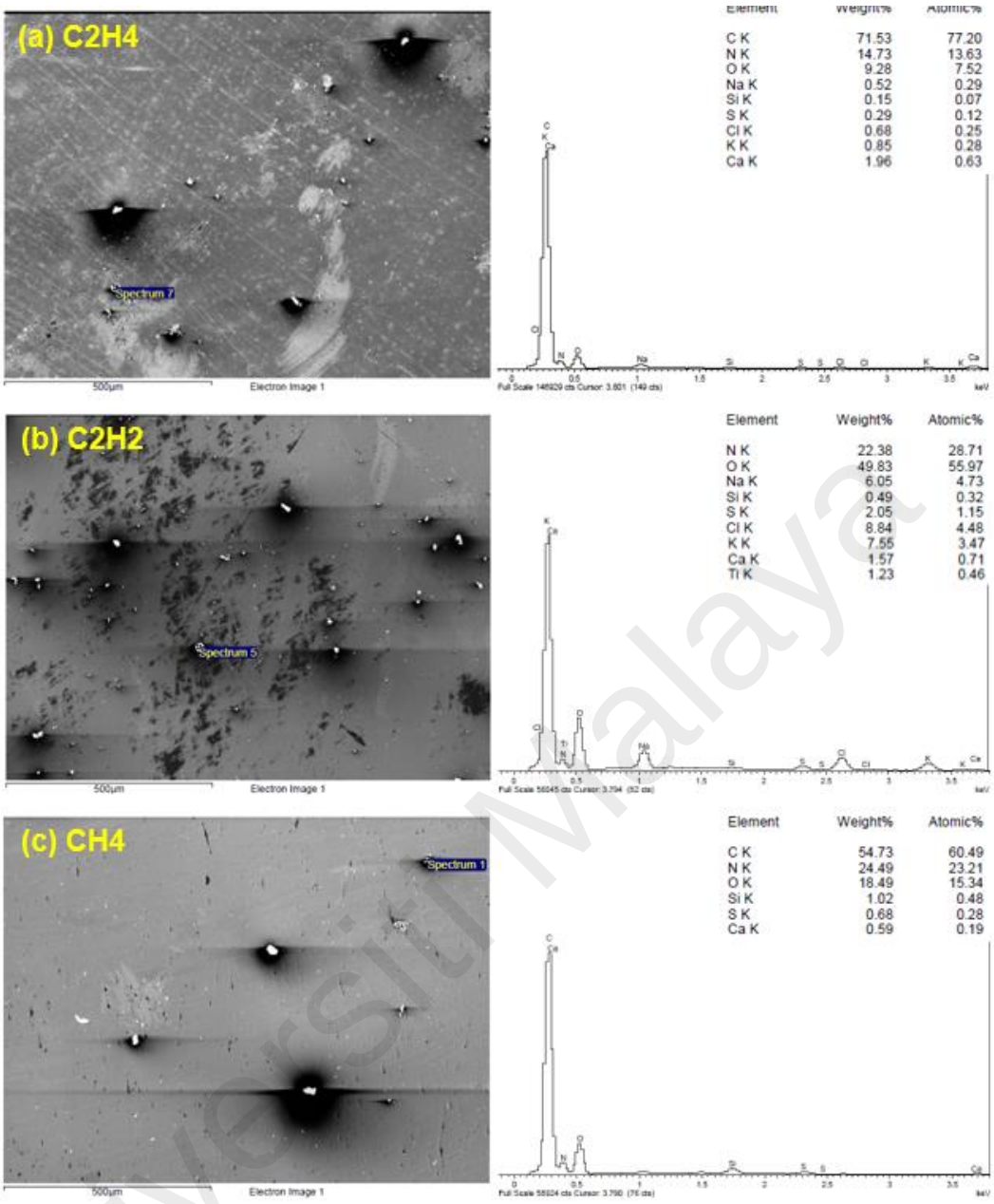

Figure 4.27 SEM-EDS of all films after wear test under BSA condition.

Generally, all sample exhibited similar properties with slight difference in surface energy, protein adsorption and wear. However, due to the difference in the Υ_p and Υ_h have resulting in different performance of samples. C_2H_4 show the better ability in sustaining protein lubrication due to high Υ_h. While C_2H_2 sample exhibit the better protein adsorption due to its high polarity chemical structure with high Υ_p.

Universiti Malaya

CHAPTER 5: CONCLUSION

5.1 Conclusion

Effect of surface modification using surface coating and surface texturing with different method have been analyzed in this study. From the result, we know that

1. The high incidence of micro pits (average depth of 27.5 μm for 6 months insert and 18 μm for 8 months insert) and scratching as the observed surface defects. The main factor that caused these wear features is wear debris that enter during the articulation motion of the implants
    a. 6 months tibial insert is observed to exhibit high-grade wear, while 8 months tibial insert is observed to possess low-grade wear.
        i. The mode of damage of 6 months tibial insert is characterized as abrasive wear and oxidation induced wear.
        ii. The mode of damage of 8 months tibial insert is characterized as abrasive wear.
    b. The reduction of mechanical properties of early retrieved UHMWPE tibial inserts is caused by changes to the molecular weight. It is believed to have contributed to the wear damage. As compared to 8 months tibial insert, 6 months tibial insert undergone approximately 86.4% of weight reduction from the standard medical grade showed the lowest mechanical properties and high-grade wear
2. Although textured samples have the ability to improve its own wear resistance, but the textured surface will increase the wear of its counterpart due to surface roughness. While the sample with only coating have better ability in protecting both film and counterpart surface.
3. a-C:H coating which is more hydrophobic have higher protein adsorption rate (313.85 ± 6.347 nm) as compared with ta-C coating (93.66 ± 0.533 nm). a-C:H coating was

Universiti Malaya

observed to have better ability (no visible wear on a-C:H coating; UHMWPE wear rate of 2.11 x10^{-7} m^3/mN under BSA condition) to protect both contact surface under protein conditions which was highly due to it higher protein adsorption ability.

4. All samples exhibit similar performance, with slight difference of surface energy (55.10 mN.m^{-1} for C_2H_4 sample; 56.10 mN.m^{-1} for C_2H_2 sample; 62.69 mN.m^{-1} for CH_4 sample), protein adsorption (277.09 ± 4.513 nm for C_2H_4 sample; 313.85 ± 6.347 nm for C_2H_2 sample; 280.72 ± 2.265 nm for CH_4 sample) and wear performance (wear scar average 858 μm for C_2H_4 sample; 1015 μm for C_2H_2 sample 978 μm for CH_4 sample under BSA condition).
    a. C_2H_4 sample have better ability in sustaining protein lubricant (lubricant sustain until 1108 turn under BS condition; 1412 turn under BSA condition).
    b. C_2H_2 sample have better protein adsorption rate (313.85 ± 6.347 nm).

5.2 Future Works

More works will be done in future to characterize the effect of surface coating and surface texturing toward the biomaterials.

- Difference texture shape and texture parameter in order to characterize the effect of texture shape and parameter in tribological behavior.
- Modification on UHMWPE material in improving functionality and performance of implants.

Universiti Malaya

REFERENCE

Abu-Amer, Y. et al. (2007). Aseptic loosening of total joint replacements: mechanisms underlying osteolysis and potential therapies. *Arthritis research & therapy*, *9 Suppl 1*(Suppl 1), S6. doi:10.1186/ar2170

Addiego, F. et. al. (2011). Does Texturing of UHMWPE Increase Strength and Toughness? A Pilot Study. Clin Orthop Relat Res (2011) 469:2318–2326

Allred, A. L. & Hensley, A. L. (1961). Electronegativities of nitrogen, phosphorus, arsenic, antimony and bismuth. Journal of Inorganic and Nuclear Chemistry. Vol. 17, Issues 1–2, 43-54.

Ahmed, A. et al. (2015). An overview of geometrical parameters of surface texturing for piston/cylinder assembly and mechanical seals. *Meccanica*, *51*(1), 9-23.

Aizawa, T. & Fukuda, T. (2013). Oxygen plasma etching of diamond-like carbon coated mold-die for micro-texturing. Surface and Coatings Technology, 215, pp.364-368.

Al-Azizi & Ala' A. (2014). Nano-Texture for A Wear-Resistance And Near-Frictionless Diamond-Like Carbon. Carbon 73, 403-412.

Alvarado, J., et al. (2003). BIOMECHANICS OF HIP AND KNEE PROSTHESES.

Al Mahmud, K. et al. (2014). Tribological characteristics of amorphous hydrogenated (*a*C: H) and tetrahedral (t*a*-C) diamond-like carbon coating at different test temperatures in the presence of commercial lubricating oil. Surface and Coatings Technology, 245, 133–47.

Anno, J.N. et al. (1968). Microasperity lubrication, J. Tribol. 90, 351-355

Ansari, F. et al. (2013). Fractography and oxidative analysis of gamma inert sterilized posterior-stabilized tibial insert post fractures: Report of two cases. *The Knee,* 20 (6), 609-613.

Arakawa, T. et al. (2001). Factors affecting short-term and long-term stabilities of proteins. Advanced Drug Delivery Reviews. Volume 46, Issues 1–3, 307-326

Universiti Malaya

Arslan, A., Masjuki, H., Varman, M., Kalam, M., Quazi, M., & Al Mahmud, K. (2015). Effects of texture diameter and depth on the tribological performance of DLC coating under lubricated sliding condition. *Applied Surface Science*, *356*, 1135-1149.

Arsoy, D. et al., 2012. Aseptic tibial debonding as a cause of early failure in a modern total knee arthroplasty design. Clinical orthopaedics and related research, 471(1), 94-101.

Aurora, A. et al. (2006). Effect of lubricant composition on the fatigue properties of ultra-high molecular weight polyethylene for total knee replacement. *Proceedings of the Institution of Mechanical Engineers, Part H: Journal of Engineering in Medicine*, *220*(4), 541–551. https://doi.org/10.1243/09544119JEIM35

Azom. (2012). Medical Applications of Stainless Steel 304. Azo materials. https://www.azom.com/article.aspx?ArticleID=6641

Bahçe, E. & Emir, E. (2019). Investigation of wear of ultra-high molecular weight polyethylene in a soft tissue behaviour knee joint prosthesis wear test simulator. Journal of Materials Research and Technology.

Balla, V. K. et al. (2010). Porous tantalum structures for bone implants: fabrication, mechanical and in vitro biological properties Acta Biomater., 6, 3349–3359

Banker J. (1992). Amide modes and protein conformation. Biochimica et Biophysica Acta, 1120, 123−143.

Besong, A.A. et al. (1998). Quantitative comparison of wear debris from UHMWPE that has and has not been sterilised by gamma irradiation. J Bone and Jt. Surg.Br. 80(2). 340-344.

Blunn, G. W. et al., 1992. Polyethylene wear in unicondylar knee prostheses. 106 Retrieved Marmor, PCA, and St. Georg tibial components compared. Acta Orthop Scand, 63(3), 247–255.

Brandt, J. M. et al., 2011. Delamination wear on two retrieved polyethylene inserts after gamma sterilization in nitrogen, The Knee, Volume 18, Issue 2, 125-129.

Universiti Malaya

Brigelius-Flohé, R. & Traber, M. G. (1999). Vitamin E: Function and metabolism. FASEB J. vol. 13, 1145–1155.

Budzynski, P. et al. (2006). Surface modification of Ti–6Al–4V alloy by nitrogen ion implantation. Wear. 261(11-12). 1271-1276.

Burnett, R. S. J. et al., 2007. Unilateral tibial polyethylene liner failure in bilateral total knee arthroplasty–bilateral retrieval analysis at 8 years. J Arthroplast, 22(5), 753–758.

CAD/CAM: Computer-Aided Design and Manufacturing, by Mikell P. Groover and Emory W. Zimmers Jr., Printice Hall of India Private Limited

Capellato, P. et al. (2013). Surface Modification on Ti-30Ta Alloy for Biomedical Application. Engineering, 2013, 5, 707-713

Cervantes, A. L. et al. (2012). Effects of surface texturing on the performance of biocompatible UHMWPE as a bearing material during in vitro lubricated sliding/rolling motion. journal of the mechanical behavior of biomedical materials 20 (2013) 45 – 53.

Ching, H. A. et al. (2014). Effects of surface coating on reducing friction and wear of orthopaedic implants. Sci. Technol. Adv. Mater. 15 014402

Choudhury, D., et al. (2018). Mechanical wear and oxidative degradation analysis of retrieved ultra high molecular weight polyethylene acetabular cups. J. Mech. Behav. Biomed. Mater. 79, 314–323.

Clarke, I. C. (1971). Human articular surface contours and related surface depression frequency studies. Ann Rheum Dis 1971; 30: 15–23.

Collier, J. P. et al. (1996). Impact of gamma sterilization on clinical performance of polyethylene in the knee. J Arthroplast, 11(4), 377–389.

Costa, L. et al. (1998). Oxidation in orthopaedic UHMWPE sterilized by gamma-radiation and ethylene oxide. Biomater. vol. 19, 659–668.

Universiti Malaya

Crowninshield R. D., et al. (2008). Clinical performance of contemporary tibial polyethylene components. J Arthroplast, 21(5), 754–761.

Demas, N. G. et al. (2016). Measurement of Thin-film Coating Hardness in the Presence of Contamination and Roughness: Implications for Tribology. *Metallurgical and Materials Transactions A, 47*(4), 1629-1640. doi: 10.1007/s11661-016-3342-9

Demehri, S. et al. (2014). Chronic allergic contact dermatitis promotes skin cancer. *J Clin Invest.* 2014;124(11):5037-5041

Diabb, J. et. al. (2009). Failure analysis for degradation of a polyethylene knee prosthesis component. Eng Fail Anal, 16:1770–3

Ding, Q. et al. (2010). Improved Tribological Behavior of DLC Films Under Water Lubrication by Surface Texturing. *Tribology Letters*, *41*(2), 439-449.

Dong, C. H. et al. (2018). Experimental Study on Surface Element Composition and Hydrophobic Properties of DLC Coating. Key Engineering Materials, Vol. 764, 58-67

Drexler, M. et al. (2013). Assuring the happy total knee replacement patient. Bone Joint J, 95 (11), 120-123.

Dudhniwala, A. G. et al. (2016). Early failure with the Journey-Deuce bicompartmental knee arthroplasty. European Journal of Orthopaedic Surgery & Traumatology. 517-521.

Elahinia, M., et al. (2019). Engineering Bone-Implant Materials. *Bioengineering (Basel, Switzerland)*, *6*(2), 51.

Eliaz, N. (2019). Corrosion of Metallic Biomaterials: A Review. *Materials*, *12*, 407.

Escudeiro, A. (2014). Adsorption of bovine serum albumin on Zr co-sputtered a-C(:H) films: Implication on wear behaviour. J Mech Behav Biomed Mater. 39, 316-27.

Fisher, J. et al (2009). Knee Society Presidential Guest Lecture: Polyethylene wear in total knees. Clin Orthop Relat Res. 2010; 468:12–18.

Universiti Malaya

Flannery, M. et al. (2008). Analysis of wear and friction of total knee replacements. Part II: Friction and lubrication as a function of wear. Wear. 265. 1009-1016. Fehring, T. K. et al. (2001). Clinical Orthopaedics and Related Research. Vol.392, 315-318

Garcia, R. M. et al. (2009). Analysis of Retrieved Ultra–High-Molecular-Weight Polyethylene Tibial Components from Rotating-Platform Total Knee Arthroplasty. The Journal of Arthroplasty, Vol. 24 No. 1, 131-138

Ghosh, S. et al. (2014). Tribological role of synovial fluid compositions on artificial joints - A systematic review of the last 10 years. Lubrication Science. 26. 10.1002/ls.1266.

Ghosh, S., & Abanteriba, S. (2016). Status of surface modification techniques for artificial hip implants. *Science and technology of advanced materials*, *17*(1), 715–735. doi:10.1080/14686996.2016.1240575

Gottimukkala, R. (2005). *Growth and characterization of diamond and diamond like carbon films with interlayer.* (M. A.), University of South Florida.

Grill, A. (1998). Diamond-like carbon - state of the art. *Diamond and Related Materials, 8*, 428-434.

Groover, M. P. et al. CAD/CAM: Computer-Aided Design and Manufacturing. Printice Hall of India Private Limited

Gupta, P. (2003). *Synthesis, structure and properties of nanolayered dlcdlc films.* (M. A.), Panjab University.

Hall, R. M. et al. (2001). Biotribology for joint replacement. Curr. Orthop. 15 (4), 281–290

Haman. J. D. et al. (2005). Surface Damage and Wear in Fixed, Modular Tibial Inserts: The Effects of Conformity and Constraint. In: Bellemans J., Ries M.D., Victor J.M. (eds) Total Knee Arthroplasty. Springer, Berlin, Heidelberg

Han, J. et al. (2008). Influence of surface roughness and contact load on friction coefficient and scratch behavior of thermoplastic olefins, Applied Surface Science, Volume 254, Issue 15, 4494-4499

Universiti Malaya

Hartley, J. G (2007) CNSE Associate Head of the Nanoengineering Constellation, CNSE Professor of Nanoengineering, CNSE Addresses Unique Nanotechnology Challenges. http://www.nanotech-now.com/columns/?article=042

Hata T, Kitazaki Y, Saito T. (1987). Estimation of the surface energy of polymer solids. J Adhes., 21:177–194.

Hauert, R. et al. (2012). Retrospective lifetime estimation of failed and explanted diamond-like carbon coated hip joint balls, Acta Biomaterialia, Vol 8, Issue 8, 3170-3176

Hench, L. L. & Polak, J. M. (2002). Third-generation biomedical materials. Science. 2002 Feb 8; 295(5557):1014-7.

Heni, B. (2019). Chapter 6 - Thermal Denaturation, Aggregation, and Methods of Prevention, Whey Proteins, Academic Press, 185-247.

Hirakawa, K. et al. (1999). Relationship between wear debris particles and polyethylene surface damage in primary total knee arthroplasty. J Arthroplast, 14(2), 165–71.

Hlady, V. et al. (1999). Methods for studying protein adsorption. *Methods in enzymology*, *309*, 402–429. doi:10.1016/s0076-6879(99)09028-x

Ho, F.Y. (2007). Mobile-bearing knees reduce rotational asymmetric wear. Clin Orthop Relat Res, 462, 143–149.

Hollar, C. M. (1995). Factors Affecting the Denaturation and Aggregation of Whey Proteins in Heated Whey Protein Concentrate Mixtures1. Journal of Dairy Science. Vol. 78, Issue 2, 260-267

Hood, R. W. et al. (1983). Retrieval analysis of total knee protheses: a method and its application to 48 total condylar protheses. J Biomed Mater Res. 17, 829–842.

Jun, F. (2019). UHMWPE Biomaterials for Joint Implants: Structures, Properties and Clinical Performance. Technology & Engineering, Springer.

Ippolito, C. et al. (2017) Process parameter optimization for hot embossing uniformly textured UHMWPE surfaces for orthopedic bearings. Procedia CIRP 65 (2017), 163- 167.

Universiti Malaya

Kang, X. et al., 2014. Mechanical Properties and Tribological Behaviour of Retrieved UHMWPE Tibial Insert in Total Knee Replacement after Implantation 30 Months. Polymers and Polymer Composites. 22, 561-567

Kitazaki Y, Hata T. (1972). Surface-chemical criteria for optimum adhesion. J Adhes., 4:123–132.

Kondo, S., Liza, S., Ohtake, N., Akasaka, H., Matsuo, M., & Iwamoto, Y. (2015). Mechanical characterization of segment-structured hydrogen-free a-C films fabricated by filtered cathodic vacuum arc method. *Surface And Coatings Technology*, *278*, 71-79.

Kovačević, N. et al. (2012). The Effect of pH Value of a Simulated Physiological Solution on the Corrosion Resistance of Orthopaedic Alloys. Acta Chim Slov. 2012 Mar;59(1):144-55.

Kurtz S. M. et al. (1999). Advances in the processing, sterilization, and crosslinking of ultra-high molecular weight polyethylene for total joint arthroplasty. Biomaterials. 20(18). 1659-1688.

Kurtz S. M. et al. (2000). The relationship between the clinical performance and large deformation mechanical behavior of retrieved UHMWPE tibial inserts. Biomaterials. 21(3). 283-291

Kurtz S. M. et al. (2003). Degradation of mechanical properties of UHMWPE acetabular liners following long-term implantation. J Arthrop. 18(7 Suppl 1), 68-78

Kurtz, S. (2004). The UHMWPE Handbook: Ultra-High Molecular Weight Polyethylene in total joint replacement, First ed. Elsevier Inc, New York.

Kurtz, S. et al. (2007). Halpern Projections of primary and revision hip and knee arthroplasty in the United States from 2005 to 2030. J Bone Surg Am, 89 (4), 780-785

Kustandi, T. S. et al. (2010). Texturing of UHMWPE surface via NIL for low friction and wear properties. J. Phys. D: Appl. Phys. 43 (2010) 015301

Kutzner, I. et al. (2017). Early aseptic loosening of a mobile-bearing total knee replacement. Acta orthopaedica, *89*(1), 77-83

Universiti Malaya

Laska, A. et. al. (2016). Failure analysis of retrieved PE-UHMWE acetabular cup s. J. Mech. Behav. Biomed. Mater. 61, 70–78.

Lee, B. S. et al., 2018. Femoral Component Varus Malposition is Associated with Tibial Aseptic Loosening After TKA. Clinical orthopaedics and related research. 476, 400-407.

Liao, Y. S. et al. (2003). The effect of frictional heating and forced cooling on the serum lubricant and wear of UHMW polyethylene cups against cobalt–chromium and zirconia balls, Biomaterials 24 (2003)3047–3059.

Liu, H. et al. (2010). Surface modification of ultra-high molecular weight polyethylene (UHMWPE) by argon plasma, Applied Surface Science, Vol. 256, Issue 12, 3941-3945.

Liskiewicz, T. & Al-Borno, A. (2015). DLC Coatings in Oil and Gas Production. Journal of Coating Science and Technology. 1. 59-68. 10.6000/2369-3355.2014.01.01.7.

Liza, S., et al. (2011). Failure analysis of retrieved UHMWPE tibial insert in total knee replacement. Eng. Fail. Anal. 18 (6), 1415–1423.

Liza, S. et. al. (2017). Deposition of boron doped DLC films on TiNb and characterization of their mechanical properties and blood compatibility. Science and Technology of Advanced Materials, VOL. 18, NO. 1, 76–87. http://dx.doi.org/10.1080/14686996.2016.1262196

Liza, S., Ohtake, N., Akasaka, H., & Munoz□Guijosa, J. M. (2016). Tribological and thermal stability study of nanoporous amorphous boron carbide films prepared by pulsed plasma chemical vapor deposition. *Science and Technology of Advanced Materials, 16*(3), 035007. doi: 10.1088/1468-6996/16/3/035007

Long, L. L., & Srinivasan, M. (2013). Walking, running, and resting under time, distance, and average speed constraints: optimality of walk–run–rest mixtures. *Journal of the Royal Society Interface*, *10*(81). http://doi.org/10.1098/rsif.2012.0980

Lum, Z. C. et al. (2018). Why total knees fail: A modern perspective review. World journal of orthopedics, 9(4), 60-64.

Universiti Malaya

Mabuchi, Y. et al. (2007). The Development of Hydrogen-free DLC-coated Valve-lifter. SAE Paper. 1. 10.4271/2007-01-1752.

Maradit Kremers, H. et al. (2015). Prevalence of Total Hip and Knee Replacement in the United States. *The Journal of Bone and Joint Surgery. American Volume*, *97*(17), 1386–1397. http://doi.org/10.2106/JBJS.N.01141

May, S. (2014). Study Reveals Little Benefit to Latest Knee and Hip Implant Technologies. http://surgicalwatch.com/2014/09/study-reveals-little-benefit-latest-knee-hip-implant-technologies/

Manmeet, K. & Singh, K. (2019). Review on titanium and titanium-based alloys as biomaterials for orthopaedic applications, Materials Science and Engineering: C, Volume 102, Pages 844-862

McCord, M. A. & Rooks, M. J. (2002). SPIE Handbook of Microlithography, Micromachining and Microfabrication.

McKellop, H, et al. (2000). Effect of sterilization method and other modifications on the wear resistance of acetabular cups made of ultra-high molecular weight polyethylene. A hip-simulator study. J Bone and Jt. Surg.Am. 82-A (12). 1708-1725

McKellop, H. A. (2007) The lexicon of polyethylene wear in artificial joints. Biomaterial. 28 (34). 5049-5057

McTighe, T. et. al. (2009). Failure Mechanism on Total Knee Arthroplasty. Joint Implant Surgery & Research Foundation Chagrin Falls, Ohio, USA.

Medel, J. et al. (2009). On the Assessment of Oxidative and Microstructure Changes after in Vivo Degradation of Historical UHMWPE Knee Components by Means of Vibrational Spectroscopies and Nanoindentation. J Biomed Mater Res A. 89(2), 530-538.

Monsees, T. K. et al. (2017). Biodegradable Ceramics Consisting of Hydroxyapatite for Orthopaedic Implants. Coatings 2017, 7, 184

Mohd, J. et al., 2014. Correlation between Contact Load and Surface Roughness in Plane Strain Extrusion. Procedia Engineering. 68, 634-638

Universiti Malaya

Muratoglu, O. K. et al. (2003). Optical analysis of surface changes on early retrievals of highly cross-linked and conventional polyethylene tibial inserts. J Arthroplasty. 18(7), 42-47.

Musib, M. K. et al. (2011). A Review of the History and Role of UHMWPE as A Component in Total Joint Replacements. International Journal of Biological Engineering. 1(1), 6-10.

Musib, M. K. et al. (2011). Response to Ultra-High Molecular Weight Polyethylene Particles. American Journal of Biomedical Engineering, 2011; 1(1): 7-12Navarro, M.et al. (2008). Biomaterials in orthopaedics. J R Soc Interface. 2008 Oct 6; 5(27): 1137–1158.

Nasab, M. B. et. al. (2010). Metallic Biomaterials of Knee and Hip - A Review. Trends Biomater. Artif. Organs. Vol. 24(2). 69-82.

Nag, S., et al. (2009). Characterization of novel borides in Ti–Nb–Zr–Ta+ 2B metal-matrix composites. Materials characterization, 60(2), 106-113.

Navarro, M., et al. (2008). Biomaterials in orthopaedics. Journal of The Royal Society Interface. 5(27), 1137-1158

Nygren, H. et al. (1994). Effect of surface wettability on protein adsorption and lateral diffusion. Analysis of data and a statistical model. Biophysical Chemistry - BIOPHYS CHEM. 49. 263-272. 10.1016/0301-4622(93)E0090-R.

Oohira, K. (2009). Characteristics and Applications of DLC films. *NTN TECHNICAL REVIEW, 77*, 90-95.

Oral, E. et al. (2005). Characterization of irradiated blends of α-tocopherol and UHMWPE. Biomaterials. vol. 26, 6657–6663.

Oral, E. et al. (2007). Diffusion of vitamin E in ultra-high molecular weight polyethylene. Biomaterials. vol. 28, 5225–5237.

Oral, E & Muratoglu, O. K. (2011). Vitamin E diffused, highly crosslinked UHMWPE: a review. Int Orthop. 35(2), 215-23

Universiti Malaya

Oztürk, O. et al. (2006). Metal ion release from nitrogen ion implanted CoCrMo orthopedic implant material. Surface & Coatings Technology. 200(20-21), 5687-5697.

Pace, C. N. et al. (1996). Forces contributing to the conformational stability of proteins. *FASEB Journal*. **10** (1), 75–83.

Pang, H. et al. (2010). Characterization of diamond-like carbon films by SEM, XRD and Raman spectroscopy. Applied Surface Science. 256. 6403-6407. 10.1016/j.apsusc.2010.04.025.

Park S.J., Kim J.K., Lee K.R., Ko D.H. (2003). Humidity dependence of the tribological behavior of diamond-like carbon films against steel ball, Diam Relat Mater, 12 (2003), p. 1517

Pou, P. et al. (2017). Laser surface texturing of Titanium for bioengineering applications, Procedia Manufacturing, Vol. 13, 694-701.

Postler, A. et al. (2018). Analysis of Total Knee Arthroplasty revision causes. BMC Musculoskeletal Disorders. 19(1), 55.

Rack, H.J. & Qazi, J.I. (2006). Titanium alloys for biomedical applications. Materials Science and Engineering: C, Volume 26, Issue 8, 1269-1277.

Ramsden, J.J. et al. (2007). The Design and Manufacture of Biomedical Surfaces. CIRP Annals-Manufacturing Technology. 56(2), 687-711

Rautray, T. R. et al. (2009). Surface Modification of Titanium and Titanium Alloys by Ion Implantation. Wiley InterScience

Rawal, B.R. et al. (2016). Life estimation of knee joint prosthesis by combined effect of fatigue and wear. Procedia Technology 23, 60 – 67

Roba, M. (2009). Interaction of Synovial Fluid Components with Artificial Hip-Joint Materials, (18273), 114.

Robertson, J. (1993). Diamond 1992 Deposition mechanisms for promoting sp3 bonding in diamond-like carbon. *Diamond and Related Materials, 2*(5), 984-989.

Universiti Malaya

Robinson, W. J. et al. (2016). Probing the molecular design of hyper-branched aryl polyesters towards lubricant applications. Scientific Reports. 6. 18624. 10.1038/srep18624.

Ronkainen H. & Holmberg K. (2001). Tribological performance of different DLC coatings in water-lubricated conditions, Wear, 249 (2001), pp. 267-271

Ronkainen H. (2001). Tribological properties of hydrogenated and hydrogen-free diamond-like carbon coatings. Technical research centre of finland, VTT publications 434

Rousseau, M. A. et al. (2006). Early mechanical failure in total knee arthroplasty. International orthopaedics, 32(1), 53-6.3

Sansone, V. et al. (2013). The effects on bone cells of metal ions released from orthopaedic implants. A review. *Clinical cases in mineral and bone metabolism : the official journal of the Italian Society of Osteoporosis, Mineral Metabolism, and Skeletal Diseases*, *10*(1), 34–40. doi:10.11138/ccmbm/2013.10.1.034

Sawae, Y. et al. (1998). Effect of synovia constituents on friction and wear of ultra-high molecular weight polyethylene sliding against prosthetic joint materials, Wear, Volume 216, Issue 2, Pages 213-219,

Sawano, H., Warisawa, S. & Ishihara, S. (2009). Study on long life of artificial joints by investigating optimal sliding surface geometry for improvement in wear resistance. Precision Eng. 33, 492–8

Schestkowa, H. et al. (2020). FTIR analysis of β-lactoglobulin at the oil/water-interface, Food Chemistry, Volume 302, 125349

Shafiei, M. (2010). Investigation of Nanostructured Thin Film Based Schottky Diodes for Gas Sensing Applications. AmirKabir University of Technology (Tehran Polytechnic), Iran, Tehran

Shenhar, A., et al. (1999). Surface modification of titanium alloy orthopaedic implants via novel powder immersion reaction assisted coating nitriding method. Materials science & engineering. A, Structural materials: properties, microstructure and processing. 268(1-2), 40-46.

Universiti Malaya

Shimizu, T., Kakegawa, T. & Yang, M. (2014). Micro-texturing of DLC Thin Film Coatings and its Tribological Performance Under Dry Sliding Friction for Microforming Operation. Procedia Engineering, 81, pp.1884-1889.

Shoji, H., D'Ambrosia, R.D., Lipscomb, P.R. (1976). Failed polycentric total knee prostheses. Journal of Bone and Joint Surgery (America volume) 58, 773–777.

Simon, U. et al. (2003). Influence of the stiffness of bone defect implants on the mechanical conditions at the interface--a finite element analysis with contact. J Biomech. 36(8), 1079-1086.

Singh, R. & Dahotre, N.B. (2007). Corrosion degradation and prevention by surface modification of biometallic materials. Journal of Materials Science: Materials in Medicine. 18(5), 725-751.

Sinha, S. K. (2006). Scratching of polymers: deformation mapping and wear modeling. Scratch. Mater. Appl. 124–135.

Stanczyk, M. & Telega, J. J. (2002). Modelling of heat transfer in biomechanics: review, part II. Orthopaedics, Acta of Bioengineering and Biomechanics 4, 3–33.

Stone, D. S. (1991). Hardness and elastic modulus of TiN based on continuous indentation technique and new correlation J. Vac. Sci. Technol. A, 9, 2543–2547

Suh, N.P. et al. (1998) Tribology of polyethylene homocomposites. Wear 1998; 214: 231–236.

Sullivan, T. (2010). Letters from Grassley: Follow-up to New York Times Article on Zimmer.
http://www.typepad.com/services/trackback/6a00e5520572bb88340133f31262e4970b

Taeger, G. et al. (2003). Comparison of Diamond-Like-Carbon and Alumina-Oxide articulating with Polyethylene in Total Hip Arthroplasty. Materialwissenschaft und Werkstofftechnik. 34. 1094 - 1100.

Thomas, K. F. et al. (2001). Early Failures in Total Knee Arthroplasty. Clinical orthopaedics and related research. 392, 315-318.

Universiti Malaya

The Digital Terror. (2016). Differentiating Physical Vapor Deposition from Chemical Vapor Deposition. http://thegadgetblog.com/differentiating-physical-vapor-deposition-from-chemical-vapor-deposition/

Ulrich-Vinther, M. et al. (2002). Recombinant adeno-associated virus-mediated osteoprotegerin gene therapy inhibits wear debris-induced osteolysis J. Bone Joint Surg. Am. A 84 1405–12

Verzola, B. et. al. (2000). Protein adsorption to the bare silica wall in capillary electrophoresis: Quantitative study on the chemical composition of the background electrolyte for minimising the phenomenon, Journal of Chromatography A, Volume 868, Issue 1, 85-99.

Vidal, C.V. & Muñoz, A.I. (2008). Effect of thermal treatment and applied potential on the electrochemical behaviour of CoCrMo biomedical alloy. Electrochimica Acta.

Villa, T., et al. (2004). Contact stresses and fatigue life in a knee prosthesis: comparisonbetween in vitro measurements and computational simulations. Journal of Biomechanics 37, 45-53.

Wang, G. C. et al. (2011). Nanostructured glass–ceramic coatings for orthopaedic applications. J. R. Soc. Interface (2011) 8, 1192–1203.

Wang, K. et al. (2012). A review of protein adsorption on bioceramics. Interface Focus, 2(3), 259–277. http://doi.org/10.1098/rsfs.2012.0012.

Wang, X. & Quinn, P. J. (2000). The location and function of vitamin E in membranes (Review) Mol. Membr. Biol. vol. 17, 143–156.

Wannomae, K. K. et al., 2006. The effect of real-time aging on the oxidation and wear of highly cross-linked UHMWPE acetabular liner. Biomaterials. 27, 1980–1987.

Wiklund, U., & Larsson, M. (2000). Low friction PVD titanium–carbon coatings. *Wear, 241*(2), 234-238. doi: 10.1016/s0043-1648(00)00381-1

Windarta, M. & Khairul, F., 2011. Influence of Applied Load on Wear Characterizations of Rail Material. Journal of Applied Sciences, 11, 1636-1641.

Universiti Malaya

Wong, J. Y. & Bronzino, J. D., 2007. Biomaterials. CRC Press, Boca Ration

Yan, Y. et al. (2014). Controlled nanodot fabrication by rippling polycarbonate surface using and AFM diamond tip. Nanoscale Res Lett. 9 (1), 372.

Yang, S. et al. (2000). Deposition and tribological behaviour of sputtered carbon hard coatings Surf. Coat. Technol., 124, 110–116

Yokel R. A. (2000). The toxicology of aluminium in the brain: a review. Neurotoxicology. 21: 813–28.

Young, S. K. et al. (1998). Friction reduction in total joint arthroplasty. Wear 1998; 222: 29–37.

Zahiri, C. A., et al. (1998). Assessing Activity in Joint Replacement Patients. The Journal of Arthroplasty 13 (8), 890-895.

Zanasi, S. (2011). Innovations in total knee replacement: new trends in operative treatment and changes in peri-operative management. European orthopaedics and traumatology. 2(1-2), 21-31

Zardiackas, L. D. et al. (2001). Structure, metallurgy and mechanical properties of a porous tantalum foam J. Biomed. Mater. Res., 58, 180–187

Zhang, B. et al. (2013). Comparison of the effects of surface texture on the surfaces of steel and UHMWPE. Tribol. Int. 65 (0), 138-145.

Zhang, B., Huang, W. & Wang, X. L. (2012). Biomimetic surface design for ultrahigh molecular weight polyethylene to improve the tribological properties. Journal of Engineering Tribology 2012 226: 705

Zhang, B. & Wang, X. L. (2012). The Design and Fabrication of Dimples Pattern on the Surface of UHMWPE. Materials Science Forum Vol. 770 (2014) pp 421-426.

Zhang, C., Fujii, M. (2015). Influence of wettability and mechanical properties on tribological performance of dlc coatings under water lubrication. Journal of Surface Engineered Materials and Advanced Technology, 5, pp. 110-123.

Universiti Malaya

Zhang, M. et al. (2004). Surface modification of UHMWPE for use in total joint replacements. Biomed Sci Instrum. 40, 13-7

Zhang, T. F., Deng, Q. Y., Liu, B., Wu, B. J., Jing, F. J., Leng, Y. X., & Huang, N. (2015). Wear and corrosion properties of diamond like carbon (DLC) coating on stainless steel, CoCrMo and Ti6Al4V substrates. *Surface and Coatings Technology, 273*, 12-19. doi: 10.1016/j.surfcoat.2015.03.031

Zhang, Y. L. et al. (2015) Numerical study of surface texturing for improving tribological properties of ultra-high molecular weight polyethylene. Biosurface and Biotribology 1 (2015), 270–277.

Zweifel, H. et al. (2009). Plastics additives handbook (6th ed.). Munich Hanser. 746.

Universiti Malaya

LIST OF PUBLICATIONS AND PAPERS PRESENTED

M. Y., Tan et al. (2019). Surface analysis of early retrieved polyethylene tibial inserts for both knees in total knee replacement, Engineering Failure Analysis.

Universiti Malaya